DEVELOPMENT OF TiAlN PVD COATING SYSTEMS FOR MACHINING OF COMPACTED GRAPHITE IRON (CGI)

Development of TiAlN PVD Coating Systems for Machining of Compacted Graphite Iron (CGI)

By

Majid Abdoos, B.Sc., M.Sc.

A Thesis

Submitted to the School of Graduate Studies in Partial Fulfilment of the Requirements for the Degree Doctor of Philosophy

McMaster University

DOCTOR OF PHILOSOPHY (2020) McMaster University

(Mechanical Engineering) Hamilton, Ontario

TITLE	Development of TiAlN PVD Coating Systems for Machining of Compacted Graphite Iron (CGI)
AUTHOR	Majid Abdoos, B.Sc., M.Sc.
SUPERVISOR	Dr. Stephen C. Veldhuis Department of Mechanical Engineering
SUPERVISORY COMITTEE	Dr. Mohamad Hamed Department of Mechanical Engineering
	Dr. André Phillion Department of Materials Science and Engineering
Page Count	xiii, 145

To my parents, for their unconditional love and support.

Acknowledgements

I would like to express my utmost gratitude to my supervisor, Dr. Stephen Veldhuis for this opportunity. Without his support and guidance, this research would not be possible. I am also grateful to my committee members, Dr. Mohamad Hamed and Dr. André Phillion for their valuable comments and advice during my studies.

I need to thank all my mentors, friends, and colleagues at the McMaster Manufacturing Research Institute (MMRI), especially Dr. Abul Fazel Arif, Dr. Sushant Rawal, Dr. Bipasha Bose, and Dr. German Fox-Rabinovich for their continuous support and guidance along the journey. I feel extremely fortunate to work alongside so many amazing people, and I will always appreciate the knowledge and experience I gained during these years.

My deepest appreciation to my mother, Fatemeh, my father, Abbas, and my sister, Mehrnaz. No word can describe how grateful I am to have your love and support in my life.

I also acknowledge that this research was supported by the Natural Sciences and Engineering Research Council of Canada (NSERC) under the CANRIMT Strategic Research Network Grant NETGP 479639-15.

Lay Abstract

With continuous improvement and optimization of the materials used in advanced industrial components, there is an increasing demand for improving machining productivity. This goal can be achieved by prolonging tool life and improving final part quality by tailoring the cutting tool according to the workpiece material. Physical vapor deposition is an effective method to alter superficial tool properties by applying a thin layer of hard coating and, thus, protecting the tool during the machining process. In the present research a TiAlN coating was developed for the machining of compacted graphite iron (CGI) by focusing on thickness, coating properties, and substrate geometry. The developed coating was able to improve tool life by 35% in comparison to commercially available coatings.

Abstract

Compacted graphite iron, with its improved mechanical properties, is the ideal candidate to replace grey cast iron in the automotive industry. Engine blocks made from CGI are lighter, smaller, and show higher fuel efficiency. However, machining compacted graphite iron is extremely challenging compared to grey cast iron, especially in continuous cutting operations. Difficulties in dry turning CGI can be attributed to a lack of a protective tribolayer and its high tendency to stick to the cutting tool, which results in built-up edge formation and adhesion wear. This research attempts to address challenges associated with CGI turning by developing a TiAlN coating with a focus on thickness and low residual stress. The mentioned coating was developed using a new technology called super fine cathode (SFC) which enables better control over residual stress generation and, therefore, enables the deposition of a TiAlN coating with higher thickness compared to its commercial range. The properties and performance of this coating were comprehensively studied using X-Ray diffraction, scanning electron microscopy, micro and nanomechanical indentation, scratch test, optical 3D microscopy, and tool wear studies. The results show that residual stress is the main measured feature limiting coating thickness and affecting wear pattern during the machining of CGI. By using a low substrate bias voltage and a high nitrogen pressure, deposition of a thick TiAlN coating under low compressive residual stress was achieved, which significantly delayed substrate exposure, reduced built-up edge formation, lowered the cutting forces, and improved tool life by 35%. Moreover, to improve the coating quality along the cutting edge, wet blasting was applied before the deposition process, which resulted in better edge quality and consistency.

Table of Contents

List of Figures

List of Tables

Abbreviations

BUE	Built up edge
CGI	Compacted graphite iron
CTE	Coefficient of thermal expansion
CVD	Chemical vapor deposition
DCI	Ductile cast iron
EDS	Energy dispersive spectroscopy
FIB	Focused ion beam
GCI	Grey cast iron
MQL	Minimum quantity lubrication
PVD	Physical vapor deposition
SEM	Scanning electron microscopy
SFC	Super fine cathode
TEM	Transmission electron microscopy
XRD	X-Ray diffraction

Chapter 1. Introduction

1.1. Background

With the continuous improvement of materials selection and development, more hard-to-cut materials are being introduced to the manufacturing industry. Thus, there is an ever-increasing need to optimize the machining process and improve cutting tools. Despite that tooling cost typically makes up only 3% of the total machining cost, its impact on the cost of labor and productivity is quite significant (Bobzin, 2016). Therefore, increasing productivity and production capacity and reducing cost are the main motivating factors driving research into tool life improvement. Most of the research performed is focused on coating development with the simple idea of providing better surface properties on the tool to withstand the dominant wear mechanism. It is only logical that in developing such a coating, a deep understanding of the wear mechanisms involved is essential. Therefore, the following sections are aimed to provide background information on different modes of tool wear, CGI and challenges associated with its machining, and PVD coating as a mean to increase tool life.

1.1.1. Tool Wear and Tool Wear Mechanisms

Tool wear is defined as material removal from the tool by physical or chemical means during the cutting process. The flank or rake face of the tool may be subjected to different modes of wear caused by a combination of adhesion, abrasion, oxidation, or diffusion (Dolinšek and Kopač, 2006). Each of these mechanisms can be involved in the wear process depending on the nature of the engagement between the tool and the workpiece, tool

geometry, surface conditions, materials involved, the external environment, and the cutting parameters such as cutting speed, feed rate, or depth of cut (Klocke and Kuchle, 2011). Tool life is then determined by the total cutting length or cutting time until the tool reaches complete failure, which is normally measured in terms of flank wear width (as shown in fig 1.1). Flank wear of 300 µm is generally considered to be the end of functional tool life, according to ISO 3685. Using a tool with a state of wear beyond 300 µm can result in increased power consumption, higher cutting forces, and higher temperature in the cutting zone, resulting in the degradation of part quality. Thus, actual tool life used in industry is often set based on desired part quality and process conditions.

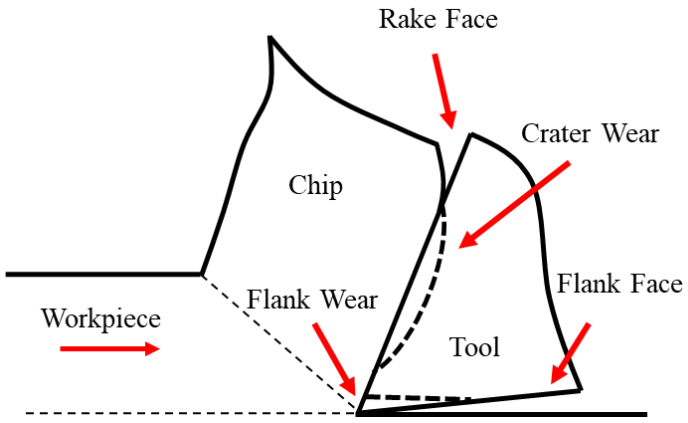

Figure 1.1. *Tool wear Schematic.*

In general, tool life plotted against cutting time/length (fig. 1.2) typically follows three stages of behaviour: the initial stage of wear is characterized by a high wear rate and adaptation of the tool/coating system to the cutting process, followed by a period of steady state wear rate, and finally catastrophic tool failure due to accelerated tool wear (Klocke and Kuchle, 2011).

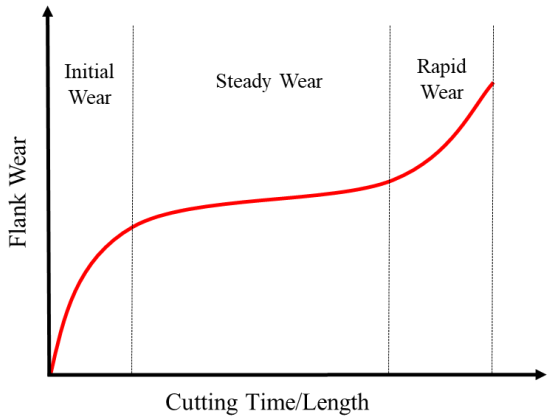

Figure 1.2. *Typical tool life curve versus cutting time/length.*

1.1.2. Tool Coating

Cutting tools with hard coatings have been used for more than 50 years in the manufacturing industry, and today around 85% of cemented carbide tools used are coated (Bobzin, 2016). Since wear occurs on the tool, it is only logical to protect this surface and improve the wear resistance of the tool with a proper coating. Consequently, coatings can provide opportunities for tool design since the bulk properties and surface properties of the tool can be adjusted separately according to the need. Coated tools are more resistant to mechanical and thermal loads compared to uncoated ones. In addition, coatings can reduce interaction between the tool and chip, lower the coefficient of friction, improve wear and fracture resistance, and thus prolong tool life (Bouzakis *et al.*, 2012).

Chemical and Physical Vapor Deposition techniques (CVD and PVD) are extensively used as the main methods for applying protective tool coatings. The performance of these coatings are strongly dependent on: composition, architecture, deposition parameters, tool geometry, and tool material (Prengel *et al.*, 2001). A timeline of different CVD and PVD coating developments can be seen in fig. 1.3.

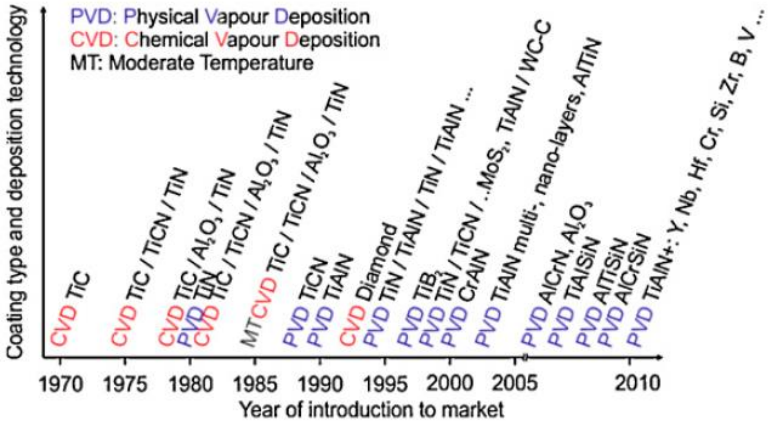

Figure 1.3. *Evolution of PVD and CVD coatings, reused with permission (Bouzakis et al., 2012).*

1.1.3. Compacted Graphite Iron (CGI)

Compacted graphite iron (CGI) is a part of the cast iron family, with mechanical properties between grey cast iron (GCI) and ductile cast iron (DCI). The graphite in CGI is randomly oriented, similar to grey cast iron; however, the graphite is thicker and possesses round edges with a unique structure, as shown in fig. 1.4. Unlike other cast irons, CGI has a complex graphite structure with a bumpy surface, providing a strong adhesion bond between the iron matrix and graphite, thus inhibiting crack propagation (Guesser, Schroeder and Dawson, 2001; Sahm, Abele and Schulz, 2002).

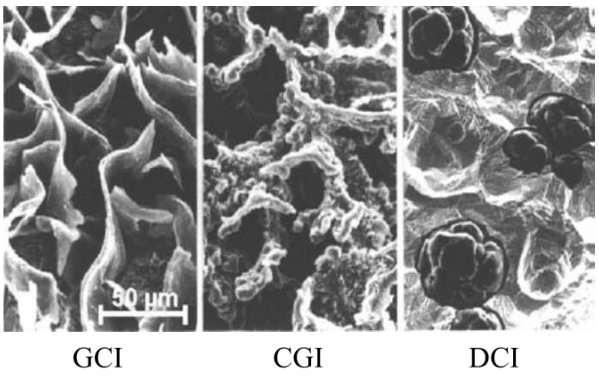

Figure 1.4. *Graphite structure in grey cast iron (GCI), compacted graphite iron (CGI), and ductile cast iron (DCI), reused with permission (Sahm, Abele and Schulz, 2002).*

The superior mechanical properties of CGI compared to grey cast iron make it a potential candidate to replace GCI in the automotive industry (Dawson and Schroeder, 2000, 2004). Dawson (Dawson and Schroeder, 2004) mentioned 10-30% lower weight and volume, reduced emissivity and higher efficiency is expected in engine blocks upon replacing grey cast iron with CGI. However, CGI has limited applications due to its lower machinability compared to GCI, as seen from the tool life comparison of both workpiece materials using various tools in fig. 1.5.

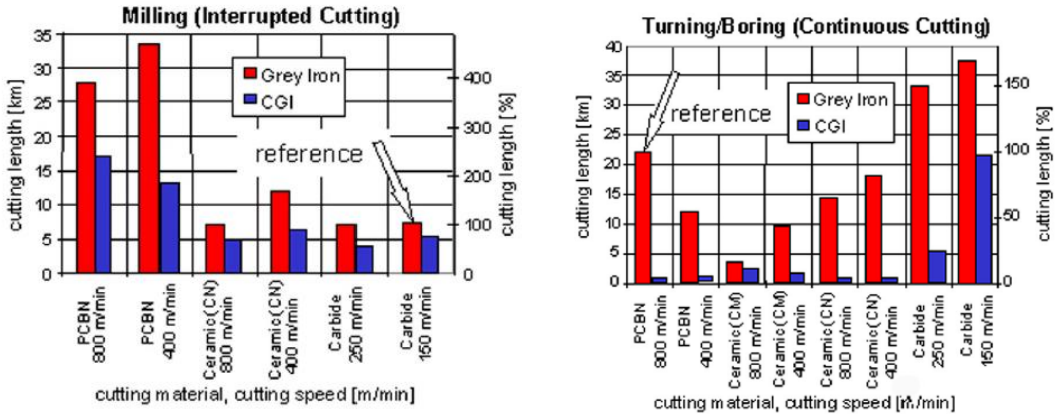

Figure 1.5. *Tool life comparison of CGI and GCI for interrupted and continuous cutting, reused with permission (Dawson et al., 2001).*

1.1.3.1 Challenges of CGI Turning

The low machinability of CGI compared to GCI is believed to be due to the following factors:

1. **Lack of sulfur:** During the machining of GCI at high cutting speeds, a dense protective MnS layer forms on the tool which can also act as a lubricant. However, in CGI, since compacted graphite particles are only stable at a low oxygen and sulfur content, sulfur cannot be added to CGI. Therefore, no protective layer forms

on the tool during the machining of CGI, which results in greater tool wear (Gastel *et al.*, 2000; Abele, Sahm and Schulz, 2002; Heck *et al.*, 2008).

2. **Lack of lubricious graphite:** Graphite in GCI helps chip formation and acts as a lubricant. Crack propagation can easily happen in the graphite while cutting GCI, and this exposed graphite lubricates the chip/tool contact area. In contrast, graphite is not easily fractured during CGI machining, usually it is deformed instead (Nayyar *et al.*, 2013).
3. **Hard abrasive particles:** Titanium may occasionally be added to CGI to stabilize the casting process. Consequently, TiC and other hard Ti particles can form, causing high abrasive wear during machining (Rosa *et al.*, 2010).
4. **Higher hardness values:** In general, CGI has higher hardness compared to GCI and therefore, it has lower machinability (Nayyar *et al.*, 2012). The hardness and mechanical strength of CGI are related to its pearlite content, which has a great influence on tool life (Nayyar *et al.*, 2013).
5. **Higher cutting temperature:** Tools experience higher temperatures when machining CGI, which can lead to a higher wear rate (Tooptong, Park and Kwon, 2018).

All the above factors contribute to different tool wear patterns, as summarized in table 1.1. In general, it can be concluded from the literature survey that abrasion and adhesion are the dominant wear modes. Chipping, BUE formation, thermal cracks, and fractures are also observed in some cases. Abrasion in the machining of CGI is mainly caused by the cementite (in pearlite) phase and hard abrasive particles that may be present in the

microstructure (Nayyar *et al.*, 2013; Tooptong, Park and Kwon, 2018). When a lubricant is present, abrasion is the dominant wear mechanism; however, under dry cutting conditions, adhesion and chipping are more significant (Rosa *et al.*, 2010; Nayyar *et al.*, 2013; Su *et al.*, 2016). In fact, the adherent layer in a dry condition can protect the tool from abrasion and therefore reduce flank wear (Tooptong, Park and Kwon, 2018). This protective adherent layer was shown to be ferrite by Nayyar et al. (Nayyar *et al.*, 2013). Adhesion is followed by the formation of a built-up edge at higher cutting speeds (Grenmyr *et al.*, 2011). According to Rosa et al. (Rosa *et al.*, 2010) adhesion and formation of a built-up edge will result in an attrition based wear mechanism: as the sticking material is being removed and redeposited during cutting, when this occurs a part of the tool will be removed with it as well. It is worth mentioning that the machinability of CGI can be affected by its composition and titanium content, nodularity, hardness, and pearlite ratio and thickness (Rosa *et al.*, 2010; Nayyar *et al.*, 2013).

1.1.3.2 Improving Tool Life with Coating

Different approaches have been taken in the past to improve tool life during the machining of CGI. These approaches include but are not limited to minimum quantity lubrication (Varghese and Balaji, 2007; Kuzu, Bijanzad and Bakkal, 2015), optimizing cutting parameters and lubricant (Wang *et al.*, 2017), high pressure coolants (Su *et al.*, 2016), altering the structure and chemical composition of CGI (Rosa *et al.*, 2010), and applying different coatings (Jindal *et al.*, 1999; Tooptong *et al.*, 2016; Wang *et al.*, 2017). Although other methods have shown promising results, there has been no systematic approach to coating design. Instead, the literature focuses on tool life comparisons of

different commercially available coatings. Table 1.1 summarizes the literature that covers coatings studied for the machining of CGI in recent years.

Table 1.1. *Coatings and their associated wear patterns studied in literature from 2008 to 2020 for turning of CGI.*

Author	Process Parameters	Tool Material/Coating
	Best Tool/Coating ★ Flank wear ● Crater wear ● Adhesion ● Chipping ● Thermal cracks ■ BUE formation ■ Fracture ■	
(Tooptong, Park and Kwon, 2018)	DoC: 2 mm Feed: 2mm/rev Speed: 200-350 m/min	WC-Co/Uncoated ●● WC-Co/Ti (C, N)/Al_2O_3 ●●●
(Wang *et al.*, 2017)	DoC: 0.9 mm Feed: 0.15 mm/rev Speed: 70 m/min Wet (varied)	WC-Co/Ti (C, N)/Al_2O_3 ★●●■ WC-Co/Al_2O_3/TiC ●● WC-Co/TiAlN/TiN ●● WC-Co/TiAlSiN ●●
(Su *et al.*, 2016)	DoC: 1 mm Feed: 0.1 mm/rev Speed: 100-300 m/min High-pressure coolant	WC-Co/Ti (C, N)/Al_2O_3 ●●●●■
(Nayyar *et al.*, 2013)	DoC: 1.5 mm Feed: 0.2 mm/rev Speed: 300 m/min Wet and dry*	WC-Co/Ti (C, N)/Al_2O_3/TiC ●●■*
(Grenmyr *et al.*, 2011)	DoC: 1.5 mm Feed: 0.3 mm/rev Speed: 200-400 m/min Wet	WC-Co/Ti (C, N)/Al_2O_3/TiC ●●■
(Rosa *et al.*, 2010)	DoC: 1 mm Feed: 0.15 mm/rev Speed: 160, 250 m/min Dry	WC-Co/TiN/Al_2O_3/TiCN ●●
(J.V.C. *et al.*, 2008)	DoC: 0.2 mm Feed: 0.5 mm/rev Speed: 160, 180, 200 m/min Dry	Si_3N_4/TiN ●●●

1.1.4. PVD Tool Coating

Physical vapor deposition is a process for depositing coatings by condensing atoms onto a substrate from a gaseous or plasma phase. The vapor might come from a solid or even liquid source. In this manner, elements, alloys and even compounds (with reactive deposition) can be deposited on substrate materials with thicknesses ranging from a few

nanometers up to several microns. Based on the fundamentals of evaporation and their source, PVD can be divided into four different techniques: vacuum evaporation, sputter deposition or sputtering, arc vapor deposition, and ion plating (Mattox, 2010).

Besides composition, coating properties can be adjusted using deposition parameters such as bias voltage, reactive gas pressure, substrate temperature, and table rotation speed. In this way, the hardness, elastic modulus, adhesion, residual stress, microstructure, and defects of a coating can be adjusted to attain desirable properties (M. Ahlgren and Blomqvist, 2005; Tillmann *et al.*, 2013; Warcholinski and Gilewicz, 2013; Elmkhah *et al.*, 2016; Cai *et al.*, 2017; Skordaris *et al.*, 2018).

In addition to the aforementioned parameters, coating properties can also be influenced by architecture. Monolayer and multilayer coatings are extensively deposited in machining applications, and each may be superior in a specific condition. While multilayer coatings are generally superior since they can prevent crack propagation, monolayer coatings show better results in some cases of wet milling due to their thermal shock resistance (Bobzin, 2016). An increased number of layers (with a similar coating thickness) results in better fracture and wear resistance due to a greater probability of crack deflection and higher hardness (Hall-Petch effect) (Stueber *et al.*, 2009; Skordaris *et al.*, 2014).

1.1.4.1 Thick PVD Coating

One of the main limitations of PVD compared to other deposition techniques is that the thickness of the coating is usually limited to 5µm. Increasing the thickness to over 5µm with conventional methods results in delamination and coating failure due to high values of residual stress (Tuffy, Byrne and Dowling, 2004). Although compressive residual stress

can increase the hardness (M. Ahlgren and Blomqvist, 2005), reduce abrasive wear and depth-of-cut notch formation (Jindal *et al.*, 1999), and increase fracture toughness by slowing crack propagation (PalDey and Deevi, 2003), high values of compressive residual stress can decrease tool life (Breidenstein and Denkena, 2013), adhesion, and, in the worst case, cause coating failure through fracture, spalling, and buckling (Teixeira, 2002; Tuffy, Byrne and Dowling, 2004; Sargade *et al.*, 2011). Thus, the key to achieving a higher coating thickness using PVD techniques is to control the excess residual stress during the coating growth.

Limited successful (Bouzakis *et al.*, 2003, 2004; Bemporad *et al.*, 2006; Skordaris *et al.*, 2016) and failed attempts (Tuffy, Byrne and Dowling, 2004; Sargade *et al.*, 2011) were made to increase the thickness of TiN or TiAlN coatings for machining purposes. A summary of studies in this area is presented in table 1.2. The most promising techniques for achieving a higher thickness mentioned in the literature, are as follows:

- Releasing the excess residual stress during deposition by using a low deposition rate for the TiAlN coating (1µm per hour) and, therefore, annealing the coating (Skordaris *et al.*, 2016).
- Using a Ti interlayer for a TiN coating to relieve the excess residual stress during layer by layer deposition (Bemporad *et al.*, 2006).

Although these methods proved to be effective at controlling residual stress, they are time-consuming and thus difficult to use for industrial scale production.

Table 1.2. *Summary of research on thick coatings.*

Author	Coating Material	Process Studied	Valuable Findings
(Vereschaka *et al.*, 2019)	Ti-TiN-(TiAlSi)N on W-Carbide (max 15µm)	Turning of AISI 321 steel	By increasing thickness, tool life was reduced. Optimum tool life was achieved with a thickness of 6-8µm.
(Vereschaka *et al.*, 2018)	Ti-TiN-(TiCrAl)N and Zr-ZrN-(ZrCrNbAl)N on W-Carbide (max 7µm)	Turning of C45 steel	Tool life is more sensitive to cutting speed when the thickness is increased. Thick coatings perform better at lower cutting speeds.
(Skordaris *et al.*, 2016)	Ti46Al54N on W-Carbide (max 8µm)	Milling of 42CrMo4 QT	Low deposition rate (1µm/h), stress, and temperature distribution were modeled for the thin and thick coating.
(Skordaris *et al.*, 2014)	Ti46Al54N on W-Carbide (max 8µm)	Milling of 42CrMo4 QT	The hardness, fatigue resistance, and tool life of the coating increased along with the number of layers due to greater resistance to crack propagation.
(Sargade *et al.*, 2011)	TiN on W-Carbide (max 6.8µm)	Turning of C40 steel	Low adhesion of the thick coating (6.8µm) was found through a scratch test, and spallation of the coating occurred during turning. Optimum thickness is reported to be 4µm.
(Mubarak, Akhter *et al.*, 2008)	TiN on HSS and D2 (max 8.7µm)	Pin on Disc and scratch test	The surface roughness and compressive residual stress of the coating increases along with its thickness.
(Tuffy, Byrne and Dowling, 2004)	TiN on W-Carbide (max 7.5µm)	Turning of SS304	High residual stress in thick coatings will cause chipping and cracking on the tool tip. Therefore, there is an optimum thickness, reported to be 3.5µm.
(Bouzakis *et al.*, 2003)	$Ti_{46}Al_{54}N$ on Carbide (max 10µm)	Milling of 42CrMo4V	The mechanical properties of the coating decrease as thickness increases, due to a coarser microstructure. 10 µm has the best tool life due to less stress concentration on the coating.
(Klocke *et al.*, 1998)	TiAlN on Cermet (max 8.8µm)	Turning of 42CrMo4V	Thick coatings have high abrasive resistance since the substrate exposure is delayed when subjected to wear.
(Posti and Nieminen, 1989)	TiN on HSS (max 10µm)	Planing, Hobbing & Turning of 42CrMo4V	Coating detachment occurs as thickness is increased. There is an optimum thickness for each application.
(Tönshoff and Mohlfeld, 1997)	$Ti_{60}Al_{40}N$ on carbide (max 6µm)	Drilling of AISI 1045	High adhesion, abrasion resistance, and tool life of thick coatings were monitored. No chipping or flaking was observed.

In the literature, thick PVD coatings are shown to be beneficial for tool life improvement due to the following reasons (Klocke *et al.*, 1998; Bouzakis *et al.*, 2003, 2004; Bemporad *et al.*, 2006; Skordaris *et al.*, 2016; Vereschaka *et al.*, 2018):

- **Delaying substrate exposure:** As the coating thickness increases, a greater volume of material is subject to wear until the substrate becomes exposed. Thus, the tool has a higher abrasive resistance.
- **Lower stress concentration on the coating:** When the coating thickness increases, edge roundness increases which results in a lower stress concentration on the coating and, therefore, longer tool life.
- **Better thermal and stress barrier:** With higher coating thicknesses, the substrate is under lower thermal and mechanical stress and, therefore, is protected more efficiently.

A technology called superfine cathode (SFC) was used in this work to deposit thick PVD coatings. This technology was developed by Kobelco to address the challenges associated with residual stress in thick coatings. Using this technology, the residual stress can be controlled in a wide range by deposition parameters.

1.1.4.2 Measurement of Residual Stress in PVD Coatings

Residual stress in PVD coatings is commonly determined using X-Ray diffraction (Perry, Sue and Martin, 1996). This method relies on measuring the interplanar distance in a particular crystallographic plane using constructive scattering of x-ray (Bragg's law). Here, the diffraction peaks shift toward higher or lower angles in the presence of stress. This change in angle is then used to measure the stress value based on different techniques

such as the commonly used $sin^2\psi$ method. It should be mention that a plane stress assumption toward the measurement of residual stress is generally used since the thickness of the coating is insignificant in comparison to the surface area. The equation below can be used as the core of $sin^2\psi$ method for residual stress measurement:

$$\sigma_\varphi = \left[\frac{E}{1+v}\right]\frac{1}{d_0}\left(\frac{\delta d_{\varphi\psi}}{\delta sin^2\psi}\right)$$

Where φ and ψ are rotation angles in sample coordinate, d is d-spacing, E is elastic modulus, v is the Poisson's ratio and σ is stress. It is worth also mentioning that d-spacing at $\psi = 0$ is commonly used as d_0 since the error of this assumption is insignificant. Other techniques such as single and two angle technique can also be used for stress measurement using XRD (Cullity, 1956).

Other methods such as 2-dimensional XRD are more complex in nature; however, can provide more information by capturing part of the diffraction ring. In this method the deformation of the Debye–Scherrer ring is mainly used to determine residual stress with the same principals as conventional XRD; however it involves 2D diffraction pattern processing and manipulation. The benefit of this method is collection of more data points with less time (He, 2003).

1.2. Research Gaps

Prior studies provide limited information on using PVD coating as a method to address issues with the machining of CGI. The data provided simply compares different commercial coatings with no systematic coating or tool design approach. Moreover, the

implementation of thick PVD coatings and their advantages in machining have not been fully explored. As such, research gaps in the literature can be summarized as follows:

- Although some work has been done in this area, the manufacturing industry still faces problems with the machinability of CGI. The main problems are identified as rapid wear due to adhesion and abrasion.
- No systematic approach to coating design based on addressing the dominant wear mechanisms has been found in the literature for the machining of CGI. Researchers have only provided data comparing different industrial coatings.
- The literature mentions that controlling the residual stress is important to achieve a thick coating; otherwise, the coating will detach from the surface. However, the relationship between thickness, residual stress, and adhesion of the coating still has not been established.
- Although several attempts were made to control residual stress and achieve thick coatings, these methods are not practical in industry.
- The potential of thick coatings in comparison to state-of-the-art available commercial coatings is not explored.
- None of the previous studies on thick coatings address how coating thickness impacts tool geometry.

1.3. Motivation and Research Objectives

Increasing productivity and product quality and reducing manufacturing costs are the main factors driving research on tool life improvement. The aim of this study is to gain a

better understanding of the advantages of thick PVD coating while working to enhance the efficiency of CGI machining. This goal requires in-depth knowledge of the wear mechanisms involved and factors affecting coating performance. The current research tries to tackle this objective with a scientific approach and design a thick TiAlN coating system. Based on the above-mentioned motivation and gaps in the literature, the main objectives of this research are defined as follows:

1. Establish the effect of coating thickness, using SFC technology, on coating properties, its impact on coating adhesion under machining loads, and cutting performance when machining CGI.
2. Determine the changes in coating residual stress and other properties by the variation of deposition parameters and its impact on tool performance.
3. Compare the performance of different monolayer and multilayer coating designs with regards to residual stress to inhibit the dominant wear mechanism.
4. Characterize the effect of edge preparation by wet blasting before coating deposition on the tool microgeometry, substrate properties, and cutting performance.

1.4. Thesis Outline

This research is divided into four major studies, each addressing one or multiple research objectives. The following chapters contain the journal articles published or submitted regarding each study. Moreover, the final chapter provides an overall conclusion on all the studies conducted. A summary of each chapter is as follows:

Chapter 1 provides a general background and literature survey on thick coatings and machining CGI. In this chapter, gaps in the literature are identified and research objectives are defined based on the motivations and literature.

Chapter 2 presents the effect of coating thickness variation on coating properties, wear characteristics, and workpiece surface integrity. In this chapter, the main factors affecting the performance of thick TiAlN coatings are identified for further investigation. This chapter addresses the first objective of this research and contains the following publication: *Abdoos, M., Yamamoto, K., Bose, B., Fox-Rabinovich, G., & Veldhuis, S. (2019). Effect of coating thickness on the tool wear performance of low stress TiAlN PVD coating during turning of compacted graphite iron (CGI). Wear, 422, 128-136.*

Chapter 3 studies the effect of bias voltage and nitrogen pressure on residual stress and other coating properties such as hardness, texture, surface roughness, and density of defects. The purpose of this study is to determine a way to adjust residual stress while maintaining other coating properties within an acceptable range. This chapter covers the second and third objectives of this research and resulted in the following publication: *Abdoos, M., Rawal, S., Arif, A. F. M., & Veldhuis, S. C. (2020). A strategy to improve tool life by controlling cohesive failure in thick TiAlN coating during turning of CGI. The International Journal of Advanced Manufacturing Technology, 106(7-8), 2793-2803.*

Chapter 4 explores different coating designs based on substrate bias voltage and altering residual stress to further improve coating performance and gain a better

understanding of the role of residual stress. This study mainly focuses on different wear mechanisms associated with residual stress. In this chapter, the second and third research objectives were addressed, and the following manuscript was published: *Abdoos, M., Bose, B., Rawal, S., Arif, A. F. M., & Veldhuis, S. C. (2020). The influence of residual stress on the properties and performance of thick TiAlN multilayer coating during dry turning of compacted graphite iron. Wear, 203342.*

Chapter 5 explores wet blasting as a method to adjust tool microgeometry before coating deposition. In this chapter, the effect of edge radius on coating quality and machining performance is studied which covers the fourth objective of this research. The following manuscript was submitted to The International Journal of Advanced Manufacturing Technology: *Abdoos, M., Graf, H., Rawal, S., Arif, A. F. M., & Veldhuis, S. C. The effect of wet blasting as a pre-deposition treatment for thick TiAlN PVD coating.*

Chapter 6 contains a summary of observations and general conclusions from the previous chapters as well as suggestions for future research directions.

1.5. Note to Reader

The reader should note that the contents of chapter 2 through chapter 5 are mainly journal publications. Although each chapter focuses on individual research objectives, similarities may be present, especially in the introduction and experimental detail sections. However, the reader is highly encouraged to go through the contents of each chapter as the aforementioned sections contain valuable information regarding each study.

1.6. References

Abele, E., Sahm, A. and Schulz, H. (2002) 'Wear Mechanism when Machining Compacted Graphite Iron', CIRP Annals - Manufacturing Technology, 51(1), pp. 53–56. doi: 10.1016/S0007-8506(07)61464-4.

Ahlgren, M. and Blomqvist, H. (2005) 'Influence of bias variation on residual stress and texture in TiAlN PVD coatings', Surface and Coatings Technology, 200(1-4 SPEC. ISS.), pp. 157–160. doi: 10.1016/j.surfcoat.2005.02.078.

Bemporad, E. et al. (2006) 'High thickness Ti/TiN multilayer thin coatings for wear resistant applications', Surface and Coatings Technology, 201(6), pp. 2155–2165. doi: 10.1016/j.surfcoat.2006.03.042.

Bobzin, K. (2016) 'High-performance coatings for cutting tools', CIRP Journal of Manufacturing Science and Technology. doi: 10.1016/j.cirpj.2016.11.004.

Bouzakis, K. D. et al. (2003) 'The influence of the coating thickness on its strength properties and on the milling performance of PVD coated inserts.', Surface and Coatings Technology, 174(175), pp. 393–401. doi: 10.1016/j.surfcoat.2003.08.003.

Bouzakis, K. D. et al. (2004) 'The effect of coating thickness, mechanical strength and hardness properties on the milling performance of PVD coated cemented carbides inserts', Surface and Coatings Technology, 177–178(178), pp. 657–664. doi: 10.1016/j.surfcoat.2003.08.003.

Bouzakis, K. D. et al. (2012) ‘Cutting with coated tools: Coating technologies, characterization methods and performance optimization’, CIRP Annals - Manufacturing Technology, 61(2), pp. 703–723. doi: 10.1016/j.cirp.2012.05.006.

Breidenstein, B. and Denkena, B. (2013) ‘Significance of residual stress in PVD-coated carbide cutting tools’, CIRP Annals - Manufacturing Technology, 62(1), pp. 67–70. doi: 10.1016/j.cirp.2013.03.101.

Cai, F. et al. (2017) ‘Influence of negative bias voltage on microstructure and property of Al-Ti-N films deposited by multi-arc ion plating’, Ceramics International, 43(4), pp. 3774–3783. doi: 10.1016/j.ceramint.2016.12.019.

Dawson, S., & Schroeder, T. (2000). Compacted graphite iron: a viable alternative. Engineering Casting Solutions AFS.

Dawson, S. and Schroeder, T. (2004) ‘Practical applications for compacted graphite iron’, AFS Transactions, 47(05), pp. 1–9.

Dawson, S., Hollinger, I., Robbins, M., Daeth, J., Reuter, U., & Schulz, H. (2001). The Effect of Metallurgical Variables on the Machinability of Compacted Graphite Iron. SAE Transactions, 110, 334-352.

Dolinšek, S. and Kopač, J. (2006) ‘Mechanism and types of tool wear; particularities in advanced cutting materials’, Journal of Achievements in Materials, 19(1), pp. 11–18.

Elmkhah, H. et al. (2016) ‘Surface characteristics for the Ti-Al-N coatings deposited by high power impulse magnetron sputtering technique at the different bias voltages’, Journal of Alloys and Compounds, 688, pp. 820–827. doi: 10.1016/j.jallcom.2016.07.013.

Gastel, M. et al. (2000) ‘Investigation of the wear mechanism of cubic boron nitride tools used for the machining of compacted graphite iron and grey cast iron’, International Journal of Refractory Metals and Hard Materials, 18(6), pp. 287–296. doi: 10.1016/S0263-4368(00)00032-9.

Grenmyr, G. et al. (2011) ‘Investigation of tool wear mechanisms in CGI machining’, International Journal of Mechatronics and Manufacturing Systems, 4(1), p. 3. doi: 10.1504/IJMMS.2011.037996.

Guesser, W., Schroeder, T. and Dawson, S. (2001) ‘Production experience with compacted graphite iron automotive components’, AFS Transactions, 109.

Heck, M. et al. (2008) ‘Analytical investigations concerning the wear behaviour of cutting tools used for the machining of compacted graphite iron and grey cast iron’, International Journal of Refractory Metals and Hard Materials, 26(3), pp. 197–206. doi: 10.1016/j.ijrmhm.2007.05.003.

J.V.C., S. et al. (2008) ‘Turning of compacted graphite iron using commercial tiN coated Si 3N4 under dry machining conditions’, 6th International Latin American Conference on Powder Technology, PTECH 2007, pp. 604–609. doi: 10.4028/www.scientific.net/MSF.591-593.604.

Jindal, P. C. et al. (1999) ‘Performance of PVD TiN, TiCN, and TiAlN coated cemented carbide tools in turning’, International Journal of Refractory Metals and Hard Materials, 17(1), pp. 163–170. doi: 10.1016/S0263-4368(99)00008-6.

Klocke, F. et al. (1998) ‘Improved Cutting Processes with Adapted Coating Systems’, CIRP Annals - Manufacturing Technology, 47(1), pp. 65–68. doi: 10.1016/S0007-8506(07)62786-3.

Klocke, F. and Kuchle, A. (2011) ‘Manufacturing Processes 1: Cutting’, in. Springer, Berlin, Heidelberg. doi: 10.1007/978-3-642-11979-8_3.

Kuzu, A. T., Bijanzad, A. and Bakkal, M. (2015) ‘Experimental Investigations of Machinability in the Turning of Compacted Graphite Iron using Minimum Quantity Lubrication’, Machining Science and Technology, 19(4), pp. 559–576. doi: 10.1080/10910344.2015.1085313.

Mattox, D. M. (2010) ‘Handbook of Physical Vapor Deposition (PVD) Processing’, in Handbook of Physical Vapor Deposition (PVD) Processing. William Andrew. doi: 10.1016/B978-0-8155-2037-5.00025-3.

Mubarak, Akhter, P. et al. (2008) ‘Effect of coating thickness on the properties of TiN coatings deposited on tool steels using cathodic arc PVD technique’, Surface Review and Letters, 15(August 2008), pp. 401–410. doi: 10.1142/S0218625X08011524.

Nayyar, V. et al. (2012) ‘An experimental investigation of machinability of graphitic cast iron grades; Flake, compacted and spheroidal graphite iron in continuous machining operations’, in Procedia CIRP, pp. 488–493. doi: 10.1016/j.procir.2012.04.087.

Nayyar, V. et al. (2013) ‘Machinability of compacted graphite iron (CGI) and flake graphite iron (FGI) with coated carbide’, International Journal of Machining and Machinability of Materials, 13(1), p. 67. doi: 10.1504/IJMMM.2013.051909.

PalDey, S. and Deevi, S. (2003) ‘Single layer and multilayer wear resistant coatings of (Ti, Al) N: a review’, Materials Science and Engineering: A, 342, pp. 58–79. doi: 10.1016/S0921-5093(03)00473-8.

Posti, E. and Nieminen, I. (1989) ‘Coating Thickness Effects on the Life of Titanium Nitride PVD Coated Tools’, Materials and Manufacturing Processes, 4(2), pp. 239–252. doi: 10.1080/10426918908956287.

Prengel, H. G. et al. (2001) ‘A new class of high performance PVD coatings for carbide cutting tools’, Surface and Coatings Technology, 139(1), pp. 25–34. doi: 10.1016/S0257-8972(00)01080-X.

Rosa, S. do N. et al. (2010) ‘Analysis of Tool Wear, Surface Roughness and Cutting Power in the Turning Process of Compact Graphite Irons with Different Titanium Content’, Journal of the Brazilian Society of Mechanical Sciences and Engineering, 32(3), pp. 234–240. doi: 10.1590/S1678-58782010000300006.

Sahm, A., Abele, E. and Schulz, H. (2002) ‘Machining of compacted graphite iron (CGI)’, Materialwissenschaft und Werkstofftechnik. WILEY-VCH Verlag, 33(9), pp. 501–506. doi: 10.1002/1521-4052(200209)33:9<501::AID-MAWE501>3.0.CO;2-W.

Sargade, V. G. et al. (2011) ‘Effect of coating thickness on the characteristics and dry machining performance of Tin film deposited on cemented carbide inserts using cfubms’, Materials and Manufacturing Processes, 26(8), pp. 1028–1033. doi: 10.1080/10426914.2010.526978.

Skordaris, G. et al. (2014) ‘Brittleness and fatigue effect of mono- and multi-layer PVD films on the cutting performance of coated cemented carbide inserts’, CIRP Annals - Manufacturing Technology, 63(1), pp. 93–96. doi: 10.1016/j.cirp.2014.03.081.

Skordaris, G. et al. (2016) ‘Film thickness effect on mechanical properties and milling performance of nano-structured multilayer PVD coated tools’, Surface and Coatings Technology, 307, pp. 452–460. doi: 10.1016/j.surfcoat.2016.09.026.

Skordaris, G. et al. (2018) ‘Bias voltage effect on the mechanical properties, adhesion and milling performance of PVD films on cemented carbide inserts’, Wear, 404–405, pp. 50–61. doi: 10.1016/j.wear.2018.03.001.

Stueber, M. et al. (2009) ‘Concepts for the design of advanced nanoscale PVD multilayer protective thin films’, Journal of Alloys and Compounds, 483(1–2), pp. 321–333. doi: 10.1016/j.jallcom.2008.08.133.

Su, G. S. et al. (2016) ‘Effects of high-pressure cutting fluid with different jetting paths on tool wear in cutting compacted graphite iron’, Tribology International, 103, pp. 289–297. doi: 10.1016/j.triboint.2016.06.029.

Teixeira, V. (2002) ‘Residual stress and cracking in thin PVD coatings’, Vacuum, 64(3–4), pp. 393–399. doi: 10.1016/S0042-207X(01)00327-X.

Tillmann, W. et al. (2013) ‘Influence of bias voltage on residual stresses and tribological properties of TiAlVN-coatings at elevated temperatures’, Surface and Coatings Technology, 231, pp. 122–125. doi: 10.1016/j.surfcoat.2012.03.012.

Tönshoff, H. K. and Mohlfeld, A. (1997) 'PVD-coatings for wear protection in dry cutting operations', Surface and Coatings Technology, 93(1), pp. 88–92. doi: 10.1016/S0257-8972(97)00027-3.

Tooptong, S. et al. (2016) 'A Preliminary Machinability Study of Flake and Compacted Graphite Irons with Multilayer Coated and Uncoated Carbide Inserts', Procedia Manufacturing, 5, pp. 644–657. doi: 10.1016/j.promfg.2016.08.053.

Tooptong, S., Park, K. H. and Kwon, P. (2018) 'A comparative investigation on flank wear when turning three cast irons', Tribology International. Elsevier Ltd, 120(December 2017), pp. 127–139. doi: 10.1016/j.triboint.2017.12.025.

Tuffy, K., Byrne, G. and Dowling, D. (2004) 'Determination of the optimum TiN coating thickness on WC inserts for machining carbon steels', Journal of Materials Processing Technology, 155–156(1–3), pp. 1861–1866. doi: 10.1016/j.jmatprotec.2004.04.277.

Varghese, K. P. and Balaji, A. K. (2007) 'Effects of tool material, tool topography and minimal quantity lubrication (MQL) on machining performance of compacted graphite iron (CGI)', International Journal of Cast Metals Research, 20(6), pp. 347–358. doi: 10.1179/136404608X320698.

Vereschaka, A. et al. (2018) 'Influence of Thickness of Multilayered Nano-Structured Coatings Ti-TiN-(TiCrAl)N and Zr-ZrN-(ZrCrNbAl)N on Tool Life of Metal Cutting Tools at Various Cutting Speeds', Coatings, 8(2), p. 44. doi: 10.3390/coatings8010044.

Vereschaka, A. et al. (2019) ‘Influence of the thickness of multilayer composite nano-structured coating Ti-TiN-(Ti,Al,Si)N on the tool life of metal-cutting tools and the nature of wear’, Coatings, 9(11). doi: 10.3390/coatings9110730.

Wang, C. et al. (2017) ‘Effect of different oil-on-water cooling conditions on tool wear in turning of compacted graphite cast iron’, Journal of Cleaner Production, 148, pp. 477–489. doi: 10.1016/j.jclepro.2017.02.014.

Warcholinski, B. and Gilewicz, A. (2013) ‘Effect of substrate bias voltage on the properties of CrCN and CrN coatings deposited by cathodic arc evaporation’, in Vacuum, pp. 145–150. doi: 10.1016/j.vacuum.2012.04.039.

Perry, A. J., Sue, J. A., & Martin, P. J. (1996). Practical measurement of the residual stress in coatings. Surface and coatings Technology, 81(1), 17-28. doi: 10.1016/0257-8972(95)02531-6.

Cullity, Bernard Dennis. Elements of X-ray Diffraction. Addison-Wesley Publishing, 1956.

He, B. B. (2003) ‘Introduction to two-dimensional X-ray diffraction’, Powder Diffraction, 18(02), pp. 71–85. doi: 10.1154/1.1577355.

Chapter 2. Effect of Coating Thickness

Abdoos, M., Yamamoto, K., Bose, B., Fox-Rabinovich, G., & Veldhuis, S. (2019). Effect of coating thickness on the tool wear performance of low stress TiAlN PVD coating during turning of compacted graphite iron (CGI). Wear, 422, 128-136.

Author's Contribution

Majid Abdoos	Designed and conducted the experiments Analyzed the results Wrote the manuscript
Kenji Yamamoto	Assisted with coating deposition and TEM
Bipasha Bose	Assisted with coating characterization
German Fox-Rabinovich	Assisted with experimental design Assisted with analyzing the data Assisted writing and editing the manuscript
Stephen Veldhuis	Supervised the project Edited the manuscript

Abstract

Compacted graphite iron (CGI), with its superior mechanical properties, is a promising candidate to replace grey cast iron in the automotive industry. However, the low machinability of CGI compared to grey cast iron, has made this transition difficult. Built up edge formation, combined with abrasive and adhesive wear is the main problem of CGI turning at moderate cutting speeds. In this study, a low compressive residual stress PVD coating was developed using newly introduced super fine cathode (SFC) technology. The main advantage of low compressive residual stress SFC coating, is the possibility of increasing its thickness compared to the commercial range of arc coatings (usually with a thickness within 1-5 µm) without any process induced spallation of the coating layer. Therefore, three different low compressive residual stress $Ti_{40}Al_{60}N$ coatings with thicknesses of around 5, 11 and 17 µm were deposited. The coatings were characterized by X-Ray diffraction, scratch test, ball crater test and nanoindentation. Furthermore, the cutting performance of the coated inserts was investigated in finish turning of CGI. An improvement of around 35% tool life is achieved for the cutting tool with the low residual stress thick coating compared to the commercial benchmark. Progression of flank wear was studied by means of TEM, SEM-EDS, optical microscopy and 3D wear measurement. Chip undersurface morphology as well as cross-sectional studies of the chip structure were performed. This was combined with analysis of the workpiece surface. Evaluation of the results obtained would help to achieve a better understanding of the wear mechanism and buildup edge formation of the studied coatings. According to the recorded data, coating thickness significantly affects cutting tool wear behavior and the mechanical properties of the coatings. A certain thickness range, specifically within 10 µm was found to be optimum.

Keywords

PVD coatings; compacted graphite iron; cutting tools; residual stress; built-up edge formation; adhesion wear

2.1. Introduction

Compacted graphite iron or CGI is from the cast iron family with its mechanical properties falling between grey cast iron and ductile cast iron. Graphite in CGI is randomly oriented similar to grey cast iron; however, it is thicker in size and has round edges with a unique structure. Unlike ductile cast iron and grey cast iron, CGI has a coral like structure with a bumpy surface that provides strong adhesion between the iron matrix and graphite. Therefore, the superior mechanical properties of CGI make it a potential replacement for grey cast iron in the automotive industry (Dawson and Schroeder, 2000, 2004). However, CGI has a lower machinability than grey cast iron since tool life variability complicates the transition (Sahm, Abele and Schulz, 2002).

It is known that poor machinability of CGI compared to grey cast iron comes from its superior mechanical properties (Nayyar *et al.*, 2012) and difference in composition (Abele, Sahm and Schulz, 2002). During machining of grey cast iron, a dense MnS layer forms on the tool, which acts as a lubricant and protects the tool from wear. As the compacted graphite structure is only stable at a low oxygen and sulfur content, no protective layer forms on the tool during machining of CGI, resulting in higher tool wear (Gastel *et al.*, 2000; Heck *et al.*, 2008). Lack of lubricating graphite due to its coral-like structure (Nayyar *et al.*, 2013), presence of hard abrasive compounds (Rosa *et al.*, 2010) and higher temperature generated during machining (Tooptong, Park and Kwon, 2018), further decreases the CGI tool life. All of these factors result in dominant adhesive and abrasive wear of the tool during CGI machining. Diffusion and oxidation wear are also reported in some cases, but their effect on tool life less significant (Da Silva *et al.*, 2011; Malakizadi

et al., 2018). Abrasive wear during machining of CGI is mostly caused by abrasive particles such as titanium or vanadium carbo-nitrides and can be reduced by controlling the chemical composition (Rosa *et al.*, 2010; Malakizadi *et al.*, 2018). On the other hand, adhesive wear followed by micro chipping, built-up edge and layer formation is more dominant at a higher cutting speed and cutting temperature (Da Silva *et al.*, 2011). Lubricating and cooling the cutting zone to achieve a lower temperature, leads to moderate success in reducing the adhesion of CGI (Su *et al.*, 2016; Wang *et al.*, 2017). Recently, Tooptong et al. (Tooptong *et al.*, 2016) explored different coatings to improve the machinability of CGI. It was reported that adhesion can be reduced via proper coating design. However, there exists no in-depth study to substantiate this claim.

PVD coatings are currently being successfully deposited on cutting tools in the thickness of 1-5µm. To improve tool life, several attempts have been made to increase the thickness beyond 5µm (Bouzakis *et al.*, 2003, 2004; Skordaris *et al.*, 2016; Yamamoto *et al.*, 2018). However, due to limitations of the deposition process provoking high residual stress distribution and strain energy, high thickness coatings are apt to early failure (Tuffy, Byrne and Dowling, 2004). Tuffy et al (Tuffy, Byrne and Dowling, 2004) observed that as the thickness of the TiN coating increases beyond 3.5 µm, tool life diminishes due to chipping and cracking at the tool tip caused by high compressive residual stress. Sargade et al (Sargade *et al.*, 2011) observed similar results for 6.7 µm thick TiN coating and reported early failure due to coating spallation. In another study, Klocke et al (Klocke *et al.*, 1998) was able to prolong the tool life during turning by increasing the thickness of the TiAlN coating to 8 µm. As the coating thickness increases, a greater volume of material is

available to wear out until substrate exposure. Bouzakis et. al (Bouzakis *et al.*, 2003, 2004) studied the effect of thickness (2-10 µm) on the mechanical properties and wear resistance of the $Ti_{46}Al_{54}N$ coating. Although an increase in thickness had a negative effect on the mechanical properties of the coating, the tool life was seen to improve in the milling application. In agreement with this study, Skordaris et al (Skordaris *et al.*, 2016) achieved an improvement in tool life by increasing the thickness of the $Ti_{46}Al_{54}N$ PVD coating to 8µm. The excess residual stress is released through a low deposition rate (1µm per hour) and therefore the coating was annealed during the deposition. The reported increase in the tool life has two causes: first, the substrate is protected for a longer duration as the thickness increases. Second, as the coating becomes thicker, edge roundness also increases, which reduces stress concentration on the coating.

Previous studies show that thick PVD coatings provide superior thermal and stress protection to the tool and increase its life by delaying substrate exposure (Skordaris *et al.*, 2016), thus improving resistance to abrasion and adhesion during the machining of CGI. This paper investigates the effect of coating thickness on edge geometry, mechanical properties of the film, adhesion, tool wear and surface integrity. In this context, 5-20 µm thick multi-layered TiAlN coatings were deposited under a low residual stress state using super fine cathode (SFC) technology and their performance was evaluated in finish turning of CGI.

2.2. Experimental Procedure

AlTiN coatings of different thicknesses were produced by a cathodic arc ion plating process using a Kobelco AIP-S20 deposition system. The system uses two SFC (super fine cathode) arc evaporation sources with extended plasma range for the deposition process. SFC is a new technology capable of depositing more than 20 µm thick coatings with low compressive residual stress. The features of this technology were detailed elsewhere (Yamamoto *et al.*, 2018). In the current study, coatings of three different thicknesses were deposited on Kennametal ISO CNGG432FS and Sandvik Coromant ISO SPGN120308 polished uncoated inserts using an arc evaporation source produced by powder metallurgy, composed of 40% Ti and 60% Al. Prior to the deposition, substrate inserts were cleaned in acetone with an ultrasonic cleaner, mounted inside the deposition chamber and then heated to 550˚ C. Ar etching was done at 1.3 Pa Ar pressure for 7.5 minutes to increase adhesion and reduce any contamination in the coating. The coatings were produced in a multilayer state using bilayers deposited with bias voltages of -30 V and -70 V, thickness of the coating is varied by adjusting the number of bilayers. The deposition parameters are given in table 2.1.

Table 2.1. *Deposition parameters for SFC deposited coatings.*

Bias voltage	Arc source current	Ar-N_2 atmosphere		Rotational speed
		Temperature	Pressure	
-30V/-70V	150 A	550˚ C	4 Pa	table rotation at 5rpm

For coating characterization, the thickness is measured with a ball crater system of a 25 mm diameter. Residual stress was measured with a 2-dimension X-Ray diffraction (XRD^2) system, Bruker D8 Discover instrument with cobalt radiation and a wavelength of

1.79 Å (K_α). Residual stress was calculated on (220) the crystallographic plane using LEPTOS software, details of the process can be found elsewhere (He, 2003). The micro-mechanical properties of the coating were evaluated on a Micro Materials NanoTest system, and nanoindentation was performed with a load control mode at a load of 100mN. The load was adjusted according to surface roughness of the samples and so that the depth of penetration would be less than 10% of the total thickness to eliminate the substrate effect. A Berkovich diamond indenter was used to perform 40 indents on each coating. To study adhesive and cohesive failure of the coating, scratch test was performed on flat coated inserts with an Anton Paar Revetest scratch tester using a Rockwell C diamond indenter with a 100 µm radius. Scratch parameters are as follows: progressive loading from 0.5 N to 100 N, scratch length of 3 mm and scratching velocity of 7.5 mm/min.

To evaluate performance of the coated tool inserts, a hollow cylindrical shape of the workpiece material (CGI) was used, with an outer diameter of 120 mm, an inner diameter of 80mm and a length of 200 mm. The workpiece consisted of 70% pearlite with 20% nodularity. CGI turning was performed using an OKUMA CNC Crown L1060 lathe CNC machine. CNGG432FC inserts with an AlTiN KC5010 coating supplied by Kennametal were used as a benchmark to compare the coating performance. The cutting test was conducted for the finishing operation under dry condition with a cutting speed of 300 m/min, feed rate of 0.2 mm/rev and 0.25 mm depth of cut. Flank wear was measured after a certain cutting length with a Keyence VHX-5000 microscope. Edge radius and volumetric difference measurement of the tool was done with an Alicona optical microscope equipped with focus variation technology. The same instrument was used for surface roughness

measurement under ISO standards 4287 and 25178. The cutting tests were continued until a maximum flank wear of 300 µm was reached according to ISO 3685 standard. During the cutting process, cutting forces were measured with a 3D component tool holder Kistler dynamometer type 9121. To better understand the wear mechanism, cutting tools were studied at certain cutting lengths using a Vega 3-TESCAN SEM equipped with EDS. FIB (focused ion beam) cross section analysis of the rake face of the tool further investigated the mechanism of wear by transmission electron microscopy (TEM) JEOL FS2200.

2.3. Results and Discussion

To evaluate the machining performance of the coating, basic understanding of its properties is needed. This section characterizes the coating by various methods such as nanoindentation, XRD and the scratch test, followed by an in-depth machining study.

2.3.1. Coating Characterization

Three different thicknesses of TiAlN coating were successfully deposited using the SFC technology. Optical inspection of the coatings showed no delamination or process-induced damage on the coating. Thickness of the coatings was measured on SPGN120308 flat inserts using a ball crater test, fig. 2.1(a) and table 2.2 shows the maximum thickness of about 17 µm. It is worth mentioning that higher deposition rate and lower deposition time comparing to literature (Skordaris *et al.*, 2016) can be achieved with the aforementioned method as shown in table 2.2. Deposition rate decreased with time; however, the change is quite insignificant. Each bilayer deposited with -30/-70 V bias voltage is approximately 400 nm. All of the coatings are in a compressive residual stress state as seen in fig. 2.1(b),

T1-T3 coatings are under low residual stress compared to the benchmark. This was expected from the nature of the SFC technology and low bias voltage implementation during the deposition process. Beside affecting the mechanical properties, the increased thickness has a significant effect on tool geometry of the coated inserts. Mean values of edge roundness from 40 measurements along the cutting edge (fig. 2.1(c)) show a drastic increase in the edge radius as the coating becomes thicker.

Table 2.2. *Coating thickness vs. deposition time.*

Coating	Total deposition time	Number of bilayer	Thickness (μm)
Benchmark (KC5010)	NA	NA	4.64 ± 0.46
T1	42 min	14	5.38 ± 0.49
T2	84 min	28	11.41 ± 0.48
T3	144 min	42	17.15 ± 0.58

Fig. 2.2(a) and (b) depicts hardness and elastic modulus of SFC deposited (T1-T3) and benchmark coatings measured by nanoindentation. Increase in the thickness has a minor effect on hardness and elastic modulus values of the coatings and mechanical strength of the coating does not decrease as was previously reported (Bouzakis *et al.*, 2004). This decrease in hardness and mechanical strength is mentioned to be due to grain growth corresponding to columnar microstructure and is not observed here due to the multilayer state of the coating. It is also worth mentioning that the coatings deposited by SFC have a higher hardness compared to the commercial coating.

To study cohesive (through the coating) and adhesive (coating/substrate interface) behavior of the coatings, two critical loads were measured during the scratch test: Lc_1, the critical load at which continuous cracking begins and Lc_2, the critical load at which the substrate is exposed. Fig. 2.2(c) and 2.2(d) show that as coating thickness increases, Lc_1

and Lc_2 values shift towards higher loads. Consequently, the failure mode spreads further away from the scratch track until total delamination and substrate exposure of the T3 coating (fig. 2.3).

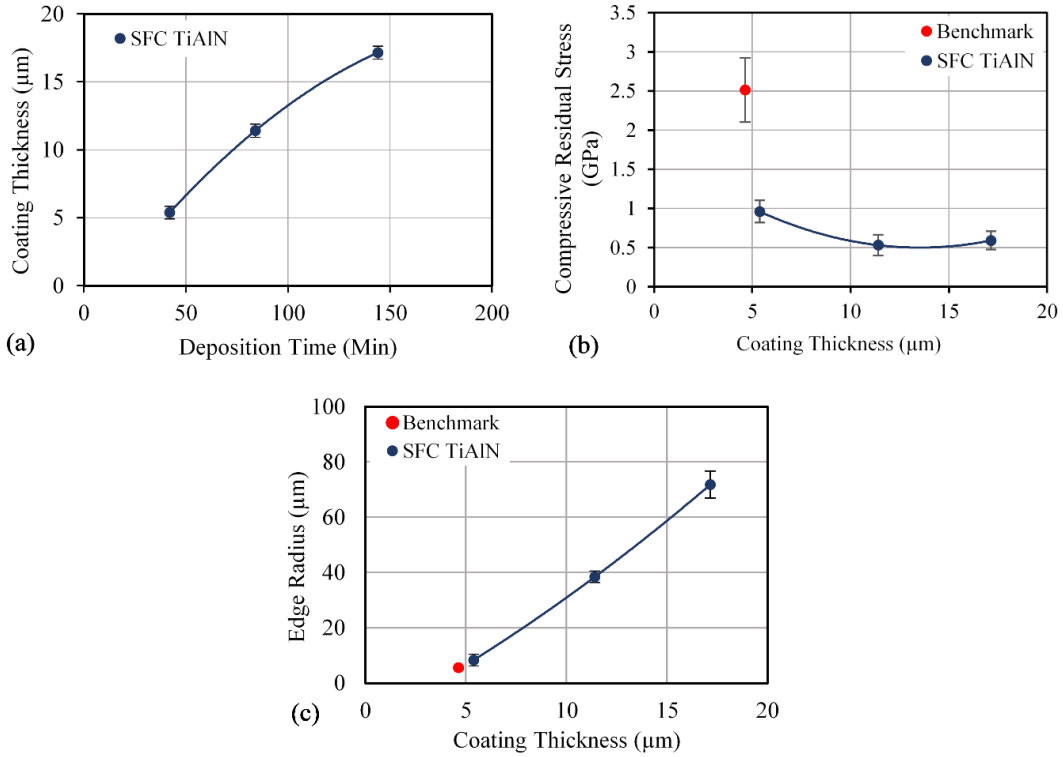

Figure 2.1. *Effect of deposition time on coating thickness (a), residual stress (b) and edge radius (c) vs. thickness.*

The effect of increasing thickness on greater critical loads and failure damage has been observed by many researchers (Heinke *et al.*, 1995; Nie *et al.*, 1999) and is believed to be due to the greater normal load required to be present on the surface to induce the same amount of shear stress in the interface (Sarin, 1993). Therefore, the variation of Lc_2 in T1-T3 is believed to be due to the difference in thickness and thus does not reliably indicate adhesion to the substrate for different coatings. However, Lc_1 can be used as a simple estimation of crack resistance (Zhang *et al.*, 2005). Comparing the different coatings in this

way, it can be concluded that SFC deposited coatings with lower compressive residual stress values are more prone to cracking and cohesive failure.

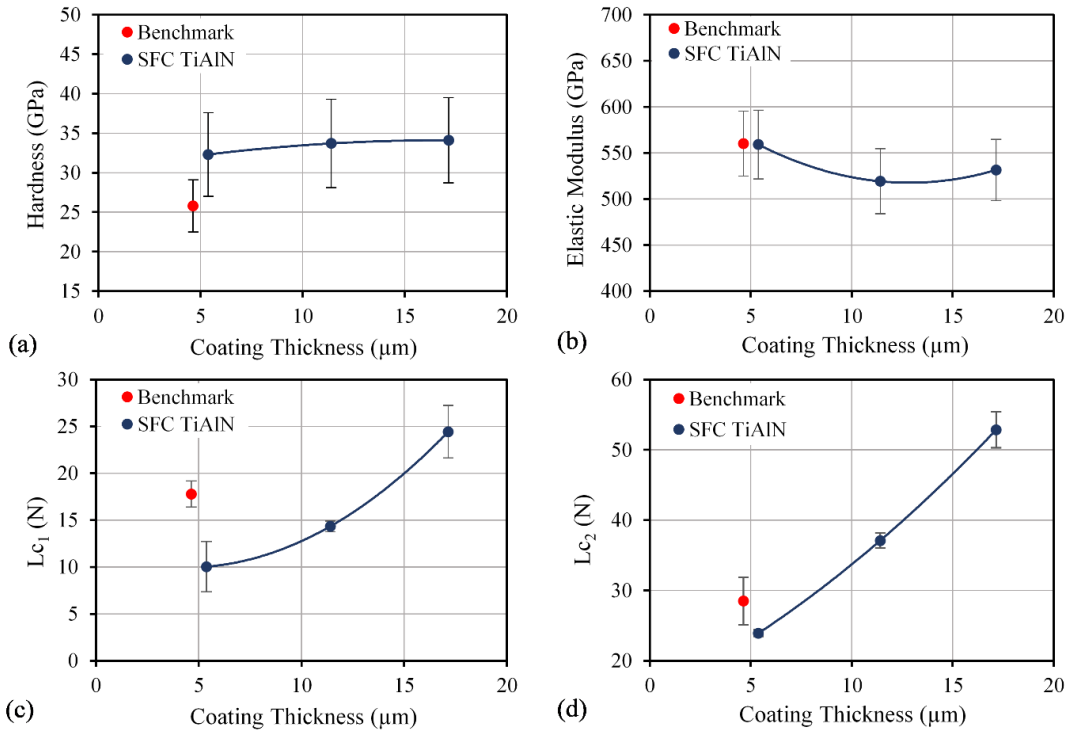

Figure 2.2. *Variation of properties with coating thickness, Hardness (a), Modulus of Elasticity (b), Lc1 (c) and Lc2 (d).*

2.3.2. Machining Studies

SFC technology makes it possible to reduce residual stress on the deposited coating and as a result, the coating becomes less resistant to cohesive failure. This factor becomes crucial when adhesive wear is manifested during dry machining of CGI. Therefore, understanding the effect of low residual stress on tool wear is of utmost importance.

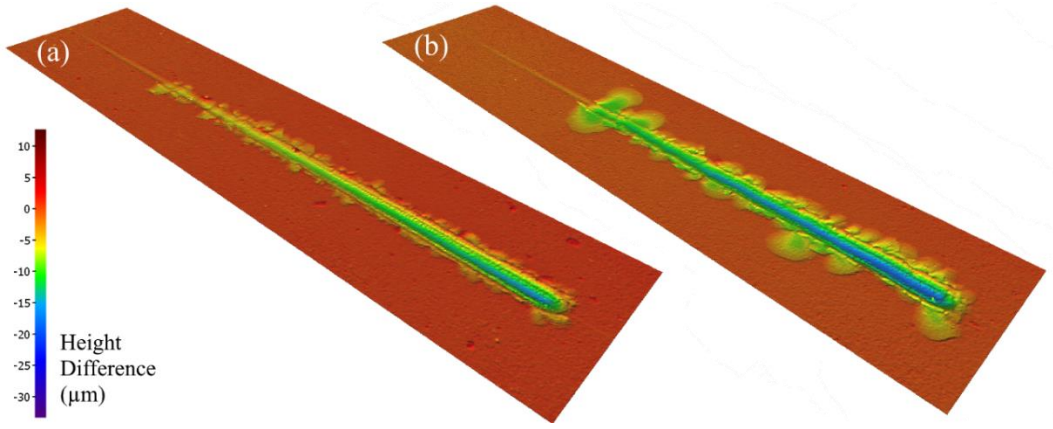

Figure 2.3. *3D scratch track map of benchmark (a) and T2 (b) coating.*

2.3.2.1 Tool Life and Cutting Force

Progression of flank wear with respect to cutting length during CGI finish turning is illustrated in fig. 2.4. Benchmark (KC5010) and T1 coatings have an almost identical tool life behavior. As coating thickness increases from T1 to T2, an improvement of around 35% in tool life is achieved. However, further thickness increase causes premature failure after a short length of cut. The premature failure of the T3 coating is strongly related to the change in tool microgeometry caused by increased thickness (fig. 2.1(b)). In fact, an increase in edge radius promotes ploughing (Denkena and Biermann, 2014) which in turn increases cutting forces (fig. 2.5), lowers stress concentration on the coating, increases heat generation as well as heat dissipation due to greater contact between the tool and workpiece/chip (Denkena and Breidenstein, 2008). Consequently, as tool life becomes more affected by it, there emerges an optimum range of cutting-edge radii and going out of this range will reduce tool life.

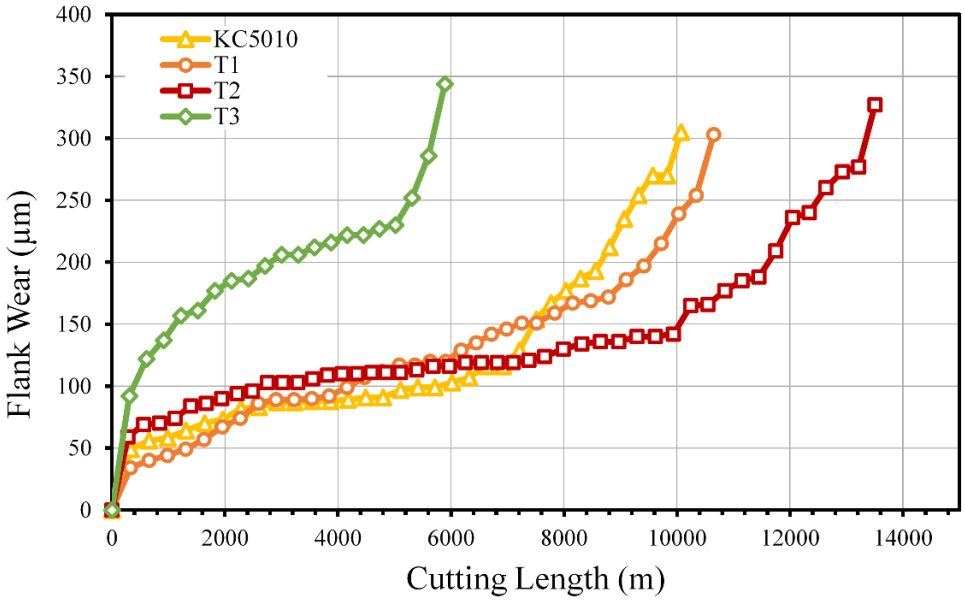

Figure 2.4. *variation of flank wear versus cutting length for different coatings.*

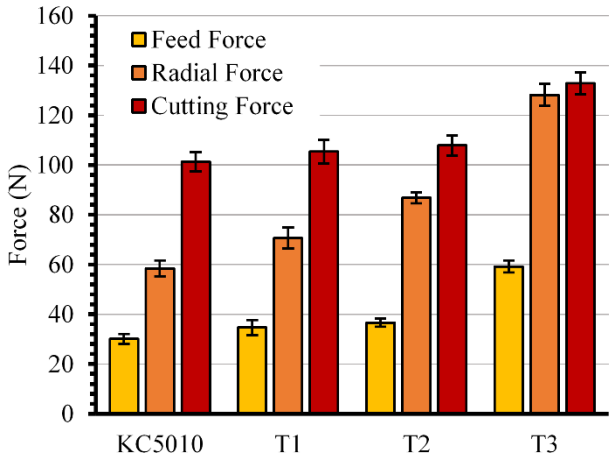

Figure 2.5. *Variation of cutting forces with coating thickness.*

Progression of tool wear is shown in fig. 2.6 with 3D difference measurement of the cutting edge. Wear is mostly focused on the cutting edge which indicates that dominant wear is caused by adhesion of CGI to the rake surface of the tool, since tests are conducted under dry condition (Nayyar *et al.*, 2013; Su *et al.*, 2016). However, the significant

difference between different coatings lies in the volume of built up edge formation, which is less extensive in case of the T1-3 coating compared to the benchmark. As the sticking material or build up edge breaks during the cutting process, it also removes some of the coating/tool material, in other words stick and slip followed by plucking action takes place. By increasing the thickness, the coating can sustain more damage and therefore reduce the volume of wear. Consequently, the T2 coating demonstrated the least volume of wear (fig. 2.7).

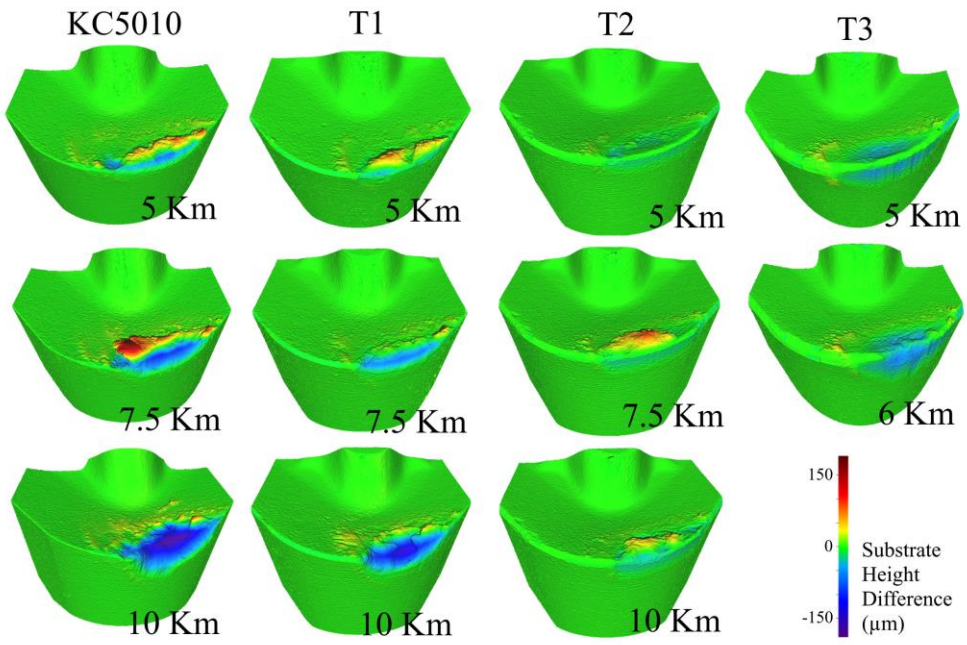

Figure 2.6. *3D difference measurement using white light interferometry during the cutting process at 5000, 7500 and 10000 m length of cut.*

To better understand BUE formation, SEM-EDS mapping was performed on the cutting edge at a steady state of wear and a 5000m length of cut. The results in fig. 2.8 show adhesive wear and CGI adhesion. Therefore, the formation of built-up edge on the rake face is followed by typical abrasive marks on the flank face of the tool. The built-up edge seems

to mainly form in the T1 and benchmark coating, since almost little to none BUE is present on the tools coated with T2 and T3. Thus, coatings deposited with the SFC technology (T1-3) could reduce formation of BUE compared to the benchmark, since even the T1 coating showed less BUE at an early stage of wear in fig. 2.9. Strong buildup formation leads to intensive damage of the surface layer of the coating and results in greater tool wear as can be seen in fig. 2.6.

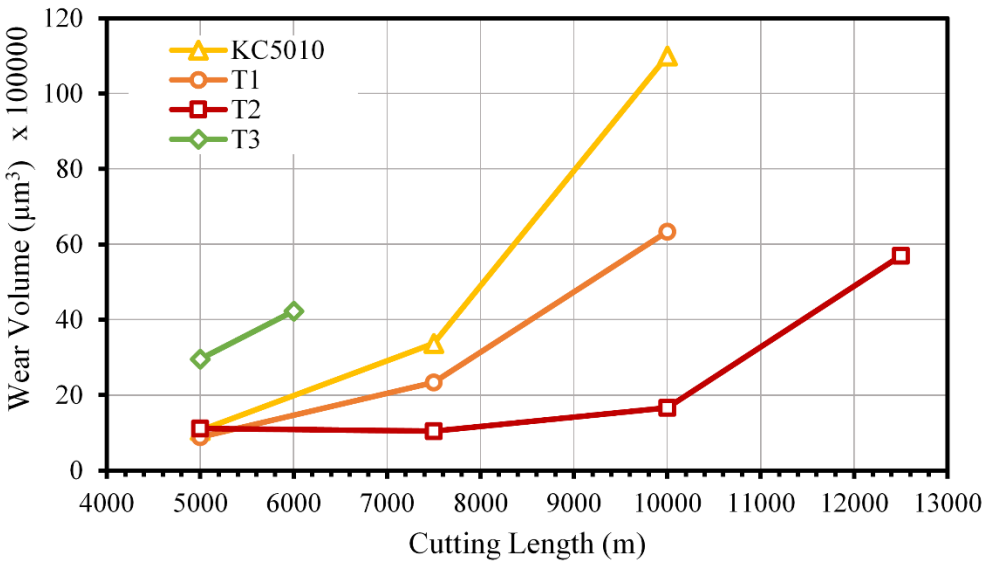

Figure 2.7. *Volumetric wear of inserts measured by white light interferometry during the cutting process.*

A lesser BUE formation probability can be correlated to lower residual stress of the T1-3 coatings. The coating deposited with SFC technology has a higher probability of cohesive failure and crack propagation would require less energy as can be seen from the critical load required for crack initiation in the scratch test (Lc_1 in table 2.2 (c)). Due to the multilayer nature of the coating, after the cracks are produced, they do not penetrate into the coating, but become deflected within the layers. Therefore, when BUE forms on coatings with low residual stress, it is readily removed by cohesive failure of the coating

taking a very small portion of the coating with itself and thus preventing catastrophic failure from happening. However, in case of the benchmark coating, since the coating possesses high resistance to cohesive failure, the BUE grows until cohesive or even adhesive failure occurs. In this manner, SFC deposited coatings (T1-T3) are capable of sustaining operation even under partial flaking of the coating.

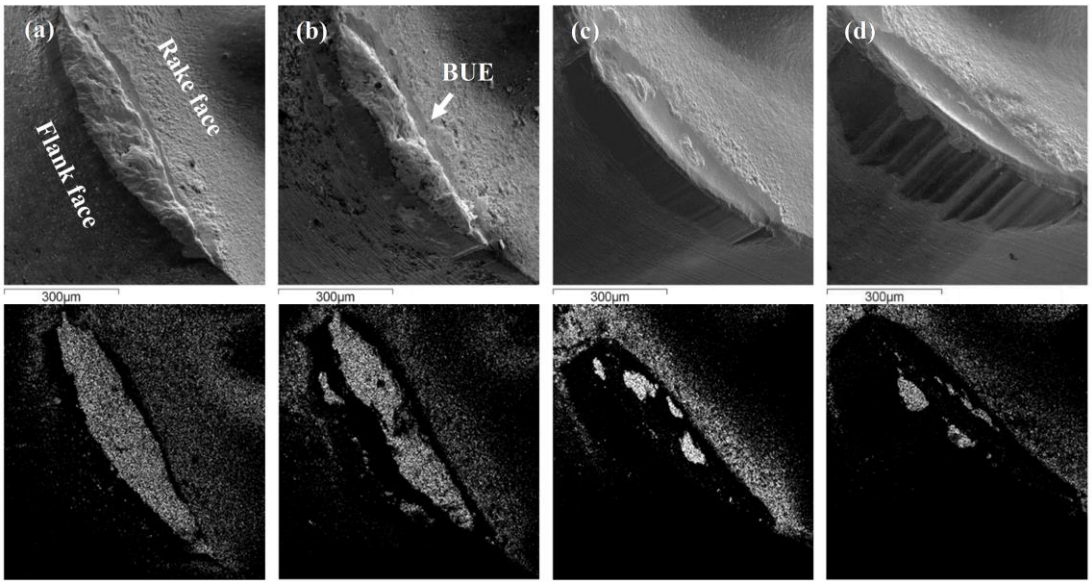

Figure 2.8. *SEM images and Fe EDS map of the tool with benchmark (a), T1 (b), T2 (c) and T3 (d) coating.*

FIB/TEM cross-section of the benchmark and T2 coating on the rake face after 400m of cutting length in fig. 2.10 (a) and (b) confirms this hypothesis. In case of fig. 2.10(a), the benchmark coating is worn out and the WC-Co substrate is exposed which could be a result of either adhesive failure in the interface or cohesive failure in the substrate. Cohesive failure in the substrate is due to stress distribution in the coating/substrate system and presence of tensile residual stress as Denkena and Breidenstein discussed (Denkena and Breidenstein, 2012). On the other hand, the TiAlN SFC multilayer coating can sustain greater adhesive damage. Layer by layer, gradual wear of the coating occurs, along with

cohesive failure and partial flaking of the coating. SEM images of the rake face after removing the BUE with $HCl+HNO_3$ in fig. 2.10 (c) and (d) clearly show substrate exposure of the benchmark tool after a short length of cut (400m), proving that partial flaking of the T2 coating is taking place on the rake face, which protects the tool from adhesion damage.

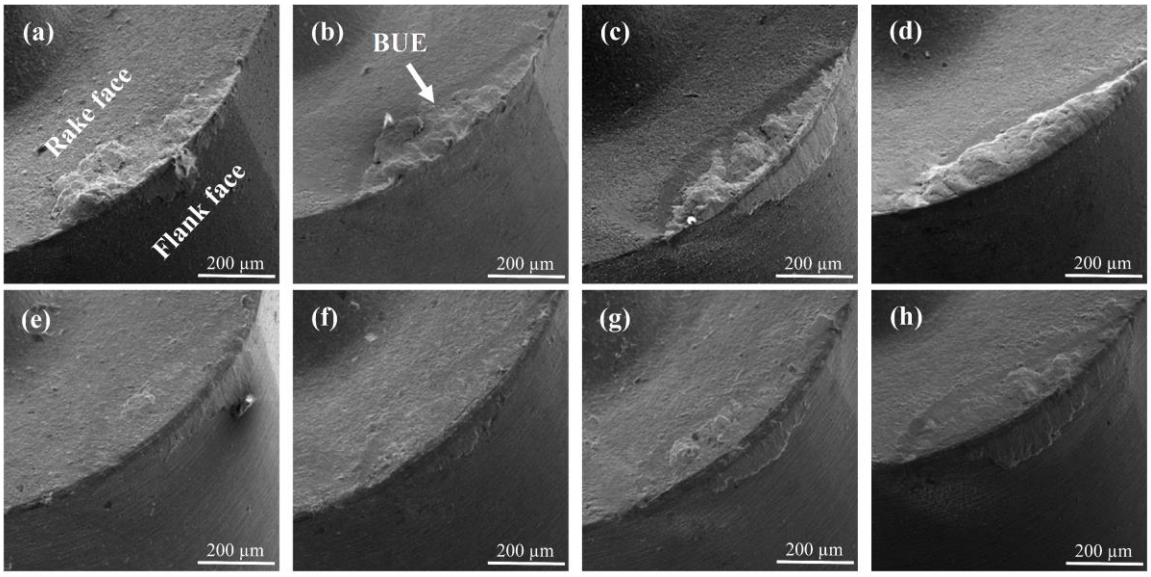

Figure 2.9. *SEM images of cutting edge with the benchmark (a)-(d) and T1 coating (e)-(h) at 25m, 75m, 150m and 400m of cutting length.*

2.3.2.2 Chip undersurface and workpiece surface integrity

SEM images of the chip undersurface collected from the early machining stage of benchmark and T2 coatings are shown in fig. 2.11 (a) and (b). It was observed that in general, chips have a smoother surface when machining with the T2 coating compared to the benchmark. To confirm this observation, surface roughness values of the chip undersurface were measured using a Lc value of 800 µm. The average value of 10 measurements on different chips showed a surface roughness (S_a) of 1.722 ± 0.254 µm upon machining with the benchmark, and 1.024 ± 0.245µm upon machining with the T2

coating. Chip undersurface morphology is an excellent indicator of the processes developing at the tool/chip interface. During machining with build-up edge formation, intensive stick-slip phenomena are taking place, which is an indication of catastrophic wear mode. This wear mode leads to severe damage of the friction surface once the build-up is broken off. This is confirmed by 3D difference measurement in fig. 2.6.

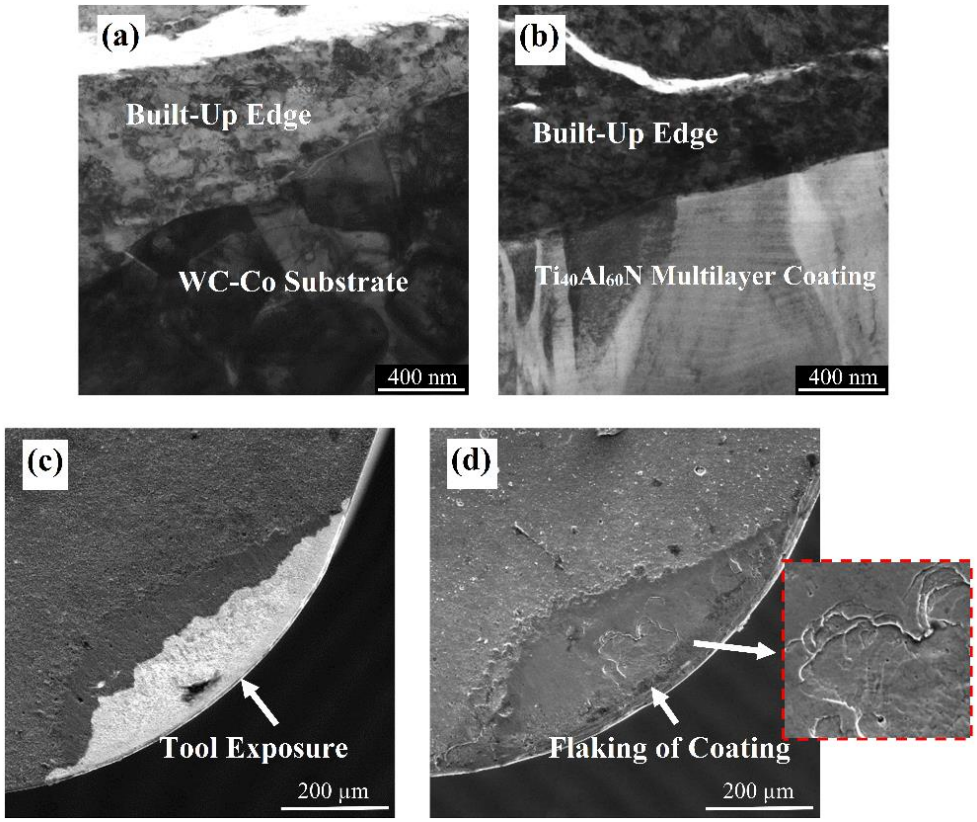

Figure 2.10. *FIB/SEM cross-section of the rake face of the tool with benchmark (a) and T2 (b) coating and SEM image of rake face after removing BUE of benchmark (c) and T2 (d) coating at 400m of cutting length.*

While built-up edge formation is impossible to entirely eliminate, it is possible to control this process by decreasing the volume of the build-ups. An efficient way to accomplish this is by adaptive response of the coated cutting tool, particularly by the partial flaking of the coating layer as was shown in the previous section. With strong buildup edge

formation, the sticking is stronger (benchmark coating). Because CGI contains a substantial amount of cementite, the sticking phase of the tool/chip interaction leads to detachment of small portions of the workpiece material on the undersurface of the chips (fig. 2.11). This results in higher roughness of the chip undersurface. If the size of the buildup is significantly reduced, then sticking intensity is lower. In contrast, the slipping phase of the interaction is enhanced and therefore chip undersurface roughness is lower when machining with the T2 coating. Cross section of the mentioned chips further proves this fact by showing a greater amount of plastic deformation (higher thickness of secondary shear deformation zone) in the chips collected while machining with the benchmark coating (fig. 2.12(a), (b)). A greater degree of plastic deformation is an indication of intensive sticking in the coating/chip interface.

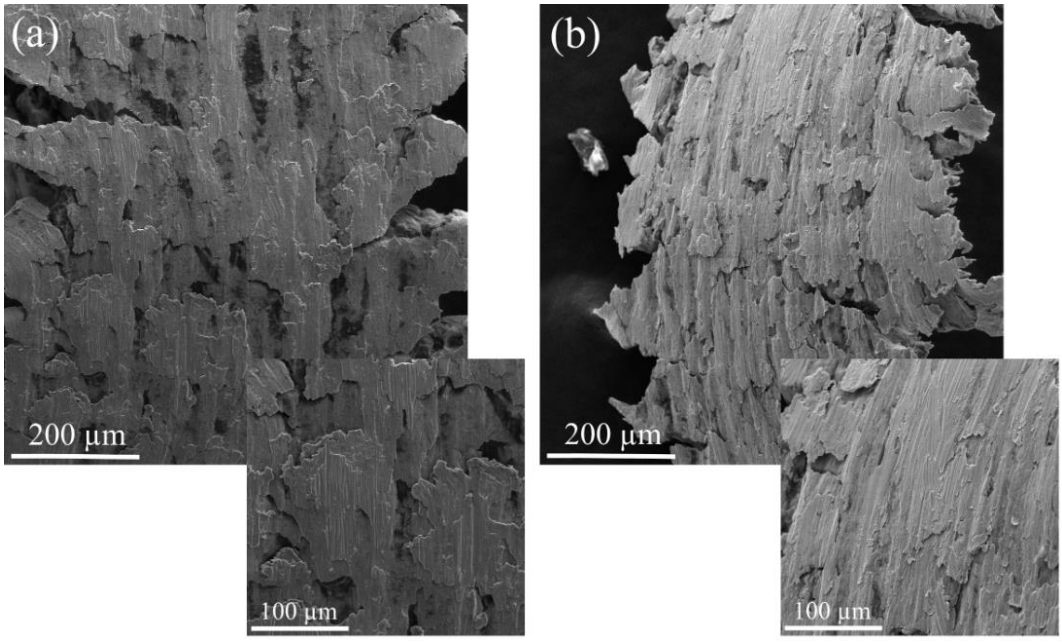

Figure 2.11. *SEM images of chip undersurface benchmark (a) and T2 (b) coating.*

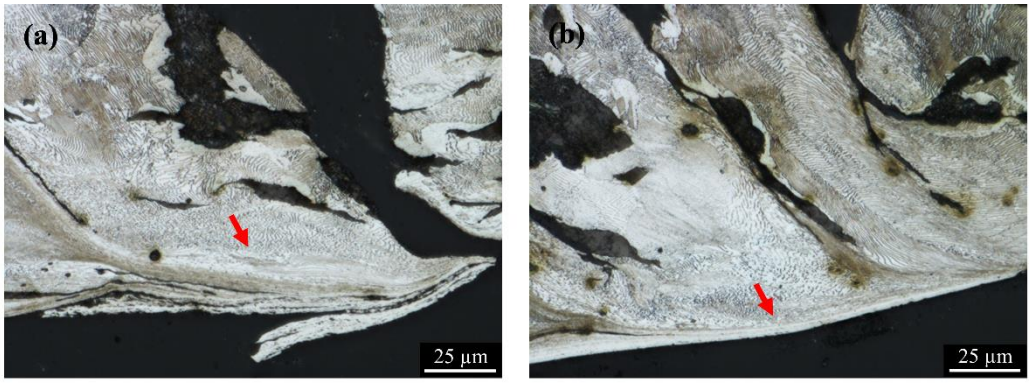

Figure 2.12. *Chip cross section benchmark (a) and T2 (b) coating.*

It is also worth mentioning that the surface quality of the machined part also improves under the low residual stress coating (T2) as shown in fig. 2.13. Mean value of roughness after 10 measurements on the machined surface shows that the R_a value is 2.507 ± 0.099 µm for the part machined with the benchmark coating, whereas the R_a value is 1.836 ± 0.070 µm for the part machined with the T2 coating. It should be noted that higher edge roundness in the T2 coating (fig. 2.1(b)) promotes ploughing, (Denkena and Biermann, 2014) which results in higher Ra values and surface roughness reduction solely as a result of lower BUE formation.

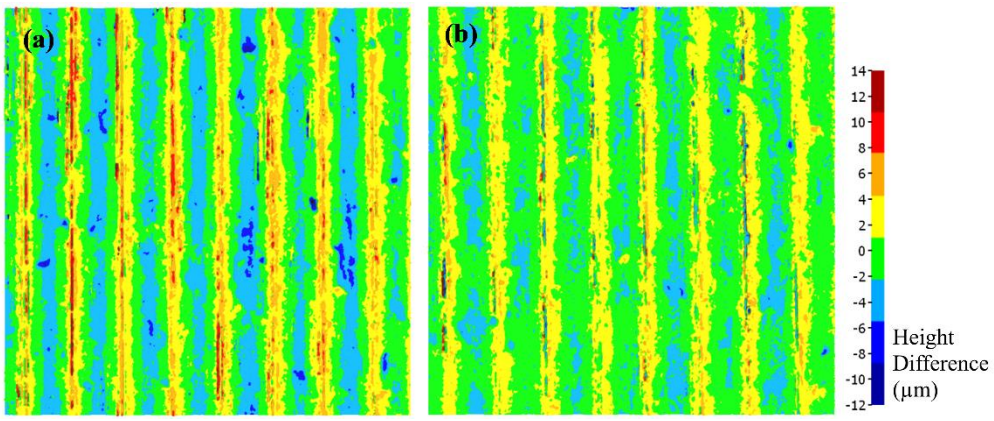

Figure 2.13. *Height difference measurement of machined surface using benchmark (a) and T2 (b) coating.*

2.4. Conclusion

The effect of PVD coating thickness on tool wear behavior, the mechanical properties of the coating, and the machining performance of CGI turning were presented in this paper. Increasing thickness above a certain value leads to greater rounding of the cutting-edge, which promotes higher cutting forces and ploughing, thus inducing an intense wear on the coated tool flank and rake surface in the case study of CGI turning.

Results show that the low residual stress multilayer TiAlN SFC coating succeeds in improving tool life and surface quality of the workpiece by decreasing built-up edge formation and delaying substrate exposure. In fact, three different factors affect the life of tools with increased coating thicknesses:

- First, SFC deposited coatings with low residual stress inhibit BUE formation due to the adaptive response of the coating layer, brought about by the partial superficial flaking of the surface layers of the coating without in-depth crack propagation into the coating layer. This is the major novelty of the obtained results.
- An increasing thickness delays substrate exposure, further increasing the tool life.
- Thickness also influences the micro-geometry of the tool, which affects cutting forces as well as thermal and mechanical loads on the coating and can lead to premature failure of the tool if not controlled.

In summary, the combination of these three factors demonstrated an improvement of around 35% in 11µm thick coatings, which could be considered to be an optimal coating thickness for this specific application.

2.5. References

Abele, E., Sahm, A. and Schulz, H. (2002) 'Wear Mechanism when Machining Compacted Graphite Iron', CIRP Annals - Manufacturing Technology, 51(1), pp. 53–56. doi: 10.1016/S0007-8506(07)61464-4.

Bouzakis, K. D. et al. (2003) 'The influence of the coating thickness on its strength properties and on the milling performance of PVD coated inserts.', Surface and Coatings Technology, 174(175), pp. 393–401. doi: 10.1016/j.surfcoat.2003.08.003.

Bouzakis, K. D. et al. (2004) 'The effect of coating thickness, mechanical strength and hardness properties on the milling performance of PVD coated cemented carbides inserts', Surface and Coatings Technology, 177–178(178), pp. 657–664. doi: 10.1016/j.surfcoat.2003.08.003.

Dawson, S. and Schroeder, T. (2000) 'Compacted Graphite Iron : A Viable Alternative', Engineering Casting Solutions AFS.

Dawson, S. and Schroeder, T. (2004) 'Practical applications for compacted graphite iron', AFS Transactions, 47(05), pp. 1–9.

Denkena, B. and Biermann, D. (2014) 'Cutting edge geometries', CIRP Annals - Manufacturing Technology, 63(2), pp. 631–653. doi: 10.1016/j.cirp.2014.05.009.

Denkena, B. and Breidenstein, B. (2008) 'Influence of the residual stress state on cohesive damage of PVD-coated carbide cutting tools', Advanced Engineering Materials, 10(7), pp. 613–616. doi: 10.1002/adem.200800063.

Denkena, B. and Breidenstein, B. (2012) ‘Residual stress distribution in PVD-coated carbide cutting tools - origin of cohesive damage’, Tribology in Industry, 34(3), pp. 158–165.

Gastel, M. et al. (2000) ‘Investigation of the wear mechanism of cubic boron nitride tools used for the machining of compacted graphite iron and grey cast iron’, International Journal of Refractory Metals and Hard Materials, 18(6), pp. 287–296. doi: 10.1016/S0263-4368(00)00032-9.

He, B. B. (2003) ‘Introduction to two-dimensional X-ray diffraction’, Powder Diffraction, 18(02), pp. 71–85. doi: 10.1154/1.1577355.

Heck, M. et al. (2008) ‘Analytical investigations concerning the wear behaviour of cutting tools used for the machining of compacted graphite iron and grey cast iron’, International Journal of Refractory Metals and Hard Materials, 26(3), pp. 197–206. doi: 10.1016/j.ijrmhm.2007.05.003.

Heinke, W. et al. (1995) ‘Evaluation of PVD nitride coatings, using impact, scratch and Rockwell- C adhesion tests’, Thin Solid Films, 270, pp. 431–438. doi: 10.1016/0040-6090(95)06934-8.

Klocke, F. et al. (1998) ‘Improved Cutting Processes with Adapted Coating Systems’, CIRP Annals - Manufacturing Technology, 47(1), pp. 65–68. doi: 10.1016/S0007-8506(07)62786-3.

Malakizadi, A. et al. (2018) ‘Effects of workpiece microstructure, mechanical properties and machining conditions on tool wear when milling compacted graphite iron’, Wear. Elsevier B.V., 410–411(May), pp. 190–201. doi: 10.1016/j.wear.2018.07.005.

Nayyar, V. et al. (2012) ‘An experimental investigation of machinability of graphitic cast iron grades; Flake, compacted and spheroidal graphite iron in continuous machining operations’, in Procedia CIRP, pp. 488–493. doi: 10.1016/j.procir.2012.04.087.

Nayyar, V. et al. (2013) ‘Machinability of compacted graphite iron (CGI) and flake graphite iron (FGI) with coated carbide’, International Journal of Machining and Machinability of Materials, 13(1), p. 67. doi: 10.1504/IJMMM.2013.051909.

Nie, X. et al. (1999) ‘Thickness effects on the mechanical properties of micro-arc discharge oxide coatings on aluminium alloys’, in Surface and Coatings Technology, pp. 1055–1060. doi: 10.1016/S0257-8972(99)00089-4.

Rosa, S. do N. et al. (2010) ‘Analysis of Tool Wear , Surface Roughness and Cutting Power in the Turning Process of Compact Graphite Irons with Different Titanium Content’, Journal of the Brazilian Society of Mechanical Sciences and Engineering, 32(3), pp. 234–240. doi: 10.1590/S1678-58782010000300006.

Sahm, A., Abele, E. and Schulz, H. (2002) ‘Machining of compacted graphite iron (CGI)’, Materialwissenschaft und Werkstofftechnik. WILEY-VCH Verlag, 33(9), pp. 501–506. doi: 10.1002/1521-4052(200209)33:9<501::AID-MAWE501>3.0.CO;2-W.

Sargade, V. G. et al. (2011) ‘Effect of coating thickness on the characteristics and dry machining performance of Tin film deposited on cemented carbide inserts using cfubms’,

Materials and Manufacturing Processes, 26(8), pp. 1028–1033. doi: 10.1080/10426914.2010.526978.

Sarin, V. K. (1993) ‘Micro-scratch test for adhesion evaluation of thin films’, Journal of Adhesion Science and Technology, 7(12), pp. 1265–1278. doi: 10.1163/156856193X00097.

Da Silva, M. B. et al. (2011) ‘Analysis of wear of cemented carbide cutting tools during milling operation of gray iron and compacted graphite iron’, Wear, 271(9–10), pp. 2426–2432. doi: 10.1016/j.wear.2010.11.030.

Skordaris, G. et al. (2016) ‘Film thickness effect on mechanical properties and milling performance of nano-structured multilayer PVD coated tools’, Surface and Coatings Technology, 307, pp. 452–460. doi: 10.1016/j.surfcoat.2016.09.026.

Su, G. S. et al. (2016) ‘Effects of high-pressure cutting fluid with different jetting paths on tool wear in cutting compacted graphite iron’, Tribology International, 103, pp. 289–297. doi: 10.1016/j.triboint.2016.06.029.

Tooptong, S. et al. (2016) ‘A Preliminary Machinability Study of Flake and Compacted Graphite Irons with Multilayer Coated and Uncoated Carbide Inserts’, Procedia Manufacturing, 5, pp. 644–657. doi: 10.1016/j.promfg.2016.08.053.

Tooptong, S., Park, K. H. and Kwon, P. (2018) ‘A comparative investigation on flank wear when turning three cast irons’, Tribology International. Elsevier Ltd, 120(December 2017), pp. 127–139. doi: 10.1016/j.triboint.2017.12.025.

Tuffy, K., Byrne, G. and Dowling, D. (2004) 'Determination of the optimum TiN coating thickness on WC inserts for machining carbon steels', Journal of Materials Processing Technology, 155–156(1–3), pp. 1861–1866. doi: 10.1016/j.jmatprotec.2004.04.277.

Wang, C. et al. (2017) 'Effect of different oil-on-water cooling conditions on tool wear in turning of compacted graphite cast iron', Journal of Cleaner Production, 148, pp. 477–489. doi: 10.1016/j.jclepro.2017.02.014.

Yamamoto, K. et al. (2018) 'Cutting Performance of Low Stress Thick TiAlN PVD Coatings during Machining of Compacted Graphite Cast Iron (CGI)', Coatings, 8(2), p. 38. doi: 10.3390/coatings8010038.

Zhang, S. et al. (2005) 'Toughness measurement of thin films: A critical review', Surface and Coatings Technology, pp. 74–84. doi: 10.1016/j.surfcoat.2004.10.021.

Chapter 3. Effect of Nitrogen Pressure and Bias Voltage

Abdoos, M., Rawal, S., Arif, A. F. M., & Veldhuis, S. C. (2020). A strategy to improve tool life by controlling cohesive failure in thick TiAlN coating during turning of CGI. The International Journal of Advanced Manufacturing Technology, 106(7-8), 2793-2803.

Author's Contribution

Majid Abdoos	Designed and conducted the experiments Analyzed the results Wrote the manuscript
Sushant Rawal	Assisted with experiment design Assisted with coating deposition
Abul Fazel Arif	Assisted with experimental design Assisted writing and editing the manuscript
Stephen Veldhuis	Supervised the project Edited the manuscript

Abstract

Beside machining condition and parameters, coating properties is one of the main factors affecting tool performance and wear pattern. These properties include coating hardness and elastic modulus, adhesion to substrate, roughness, defects and most importantly residual stress. In general, the properties of a physical vapor deposition (PVD) coating can be controlled by adjusting deposition parameters such as substrate bias voltage and nitrogen pressure. Therefore, a coating can be tailored to withstand a specific wear mode which is dominant in machining the workpiece material. In this work a strategy is suggested to decrease adhesion wear and formation of built up edge during machining of compacted graphite iron (CGI). This strategy involves deposition of thick TiAlN coating with low residual stress in order to promote cohesive failure within the coating. For this purpose, monolayer Ti40Al60N PVD coatings with high thickness (5-10 µm) were deposited under various deposition parameters. A comprehensive coating characterization was done using scanning electron microscope (SEM), X-Ray diffraction (XRD), nanoindentation and scratch test. Tool life of selected coatings were then tested under dry finishing of compacted graphite iron and wear pattern was investigated with optical and scanning electron microscope. The results showed that coating under low compressive residual stress is successful in reducing sticking and built up edge formation. This phenomenon happens with gradual cohesive failure of the coating under adhesion wear, resulting in a higher tool life under adhesive wear.

Keywords

Thick PVD coating; TiAlN; Residual stress; Adhesive wear; Built-up edge reduction; Coating deposition

3.1. Introduction

Vapor deposition techniques (PVD and CVD) are widely used to protect tools and increase tool life in manufacturing industries. Compared to CVD, PVD coatings are normally under high compressive residual stress which increases hardness and fracture toughness and limits thickness due to the accumulation of high compressive residual stresses with coating growth and failure of thick coating by spallation (Tuffy, Byrne and Dowling, 2004). It is well known that mechanical properties and performance of hard PVD coatings depend on the method of deposition, coating architecture and the process parameters such as bias voltage, deposition temperature, reactive gas pressure and table rotation speed (Yu *et al.*, 2008; Chokwatvikul, Larpkiattaworn and Surinphong, 2011; Tillmann *et al.*, 2013; Grigoriev *et al.*, 2017; Yongqiang *et al.*, 2018). Among the deposition parameters, the contributions of substrate bias voltage and reactive gas pressure on coating properties are broadly investigated. Adjusting the mentioned parameters will affect ion bombardment energy, one of the most important deposition factors that determines coating characteristics such as residual stress, texture, and structure (Elmkhah *et al.*, 2016).

Many researchers attempted to gain a better understanding of the deposition process of TiN-TiAlN coating family in order to design a coating with favorable properties. In general, a higher substrate bias voltage is shown to increase bombardment energy and result in a higher compressive residual stress, hardness and fracture toughness, thereby improving tool life (G. Skordaris *et al.*, 2017; Skordaris *et al.*, 2018). However, increase in compressive residual stress in the coating reduces adhesion due to high interfacial stresses which might

lead to spontaneous spallation and coating failure (M. Ahlgren and Blomqvist, 2005). Therefore, the compressive residual stress of the coating, should be a compromise between good adhesion and mechanical properties. Conversely, nitrogen pressure was shown to have an opposite effect on residual stress, as lower compressive values were observed at a higher nitrogen pressure (Carrasco *et al.*, 2002). It is also mentioned that nitrogen pressure affects properties such as grain size, structure, preferential orientation and coating defects (Zhou *et al.*, 2009). These properties will directly affect hardness, elastic modulus and coating adhesion (Bujak, Walkowicz and Kusiński, 2004). In this regard, ratio of defects has the most significant role which increases along with nitrogen pressure and correlates to the amount and size of the macroparticles. It is also worth mentioning that both substrate bias voltage and nitrogen pressure can affect composition of the coating which might lead to change in other properties of the coating such as hot hardness and oxidation resistance (Cai *et al.*, 2011, 2017).

In a coating/substrate system, adhesion failure is referred to detachment of the coating from substrate and cohesion damage is defined as failure of the coating from within itself. Cohesive and adhesive failure in a PVD coating substrate system is significantly controlled by residual stress state and value (Tillmann *et al.*, 2013). In this regards its mentioned tensile residual stress promotes cohesive failure and compressive residual stress delays it due to hindering crack propagation (Denkena and Breidenstein, 2008, 2012). However, both compressive and tensile residual stresses weaken coating/substrate bond at the interface. In extreme cases if the interface is overstressed, the coating will fail by

delamination (tensile residual stress) or buckling (compressive residual stress) (Teixeira, 2001, 2002).

Compacted graphite iron shows a high tendency for sticking, built-up edge formation and adhesion/attrition wear in dry machining (Su *et al.*, 2016; de Sousa, Sales and Machado, 2018; Tooptong, Park and Kwon, 2018). Therefore, use of CGI is greatly limited despite its superior mechanical properties as it shows a significant lower tool life comparing to commonly used grey cast iron (Abele, Sahm and Schulz, 2002; Dawson and Schroeder, 2004). Previous researchers showed that a greater thickness of the coating can delay substrate exposure, better protect the tool and increase tool life (Bouzakis *et al.*, 2004; Skordaris *et al.*, 2016; Bar-Hen and Etsion, 2017). However, the question arises how to deposit thick coating with lower residual stress to avoid spallation.

In recent studies by the authors (Yamamoto *et al.*, 2018; Abdoos *et al.*, 2019), an attempt was made to increase coating thickness for machining application by using a new arc ion deposition technology known as super fine cathode (SFC). SFC provides an extended plasma range due to its tuned magnetic field around cathode. Therefore, the results of an exploratory work reported in (Yamamoto *et al.*, 2018) showed the ability of SFC process to deposit thick TiAlN coatings up to 15 µm thickness in mono- and multi-layer architecture without spallation. In addition, the deposited coatings had low values of compressive residual stress (500-1000 MPa) as compared to commercially available coatings and an improvement in the tool performance was also observed for wet finish turning of CGI. Most TiAlN PVD coatings reported in literature are under high compressive residual stress, normally 2-5 GPa (PalDey and Deevi, 2003). Next, the

$Ti_{40}Al_{60}N$ coatings of different thicknesses (around 5, 11 and 17 μm) were deposited in a multi-bilayer architecture under same deposition condition and the thickness of the coatings were varied by adjusting the number of bilayers (Abdoos *et al.*, 2019). The effect of coating thickness on edge geometry, mechanical properties of the coating, tool wear, and surface integrity of the machined surface was investigated in dry finish turning of CGI. Results showed improvements in tool life (up to 35%) and surface quality of the workpiece by decreasing built-up edge formation and delaying substrate exposure. It was proposed that this behavior was a result of low compressive residual stress of the coating and corresponding reduction in sticking due to gradual cohesive failure (Abdoos *et al.*, 2019). Although the coating deposition rate, macroparticle density, coating composition, structure and texture, coating properties, temperature and others may influence the gradual cohesive failure, the prior studies showed that the residual stress was the main factor controlling cohesive/adhesive behavior of a coating (Teixeira, 2001, 2002; Denkena and Breidenstein, 2012; Tillmann *et al.*, 2013). Therefore, it is essential to know how much residual stress is beneficial and how it can be controlled.

The above literature review shows that several studies have been reported on the effect of deposition parameters on the PVD coating properties and residual stress, there is scarcity of literature on deposition parameters effect on the thick SFC coating properties and wear mechanism in dry finish turning. Therefore, in this paper, an in-depth study was conducted to control residual stress using deposition parameters (substrate bias voltage and nitrogen pressure), while monitoring mechanical properties of the coating to ensure sufficient quality. In this regard, thick monolayer $Ti_{40}Al_{60}N$ coatings were deposited with thickness

(5-10 µm) to formulate a strategy for reducing adhesion and formation of built-up edge in dry finish turning of CGI workpiece. This was done through low compressive residual stress and promotion of gradual cohesive failure of thick TiAlN coating. Finally, selected coatings having different residual stress values were tested under dry finish cutting conditions to validate the tool performance and study tool wear pattern based on residual stress and mechanical properties.

3.2. Experimental Procedure

Coatings with variation of substrate bias voltage and nitrogen pressure were deposited with cathodic arc ion deposition method using a Kobelco AIP-S20 system. Super Fine Cathode (SFC) technology was used during deposition to obtain better control of residual stress generation. Deposition was performed by two arc sources with a 40 at.% Ti and 60 at.% Al composition manufactured using powder metallurgy. Sandvik Coromant ISO SPGN120308 flat inserts and Kennametal ISO CNGG432FS uncoated inserts were used as the substrate for material characterization and machining studies respectively. Prior to deposition, all the substrates were cleaned in acetone with an ultrasonic cleaner. The substrates were then mounted into the deposition chamber, preheated to 550°C and etched by Ar at 1.3 Pa pressure for 7.5 minutes to reduce any potential contamination and increase adhesion. Coatings were deposited using a fixed deposition time of 84 minutes in a monolayer state at various bias voltages and fixed nitrogen pressure and vice versa. Details of the deposition process can be found in table 3.1. These conditions are set in order to cover common range of deposition parameters.

Table 3.1. *Deposition parameters.*

	Temperature	Bias voltage (V)	N_2 pressure (Pa)	Arc Currents (A)	Rotation Speed (RPM)
Bias variation	550°C	-30, -70, -110, -150	4	150	5
Pressure variation	550°C	-70	1, 2.5, 4, 5.5	150	5

After deposition, thickness measurement was performed using a BC-2 Miba Coating Group ball crater system and a steel ball with the diameter of 20mm, diamond paste was used to accelerate the wear. Deposition rate was then calculated based on coating thickness and deposition time. A Vega II LSU TESCAN scanning electron microscopy equipped with an Oxford X-Max 80 EDS was used to analyze the coating surface and perform composition measurements. To determine residual stress and acquire diffraction pattern, samples were analyzed using a Bruker D8 Discover instrument equipped with a cobalt target and an X-Ray wavelength of 1.79Å (K_α). Residual stress was determined using LEPTOS software on (200) crystallographic plane since it was the only available peak with significant intensity in all the samples. It is worth mentioning that the instrument uses a 2-dimensional X-Ray system, the details of which can be found elsewhere (He, 2003).

Mechanical tests were performed on the coating with an Anton-Paar Revetest scratch tester and an NHT^3 nanoindentation tester. Scratch test was done using a Rockwell C diamond indenter with a tip radius of 100µm in a length of 3mm, scratch velocity of 7.5mm and a progressive load increasing from 0.5 to 100N. The critical adhesion failure load (L_{C2}) was measured after the scratch test, per the ASTM C1624-05 standard. To measure hardness and elastic modulus of the coatings, nanoindentation was performed on the

samples using load control mode and a maximum load of 100mN. The indentation load was selected such that the penetration depth does not exceed 10% thickness of the coating.

The cutting performance of selected coatings was tested during finish turning of CGI under dry condition with cutting speed of 300 m/min, depth of cut of 0.25 mm and feed rate of 0.2 mm/rev. An OKUMA CNC Crown L1060 lathe CNC machine was used for this purpose. The CGI workpiece consisted of 70% pearlite and 10% ferrite with 20% nodularity. Workpiece was in the shape of a hollow cylinder with inner and outer diameter of 120 and 80 mm, and a length of 200 mm. Flank wear was measured after machining for a certain cutting length, using a Keyence VHX-5000 microscope. A flank wear of 300µm was set for tool failure criteria in accordance to ISO-3685 standard. Moreover, the tools were further inspected with SEM and Bruker Alicona InfiniteFocus microscope. All the surface roughness measurements were done using Bruker Alicona InfiniteFocus microscope in accordance to ISO 4287 and 25178 standards.

3.3. Coating characterization and properties

3.3.1. Coating deposition rate

Fig. 3.1 illustrates the change in deposition rate with bias voltage and nitrogen pressure. In both cases, the deposition rate increased up to a maximum point after which it subsequently began to decrease. Therefore, two opposing factors control the deposition rate with regards to both bias voltage and nitrogen pressure. This can be explained with bombardment energy and re-sputtering of already deposited atoms. Re-sputtering is an inseparable phenomenon in physical vapor deposition techniques and it strongly correlates

with bombardment energy which is affected by the deposition parameters. In general bombardment energy and re-sputtering increase with higher bias voltage and lower nitrogen pressure (Bubenzer *et al.*, 1983). As nitrogen pressure increases, bombardment energy is reduced due to the higher chance of particle collision and a lower mean free path. This reduces the chance of re-sputtering and increases the deposition rate up to a nitrogen pressure of 4Pa. However, higher nitrogen pressure also promotes "target poisoning" which results in the target being covered by its nitride with higher melting point than its metallic form (Vaz *et al.*, 2005). This will, in fact affect the area of the target contributing to the deposition process and ultimately lead to a lower deposition rate at a nitrogen pressure of 5.5Pa. In the case of substrate bias voltage, the deposition rate seems to initially increase with higher substrate bias until reaching its maximum value at a substrate bias voltage of -70 V. This can be explained with higher ion flux reaching the substrate and contributing to coating growth at a low substrate bias voltage as Raveh et al. (Raveh *et al.*, 1999) mentioned. As substrate bias voltage is further increased, the re-sputtering effect and higher degree of ion peening become the dominant factors in controlling the deposition rate and reduce rates are observed. Similar effect in deposition rate is reported by Devia et al. (Devia *et al.*, 2011a).

3.3.2. Macroparticle density

Macroparticles are droplets of molten material emitted from the target that get deposited on the substrate. These particles are a part of the defects introduced into the coating during deposition and are considered one of the disadvantages of arc ion deposition techniques. Macroparticles have a detrimental effect on mechanical properties, performance and

topography of the coating as addressed by many researchers (Bujak, Walkowicz and Kusiński, 2004; Cai *et al.*, 2011), therefore a high density of macroparticle is generally avoided. Fig. 3.2 shows the variation of macroparticle density with substrate bias voltage and nitrogen pressure. The density is calculated from SEM micrographs by dividing the area covered by macroparticles by the total area of the image. It can be seen that macroparticle density decreases with substrate bias voltage and increases with nitrogen pressure up to 4Pa. However, there is a drastic decrease in the density with nitrogen pressure of 5.5Pa. This can be attributed to the target poisoning effect as mentioned in the previous section since targets produce a lower number of molten particles while covered with its nitride due to higher melting point (Vaz *et al.*, 2005).

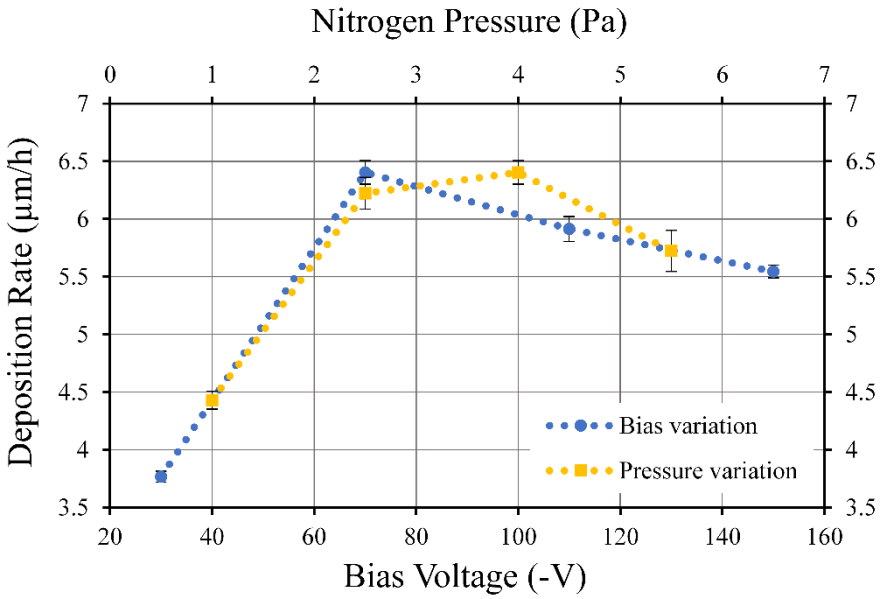

Figure 3.1. *Coating deposition rate as a function of bias voltage and nitrogen pressure.*

The increase in substrate bias voltage and decrease in nitrogen pressure have a filtration effect on macroparticles since a lower density is observed. A similar observation was

reported by many researchers (Warcholinski *et al.*, 2012; Taghavi Pourian Azar, Er and Ürgen, 2018) and two main mechanisms were proposed to explain the results. The first mechanism states that loose macroparticles on the surface of the coating are being removed by high energy ion bombardment (Warcholinski *et al.*, 2012). As the bombardment energy increases with higher bias voltage and lower nitrogen pressure, the accelerated ions have higher momentum and therefore remove macroparticles with a higher efficiency. The second mechanism involves the electrical repulsion effect where macroparticles become negatively charged while traveling towards the substrate due to random collision with ions, electrons and neutral atoms. These charged macroparticles are then repelled from the electric field near the substrate (Cai *et al.*, 2017). The change in macroparticle density is also evident from the SEM micrographs shown in fig. 3.3.

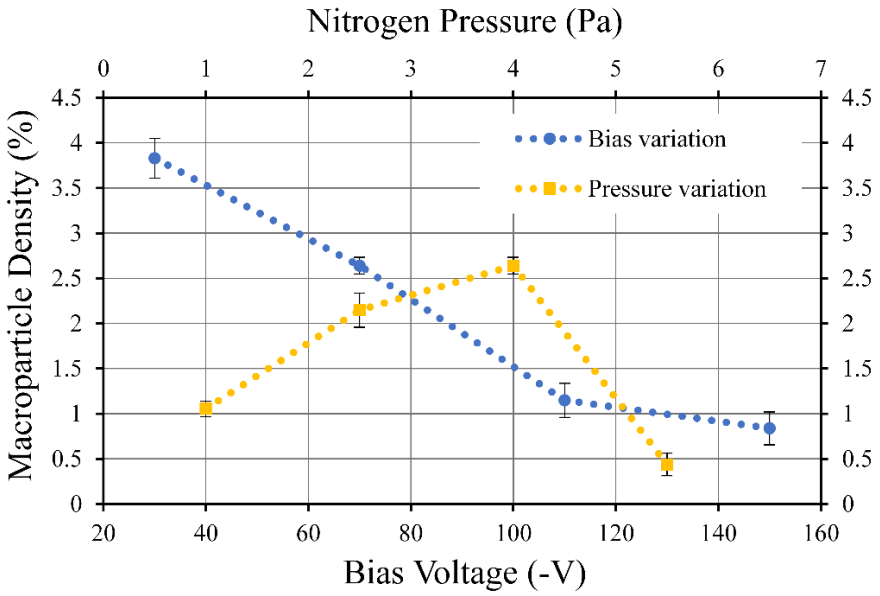

Figure 3.2. *Microparticle density of the deposited coatings under different substrate bias voltages and nitrogen pressures.*

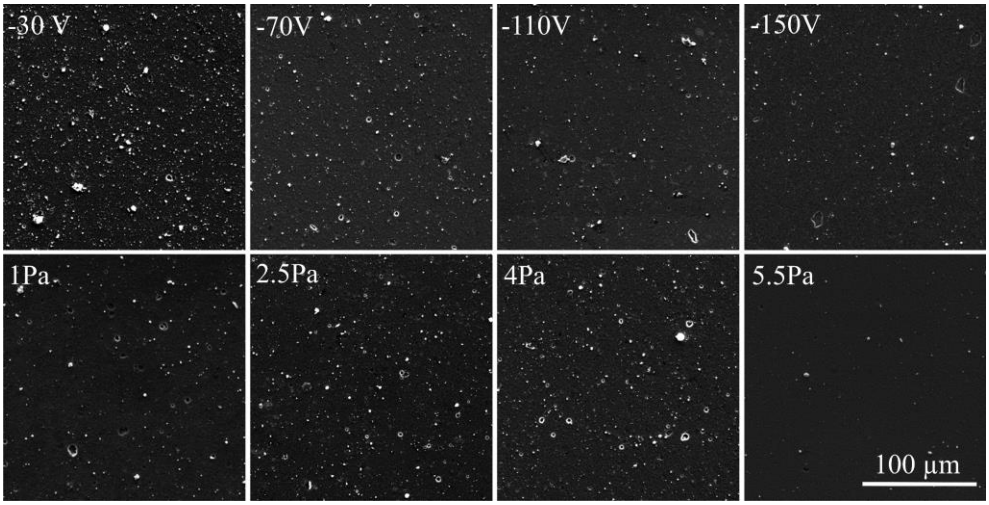

Figure 3.3. *SEM micrographs of coatings deposited with varying bias voltage and nitrogen pressure.*

3.3.3. Coating Composition, Structure and Texture

Composition of the deposited coatings was measured using energy dispersive X-ray spectroscopy (EDS). With varying substrate bias voltage and pressure, an insignificant Al:Ti ratio variation between 41:59 to 43:57 was seen as shown in fig. 3.4. This slight change is reported to be due to "selective re-sputtering" effect which refers to Al atoms get selectively re-sputtered due to their lower atomic weight compared to Ti atoms with higher bombardment energy (Zhang *et al.*, 2012). The deposited TiAlN coatings showed a monolayer dense columnar structure as shown in the coating fracture cross section in fig. 3.5. X-Ray Diffraction pattern of the TiAlN coatings deposited at varying substrate bias voltages and nitrogen pressures shown in fig. 3.6 indicated predominant (200) crystallographic orientation in all the samples (peaks were identified using ICDD PDF 04-015-2554). However, the intensity of this peak was reduced with increase in bias voltage and decrease in pressure. It is known that the texture or preferential orientation of the TiN-coating family is determined by the competition between the surface and strain energy

(Devia *et al.*, 2011a). If strain energy is dominant, preferential orientation is (111) with high packing density in favour of releasing the compressive residual stress (Li and Wang, 2003). Otherwise, if surface energy is predominant, (200) crystallographic orientation is preferred. Lack of (111) orientation in all the deposited samples, confirms the ability of SFC technology to control and reduce strain energy generated during deposition.

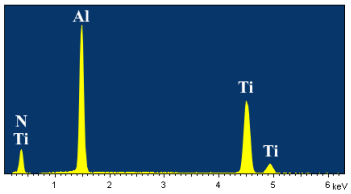

Bias Voltage (V)	N_2 Pressure (Pa)	Al (at. %)	Ti (at. %)	N (at. %)	Al:Ti Ratio
-30	4	25.4 ± 0.3	18.6 ± 0.3	56.0 ± 0.5	58:42
-70	4	25.5 ± 0.3	18.7 ± 0.3	55.8 ± 0.5	58:42
-110	4	25.1 ± 0.3	19.1 ± 0.3	55.8 ± 0.5	57:43
-150	4	25.1 ± 0.3	18.4 ± 0.3	56.5 ± 0.5	58:42
-70	1	25.5 ± 0.3	19.2 ± 0.3	55.3 ± 0.5	57:43
-70	2.5	25.5 ± 0.3	19.1 ± 0.3	55.3 ± 0.5	57:43
-70	4	25.5 ± 0.3	18.7 ± 0.3	55.8 ± 0.5	58:42
-70	5.5	26.5 ± 0.3	18.3 ± 0.3	55.2 ± 0.5	59:41

Figure 3.4. *EDS spectrum and composition of the deposited coatings.*

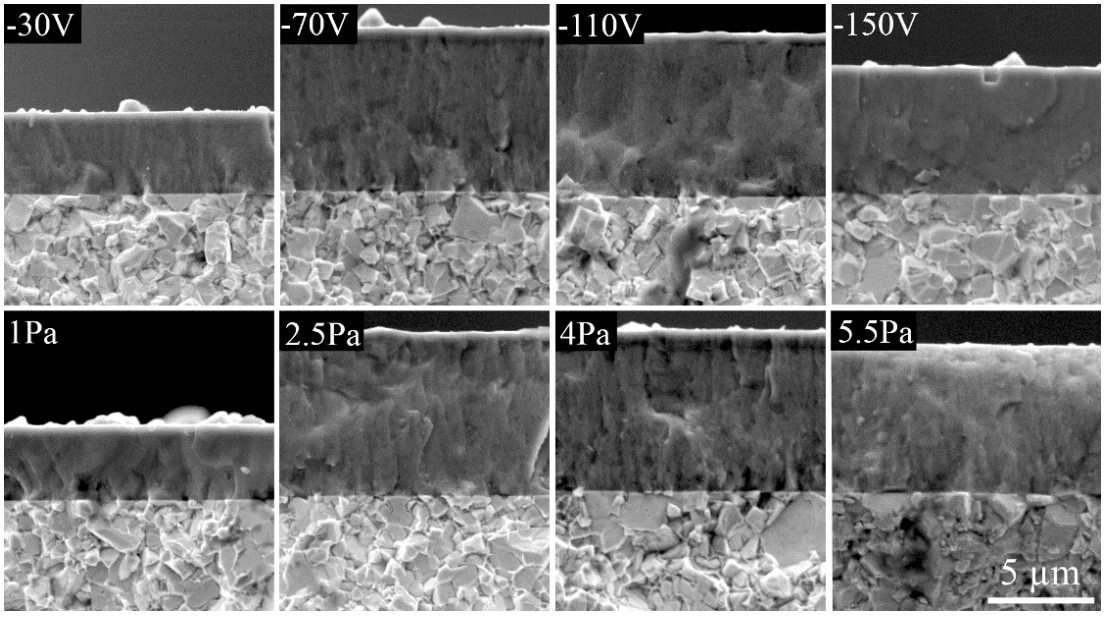

Figure 3.5. SEM fracture cross section of TiAlN coating deposited under various *substrate bias voltage and nitrogen pressure.*

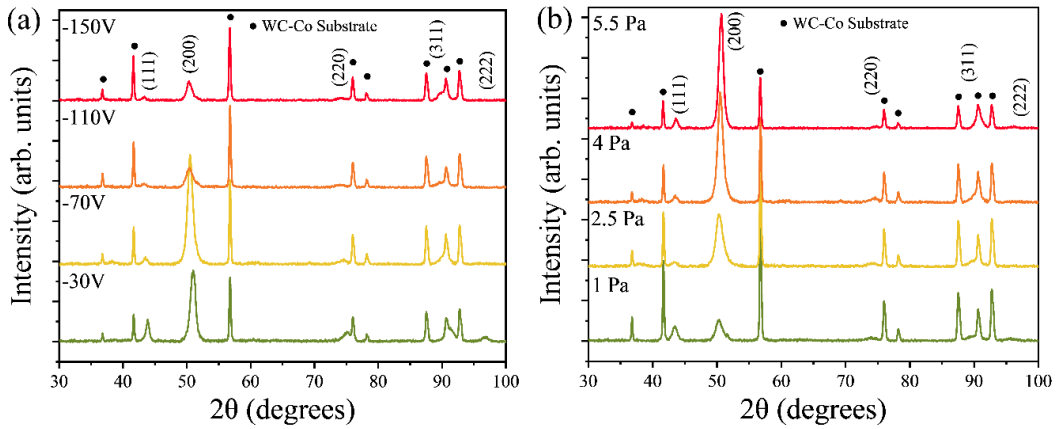

Figure 3.6. *X-Ray pattern of coatings deposited at various substrate bias voltages (a) and various nitrogen pressures (b).*

3.3.4. Residual stress

Residual stress is one of the most important factors of PVD coatings affecting its properties and performance. This residual stress mainly originates from the growth process and difference in coefficient of thermal expansion (CTE) between the coating and substrate (Teixeira, 2002). In general, PVD coatings are under compressive residual stress of -2 to -5 GPa, which increases the coating resistance to indentation and cracking (PalDey and Deevi, 2003; Höling *et al.*, 2005). The variation of residual stress for the deposited TiAlN coatings with respect to substrate bias voltage and nitrogen pressure is presented in fig. 3.7. An average compressive residual stress of -0.48 GPa was observed at a substrate bias voltage of -30 V with its value increasing at a higher bias voltage, resulting in a compressive residual stress value of -3.29 GPa at -150 V. An opposite trend was observed with nitrogen pressure, as compressive residual stress decreased from -4.72 GPa at a nitrogen pressure of 1 Pa to -0.64 GPa at a nitrogen pressure of 5.5 Pa. This change in residual stress with the mentioned process parameters is well known to be due to the change

in ion bombardment energy as higher bombardment energy results in higher compressive residual stress in the coating (Lewis *et al.*, 2004). As mentioned, it is a unique ability of the SFC technology to produce a dense thick coating under very low (less than -1GPa) compressive residual stresses which would not be achievable with other deposition methods.

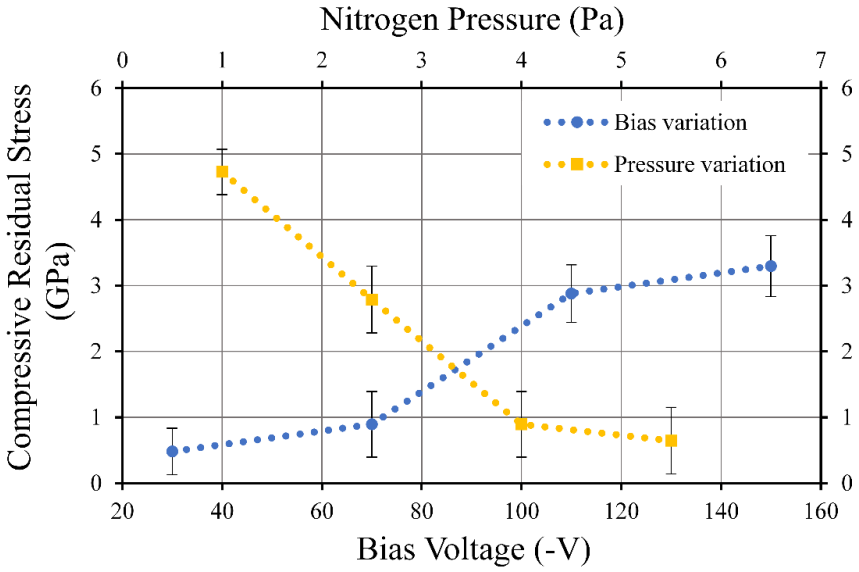

Figure 3.7. *Variation of mean residual stress of the coating with bias voltage and nitrogen pressure.*

3.3.5. Coating Properties

Table 3.2 presents various characteristics of the deposited TiAlN coatings. In general, hardness, elastic modulus and surface roughness of a PVD coating, can be affected by grain size (Hall Petch effect), residual stress, texture, macroparticle density and composition. In this context, there seems to be a very minor difference in the deposited coatings characteristics as multiple factors are affecting each property. As an example, hardness seems to be mostly affected by compressive residual stress as it is following a similar trend.

On the other hand, the impact of macroparticle density on hardness seems to be insignificant.

Adhesion of the deposited coatings presented by Lc_2 seems to decrease with substrate bias voltage. In this regard Zhang et al. (Zhang *et al.*, 2012) mentioned that as bombardment energy is increased, two opposing factors are affecting adhesion of the coating. At a higher bombardment energy, the implantation of atoms is enhanced which can increase adhesion, however this also increases the compressive residual stress which can reduces the overall adhesion of the coating by introducing stresses in the interface. It should be also noted that thickness has a major impact in adhesion measured from scratch test as similar load produces higher stresses in the coating/substrate interface with a thinner coating (Bull and G.-Berasetegui, 2006). Since deposition time is fixed in this study, the thickness varies and therefore lower Lc2 was seen in bias voltage of -30 V.

Table 3.2. *Characteristics of the deposited coatings.*

Bias Voltage (V)	N_2 pressure (Pa)	Thickness (µm)	Hardness (GPa)	Elastic Modulus (GPa)	Surface Roughness - S_a (nm)	Lc_2 (N)
-30	4	5.3 ± 0.1	30.1 ± 2.5	521.6 ± 75.2	336 ± 4	21.3 ± 0.6
-70	4	8.9 ± 0.2	33.3 ± 3.0	446.3 ± 53.9	528 ± 5	33.7 ± 1.6
-110	4	8.3 ± 0.2	34.0 ± 2.0	433.0 ± 30.1	416 ± 13	27.7 ± 1.1
-150	4	7.8 ± 0.1	34.6 ± 2.9	456.4 ± 23.3	452 ± 7	23.2 ± 1.1
-70	1	6.2 ± 0.1	36.8 ± 2.8	467.0 ± 47.6	460 ± 9	20.5 ± 2.0
-70	2.5	8.7 ± 0.2	35.4 ± 2.6	453.6 ± 43.3	497 ± 3	30.3 ± 1.1
-70	4	8.9 ± 0.2	33.3 ± 3.0	446.3 ± 53.9	528 ± 5	33.7 ± 1.6
-70	5.5	7.9 ± 0.2	33.3 ± 2.5	470.4 ± 59.3	546 ± 2	35.3 ± 0.3

Overall, all the deposited coatings show insignificant difference in hardness and elastic modulus. However, from a practical standpoint target poisoning should be avoided and high deposition rate is preferred. Moreover, high coating adhesion is necessary for machining

application. Therefore, according to the schematic shown in fig. 3.8, substrate bias voltage of -70Pa to -110Pa and nitrogen pressure of 2.5Pa to 4Pa is the ideal range of deposition parameters for machining application.

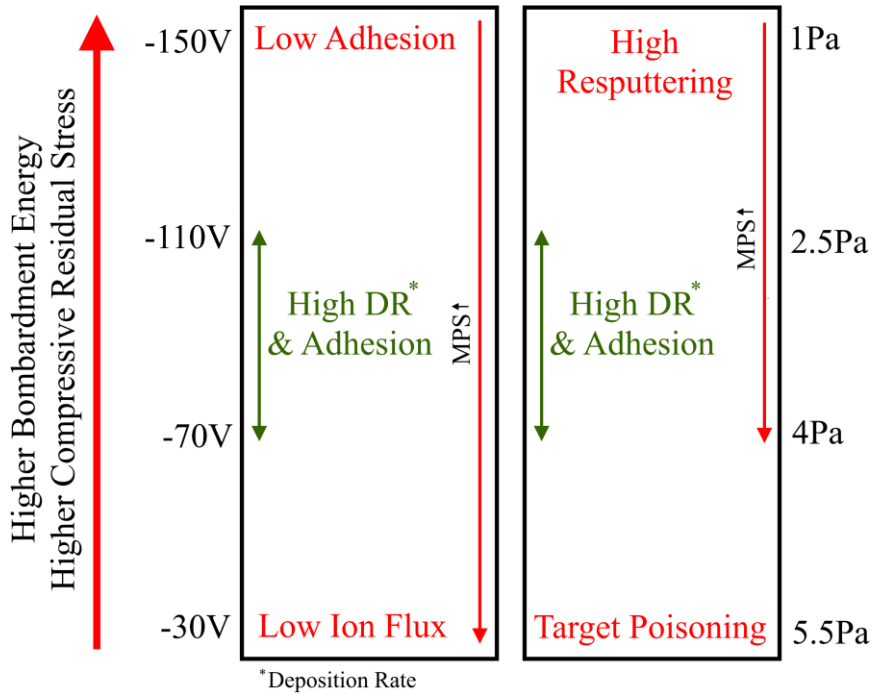

Figure 3.8. *Schematic effect of deposition parameters.*

3.4. Machining Tests

Machining test was done with the purpose of showing the effect residual stress on tool performance and wear pattern. With residual stress as the main criteria, TiAlN coatings deposited at a nitrogen pressure of 4Pa and bias voltage of -70V and -110V were chosen for machining studies. The selected coatings are under compressive residual stress of -0.89 GPa and -2.87 GPa respectively while maintaining a close and acceptable range of

mechanical properties. As mentioned, the purpose of the machining experiment is to elaborate the importance of residual stress and its effect on wear pattern.

As it can be seen in fig. 3.9, a 40% higher tool life was achieved with the TiAlN coating deposited at a -70 V bias voltage compared to the coating deposited at a -110 V bias voltage. Initial cutting forces in fig. 3.10(a), shows insignificant difference between two coatings as similar geometry and edge radius (25-27 µm) was achieved in both tools. Moreover, as illustrated in fig. 3.10(b), less workpiece material is sticking to the coating under lower bias voltage at different cutting stages. To investigate the difference in the wear pattern of the aforementioned coatings, cutting edges were studied at different cutting lengths using SEM as shown in fig. 3.11. A high degree of built-up edge formation was observed on the TiAlN coating deposited at -110 V, whereas the built-up edge seems to be drastically lower on the TiAlN coating deposited at -70 V. Moreover, there are signs of flaking on the coating, which indicates the presence of cohesive failure with lower residual stress. BUE formation in dry machining of CGI has been observed by many researchers as adhesion is the dominant wear mode in dry condition and the sticking material is mentioned to be ferrite (Rosa *et al.*, 2010; Nayyar *et al.*, 2013). This condition leads to removal of material from tool/coating system as the unstable sticking material or BUE gets removed and redeposited during the cutting process. As mentioned, this wear process seems to be less aggressive or delayed in the coating deposited under lower bias voltage despite its similar characteristics (except residual stress) to coating deposited at -110 V bias. Therefore, this behavior can be linked to difference in compressive residual stress value of the coatings.

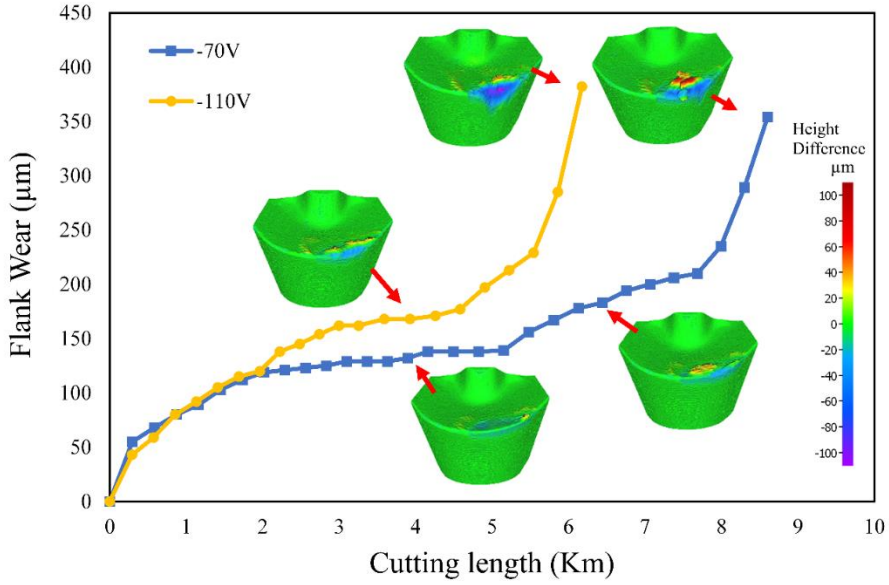

Figure 3.9. *Tool life behavior of selected coatings.*

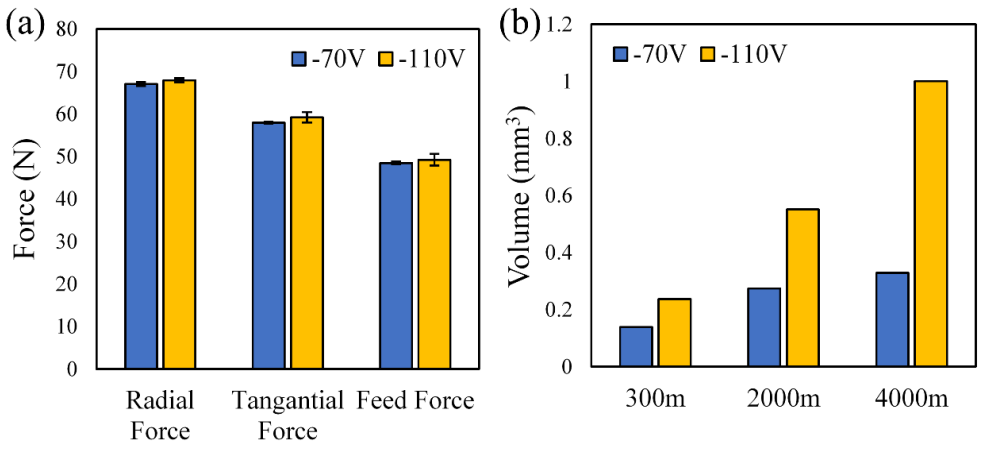

Figure 3.10. *Initial cutting forces (a) and volume of material sticking on the tool (b).*

Regarding the role of residual stress in machining, it is reported that for protecting the tool, compressive residual stress is needed to prevent cohesive failure of the coating (Breidenstein and Denkena, 2013). However, there is an upper limit and increasing the compressive residual stress after a critical value can result in coating and tool failure due to poor adhesion. Therefore, a compromise between good adhesion and cohesive failure

resistance should be applied. However, this research contends that low compressive residual stress and low cohesive failure resistance of the coating can be beneficial in some cases as it reduces adhesive wear and built-up edge formation. In case of the coating with low compressive residual stress, when adhesion occurs between the generated chip and the TiAlN coating, the sticking material gets removed due to easily generation of cracks and failure of the coating within itself (cohesive failure). This leads to partial flaking of the coating and built-up edge formation which can be seen in fig. 3.11. In contrast with a high value of compressive residual stress (TiAlN coating deposited at -110V), sticking material accumulates on the cutting edge, which results in removal of chunks of coating/tool material as previously showed by the authors (Abdoos *et al.*, 2019). Therefore, gradual coating removal or the partial flaking mechanism of the coating under low compressive residual stress increases tool life under dominance of adhesive wear.

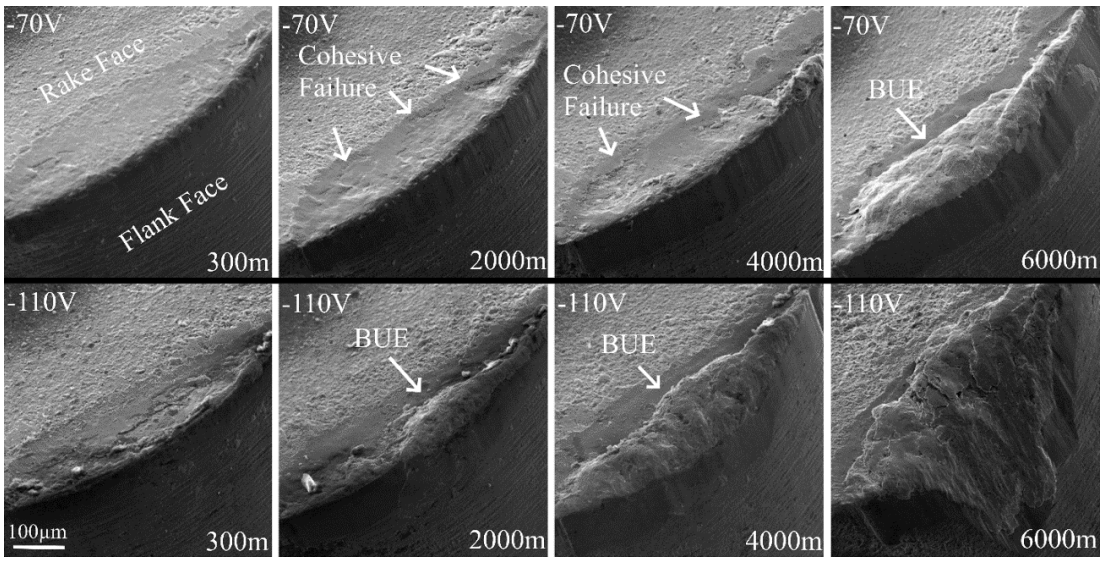

Figure 3.11. Progression of tool wear with low (-70V bias voltage) and high residual *stress coating (-110V bias voltage) at 2000m of cut intervals.*

3.5. Conclusions

The purpose of this study was to introduce a strategy to reduce adhesion damage and formation of built-up edge and subsequently improve tool life through the adjustment of deposition parameters of TiAlN SFC PVD coating. It was found that value of the residual stress is one the main factors controlling the failure mode of the coating subjected to sticking and attrition wear. With the implementation of low compressive residual stresses during the deposition of a thick TiAlN coating, a 40% improvement in tool life was achieved. Moreover, the mentioned coating showed lower built-up edge formation. The following is a summary of main findings of this research:

- The majority of coating properties can be controlled during deposition with varying substrate bias voltage and nitrogen pressure. These properties are under the influence of bombardment energy, re-sputtering effect, and target poisoning. The bombardment energy increases with substrate bias voltage and reduces with nitrogen pressure, while the re-sputtering of the already deposited atoms follows the same trend. It is also worth mentioning that, in the current study target poisoning was dominant at a nitrogen pressure of 5.5 Pa.

- All deposited TiAlN coatings featured a dense columnar structure with preferential orientation of (200) since low strain energy is generated during deposition. Change in composition with bias voltage and nitrogen pressure is insignificant.

- Coating macroparticle density decreased with substrate bias voltage and increased with nitrogen pressure up to 4Pa. In all the cases macroparticle density was significantly low and therefore showed no effect on hardness.
- Variation of hardness and elastic modulus with deposition parameters was found to be insignificant. Hardness was increased slightly at a higher bias voltage and lower nitrogen pressure which can be attributed to higher compressive residual stresses.
- Residual stress is the main affected property during deposition, which directly increases with the bombardment energy. Tool life and coating failure mechanisms are highly dependent on the residual stress of the coating. A lower compressive residual stress proved to be favorable in the presence of adhesive wear since it lowers sticking and built of edge formation. In this regard coating deposited under substrate bias voltage of -70V and nitrogen pressure of 4Pa showed the best performance.

3.6. References

Abdoos, M. et al. (2019) ‘Effect of coating thickness on the tool wear performance of low stress TiAlN PVD coating during turning of compacted graphite iron (CGI)’, Wear. Elsevier B.V., 422–423(January), pp. 128–136. doi: 10.1016/j.wear.2019.01.062.

Abele, E., Sahm, A. and Schulz, H. (2002) ‘Wear Mechanism when Machining Compacted Graphite Iron’, CIRP Annals - Manufacturing Technology, 51(1), pp. 53–56. doi: 10.1016/S0007-8506(07)61464-4.

Ahlgren, M. and Blomqvist, H. (2005) ‘Influence of bias variation on residual stress and texture in TiAlN PVD coatings’, Surface and Coatings Technology, 200(1-4 SPEC. ISS.), pp. 157–160. doi: 10.1016/j.surfcoat.2005.02.078.

Bar-Hen, M. and Etsion, I. (2017) ‘Experimental study of the effect of coating thickness and substrate roughness on tool wear during turning’, Tribology International, 110, pp. 341–347. doi: 10.1016/j.triboint.2016.11.011.

Bouzakis, K. D. et al. (2004) ‘The effect of coating thickness, mechanical strength and hardness properties on the milling performance of PVD coated cemented carbides inserts’, Surface and Coatings Technology, 177–178(178), pp. 657–664. doi: 10.1016/j.surfcoat.2003.08.003.

Breidenstein, B. and Denkena, B. (2013) ‘Significance of residual stress in PVD-coated carbide cutting tools’, CIRP Annals - Manufacturing Technology, 62(1), pp. 67–70. doi: 10.1016/j.cirp.2013.03.101.

Bubenzer, A. et al. (1983) ‘Rf-plasma deposited amorphous hydrogenated hard carbon thin films: Preparation, properties, and applications’, Journal of Applied Physics, 54(8), pp. 4590–4595. doi: 10.1063/1.332613.

Bujak, J., Walkowicz, J. and Kusiński, J. (2004) ‘Influence of the nitrogen pressure on the structure and properties of (Ti,Al)N coatings deposited by cathodic vacuum arc PVD process’, Surface and Coatings Technology, 180–181, pp. 150–157. doi: 10.1016/j.surfcoat.2003.10.058.

Bull, S. J. and G.-Berasetegui, E. (2006) ‘An overview of the potential of quantitative coating adhesion measurement by scratch testing’, Tribology and Interface Engineering Series, 51, pp. 136–165. doi: 10.1016/S0167-8922(06)80043-X.

Cai, F. et al. (2011) ‘Effect of nitrogen partial pressure on Al-Ti-N films deposited by arc ion plating’, Applied Surface Science, 258(5), pp. 1819–1825. doi: 10.1016/j.apsusc.2011.10.053.

Cai, F. et al. (2017) ‘Influence of negative bias voltage on microstructure and property of Al-Ti-N films deposited by multi-arc ion plating’, Ceramics International, 43(4), pp. 3774–3783. doi: 10.1016/j.ceramint.2016.12.019.

Carrasco, C. A. et al. (2002) ‘The relationship between residual stress and process parameters in TiN coatings on copper alloy substrates’, Materials Characterization, 48(1), pp. 81–88. doi: 10.1016/S1044-5803(02)00256-5.

Chokwatvikul, C., Larpkiattaworn, S. and Surinphong, S. (2011) ‘Effect of Nitrogen Partial Pressure on Characteristic and Mechanical Properties of Hard Coating TiAlN Film’, Journal of Metals, Materials and Minerals, 21(1), pp. 115–119.

Dawson, S. and Schroeder, T. (2004) ‘Practical applications for compacted graphite iron’, AFS Transactions, 47(05), pp. 1–9.

Denkena, B. and Breidenstein, B. (2008) ‘Influence of the residual stress state on cohesive damage of PVD-coated carbide cutting tools’, Advanced Engineering Materials, 10(7), pp. 613–616. doi: 10.1002/adem.200800063.

Denkena, B. and Breidenstein, B. (2012) ‘Residual stress distribution in PVD-coated carbide cutting tools - origin of cohesive damage’, Tribology in Industry, 34(3), pp. 158–165.

Devia, D. M. et al. (2011) ‘TiAlN coatings deposited by triode magnetron sputtering varying the bias voltage’, Applied Surface Science, 257(14), pp. 6181–6185. doi: 10.1016/j.apsusc.2011.02.027.

Elmkhah, H. et al. (2016) ‘Surface characteristics for the Ti-Al-N coatings deposited by high power impulse magnetron sputtering technique at the different bias voltages’, Journal of Alloys and Compounds, 688, pp. 820–827. doi: 10.1016/j.jallcom.2016.07.013.

Grigoriev, S. N. et al. (2017) ‘Comparative analysis of cutting properties and nature of wear of carbide cutting tools with multi-layered nano-structured and gradient coatings produced by using of various deposition methods’, The International Journal of Advanced Manufacturing Technology, 90(9–12), pp. 3421–3435. doi: 10.1007/s00170-016-9676-z.

He, B. B. (2003) ‘Introduction to two-dimensional X-ray diffraction’, Powder Diffraction, 18(02), pp. 71–85. doi: 10.1154/1.1577355.

Höling, A. et al. (2005) ‘Mechanical properties and machining performance of Ti1-xAlxN-coated cutting tools’, Surface and Coatings Technology, 191(2–3), pp. 384–392. doi: 10.1016/j.surfcoat.2004.04.056.

Lewis, D. B. et al. (2004) ‘Interrelationship between atomic species, bias voltage, texture and microstructure of nano-scale multilayers’, Surface and Coatings Technology, 184(2–3), pp. 225–232. doi: 10.1016/j.surfcoat.2003.11.005.

Li, M. and Wang, F. (2003) ‘Effects of nitrogen partial pressure and pulse bias voltage on (Ti,Al)N coatings by arc ion plating’, Surface and Coatings Technology, 167(2–3), pp. 197–202. doi: 10.1016/S0257-8972(02)00895-2.

Nayyar, V. et al. (2013) ‘Machinability of compacted graphite iron (CGI) and flake graphite iron (FGI) with coated carbide’, International Journal of Machining and Machinability of Materials, 13(1), p. 67. doi: 10.1504/IJMMM.2013.051909.

PalDey, S. and Deevi, S. (2003) ‘Single layer and multilayer wear resistant coatings of (Ti, Al) N: a review’, Materials Science and Engineering: A, 342, pp. 58–79. doi: 10.1016/S0921-5093(03)00473-8.

Raveh, A. et al. (1999) Graded Al-AlN, TiN, and TiAlN multilayers deposited by radio-frequency reactive magnetron sputtering, Surface and Coatings Technology. doi: 10.1016/S0257-8972(99)00054-7.

Rosa, S. do N. et al. (2010) ‘Analysis of Tool Wear , Surface Roughness and Cutting Power in the Turning Process of Compact Graphite Irons with Different Titanium Content’, Journal of the Brazilian Society of Mechanical Sciences and Engineering, 32(3), pp. 234–240. doi: 10.1590/S1678-58782010000300006.

Skordaris, G. et al. (2016) ‘Film thickness effect on mechanical properties and milling performance of nano-structured multilayer PVD coated tools’, Surface and Coatings Technology, 307, pp. 452–460. doi: 10.1016/j.surfcoat.2016.09.026.

Skordaris, G. et al. (2017) ‘Effect of PVD film’s residual stresses on their mechanical properties, brittleness, adhesion and cutting performance of coated tools’, CIRP Journal of

Manufacturing Science and Technology. Elsevier, 18, pp. 145–151. doi: 10.1016/j.cirpj.2016.11.003.

Skordaris, G. et al. (2018) ‘Bias voltage effect on the mechanical properties, adhesion and milling performance of PVD films on cemented carbide inserts’, Wear, 404–405, pp. 50–61. doi: 10.1016/j.wear.2018.03.001.

de Sousa, J. A. G., Sales, W. F. and Machado, A. R. (2018) ‘A review on the machining of cast irons’, International Journal of Advanced Manufacturing Technology. The International Journal of Advanced Manufacturing Technology, 94(9–12), pp. 4073–4092. doi: 10.1007/s00170-017-1140-1.

Su, G. S. et al. (2016) ‘Effects of high-pressure cutting fluid with different jetting paths on tool wear in cutting compacted graphite iron’, Tribology International, 103, pp. 289–297. doi: 10.1016/j.triboint.2016.06.029.

Taghavi Pourian Azar, G., Er, D. and Ürgen, M. (2018) ‘The role of superimposing pulse bias voltage on DC bias on the macroparticle attachment and structure of TiAlN coatings produced with CA-PVD’, Surface and Coatings Technology, 350, pp. 1050–1057. doi: 10.1016/j.surfcoat.2018.02.066.

Teixeira, V. (2001) ‘Mechanical integrity in PVD coatings due to the presence of residual stresses’, in Thin Solid Films, pp. 276–281. doi: 10.1016/S0040-6090(01)01043-4.

Teixeira, V. (2002) ‘Residual stress and cracking in thin PVD coatings’, Vacuum, 64(3–4), pp. 393–399. doi: 10.1016/S0042-207X(01)00327-X.

Tillmann, W. et al. (2013) ‘Influence of bias voltage on residual stresses and tribological properties of TiAlVN-coatings at elevated temperatures’, Surface and Coatings Technology, 231, pp. 122–125. doi: 10.1016/j.surfcoat.2012.03.012.

Tooptong, S., Park, K. H. and Kwon, P. (2018) ‘A comparative investigation on flank wear when turning three cast irons’, Tribology International. Elsevier Ltd, 120(December 2017), pp. 127–139. doi: 10.1016/j.triboint.2017.12.025.

Tuffy, K., Byrne, G. and Dowling, D. (2004) ‘Determination of the optimum TiN coating thickness on WC inserts for machining carbon steels’, Journal of Materials Processing Technology, 155–156(1–3), pp. 1861–1866. doi: 10.1016/j.jmatprotec.2004.04.277.

Vaz, F. et al. (2005) ‘Influence of nitrogen content on the structural, mechanical and electrical properties of TiN thin films’, Surface and Coatings Technology, 191(2–3), pp. 317–323. doi: 10.1016/j.surfcoat.2004.01.033.

Warcholinski, B. et al. (2012) ‘An analysis of macroparticle-related defects on CrCN and CrN coatings in dependence of the substrate bias voltage’, in Vacuum, pp. 1235–1239. doi: 10.1016/j.vacuum.2011.04.023.

Yamamoto, K. et al. (2018) ‘Cutting Performance of Low Stress Thick TiAlN PVD Coatings during Machining of Compacted Graphite Cast Iron (CGI)’, Coatings, 8(2), p. 38. doi: 10.3390/coatings8010038.

Yongqiang, W. et al. (2018) ‘Characterization and mechanical properties of TiN/TiAlN multilayer coatings with different modulation periods’, International Journal of Advanced

Manufacturing Technology. The International Journal of Advanced Manufacturing Technology, 96(5–8), pp. 1677–1683. doi: 10.1007/s00170-017-0832-x.

Yu, D. et al. (2008) 'Optimization of hybrid PVD process of TiAlN coatings by Taguchi method', Applied Surface Science. North-Holland, 255, pp. 1865–1869. doi: 10.1016/j.apsusc.2008.06.204.

Zhang, G. P. et al. (2012) 'Influence of pulsed substrate bias on the structure and properties of Ti-Al-N films deposited by cathodic vacuum arc', Applied Surface Science, 258(19), pp. 7274–7279. doi: 10.1016/j.apsusc.2012.03.100.

Zhou, T. et al. (2009) 'Influence of N2partial pressure on mechanical properties of (Ti,Al)N films deposited by reactive magnetron sputtering', Vacuum, 83(7), pp. 1057–1059. doi: 10.1016/j.vacuum.2009.01.001.

Chapter 4. Influence of Residual Stress

Abdoos, M., Bose, B., Rawal, S., Arif, A. F. M., & Veldhuis, S. C. (2020). The influence of residual stress on the properties and performance of thick TiAlN multilayer coating during dry turning of compacted graphite iron. Wear, 203342.

Author's Contribution

Majid Abdoos	Designed and conducted the experiments Analyzed the results Wrote the manuscript
Bipasha Bose	Assisted with coating characterization
Sushant Rawal	Assisted with experiment design Assisted with coating deposition
Abul Fazel Arif	Assisted with experimental design Assisted writing and editing the manuscript
Stephen Veldhuis	Supervised the project Edited the manuscript

Abstract

TiAlN is one of the most widely used physical vapor deposition (PVD) coatings in the manufacturing industry. Naturally, the performance of this coating is dependent on its properties, which can be tuned and optimized according to the application. Residual stress is one of the properties which affects hardness, fracture toughness, and adhesion of the coating. Although it is difficult to make a general recommendation for what residual stress values are desirable, individual recommendations can be made based on a specific workpiece material and tool wear mechanism. In this regard, adhesion wear and the formation of built-up edge were identified as the dominant wear mechanism during dry turning of compacted graphite iron and a coating's residual stress should be adjusted to minimize the damage from adhesion wear. Therefore, the present work investigates cutting performance and related coating properties of multilayer thick TiAlN coating with different residual stress designs. For this purpose, residual stress was adjusted by varying the substrate bias voltage during the deposition process. The effect of residual stress on properties such as hardness, yield strength, and adhesion were studied by nanoindentation and scratch tests. Moreover, the dominant wear pattern, especially on the rake face and cutting edge, was thoroughly studied using a scanning electron microscope (SEM). The results showed increased mechanical properties such as hardness and yield strength with higher substrate bias voltages and therefore higher residual stresses. However, the coating with the lowest compressive residual stress outperformed the other coatings during machining due to a combination of high adhesion to the substrate and low as-deposited defects which effectively delayed cutting-edge exposure.

Keywords

PVD coatings; Cutting tools; Residual stress; Compacted graphite iron; Dry turning; Adhesion wear

4.1. Introduction

Physical vapour deposition (PVD) coatings are commonly used in the manufacturing industry to enhance the mechanical, tribological, and thermal properties of cutting tools. Consequently, a coated tool can provide lower machining costs, improved tool performance, and increased productivity in machining difficult to machine materials, such as compacted graphite iron (CGI) (Bobzin, 2016). Due to its superior mechanical properties and unique structure of graphite, compacted graphite iron is the ideal candidate for replacing grey cast iron in the automotive industry. In this regard Dawson (Dawson and Schroeder, 2004) mentioned that a weight and volume reduction of 10-30%, lower emissivity and higher efficiency is expected in engine blocks when replacing grey cast iron with CGI. However, CGI has a significantly reduced tool life in machining, especially in continuous cutting operations. For this reason, application of CGI is limited as CGI engines are not cost-efficient. Thus, to solve this problem and overcome the difficulties in machining of CGI there is a need for better tooling and coating design. The poor machinability of CGI compared to grey cast iron is mainly attributed to the following factors: lack of sulfur and the ability to form a protective tribolayer during machining (Heck *et al.*, 2008), lack of lubricious graphite and high adhesion to the tool (Nayyar *et al.*, 2013), higher hardness (Nayyar *et al.*, 2012) and higher cutting temperature (Tooptong, Park and Kwon, 2018). Therefore, a combination of abrasion, adhesion and built-up edge formation, chipping, and tool fracture is observed depending on the machining process (Wang *et al.*, 2017; Tooptong, Park and Kwon, 2018). Generally, in wet machining of CGI, abrasion is the dominant wear mode, and under dry cutting conditions, adhesion, built-up edge

formation, and chipping are more significant (Rosa *et al.*, 2010; Su *et al.*, 2016). Sticking of the workpiece material, followed by built-up edge formation, triggers a subsequent attrition mechanism which gradually removes coating/tool material and destroys the cutting edge (Rosa *et al.*, 2010). Naturally, these factors should all be considered for selecting a proper coating and tailoring its properties for machining CGI. To this end, recent studies done by the authors revealed residual stress to be a crucial factor in determining coating life when facing adhesion wear (Abdoos *et al.*, 2019, 2020).

In general, stress in a PVD coating is generated by (i) interactions of the microstructure and defects during coating growth, (ii) peening of the already deposited coating by high energy particles, and (iii) cooling from the initial deposition temperature due to differences in the coefficient of thermal expansion (CTE) between the coating and substrate (Teixeira, 2001, 2002). The magnitude of the generated residual stress depends on the deposition parameters, such as the substrate bias voltage and reactive gas pressure (Cai *et al.*, 2017). Naturally, this residual stress, mostly compressive in nature, is associated with other coating properties such as adhesion, fracture toughness, and hardness (Denkena and Breidenstein, 2008; Breidenstein *et al.*, 2016). Aside from deposition parameters, residual stress is often impacted by post processing such as hard particle micro blasting (Tanaka *et al.*, 2016) and annealing, (Fox-Rabinovich *et al.*, 2008) or through architecture and interlayer design (Bemporad *et al.*, 2006; Ali, Sebastiani and Bemporad, 2015). In cutting applications, compressive residual stress is often preferred as it enhances mechanical properties, such as hardness, and delays crack initiation and propagation (G Skordaris *et al.*, 2017). Thus, high compressive residual stress is generally associated with better cutting

performance. Prior studies in this area have shown an improvement to hardness, cohesion, yield, and rupture stress by increasing residual stress (Skordaris *et al.*, 2018). However, this effect is known to plateau at a certain point. For instance, enhancements in mechanical properties of TiAlN coatings with compressive residual stresses higher than 2 GPa were found insignificant (G Skordaris *et al.*, 2017). Instead, with residual stresses higher than this, the coating becomes brittle, and fracture occurs at a lower plastic deformation level (Bouzakis, G. Skordaris, *et al.*, 2011). Additionally, an increase in stress at the coating/substrate interface results in reduced adhesion, which leads to complete delamination in extreme cases (M Ahlgren and Blomqvist, 2005). Similarly, an accumulation of compressive stress during coating growth may result in premature coating delamination, thus limiting coating thickness (Tuffy, Byrne and Dowling, 2004). To address this problem, several attempts have been made in order to produce functional graded coatings by generating a combination of low compressive stress at the coating/substrate interface and high compressive residual stress at the surface. This provided strong adhesion with sufficient mechanical properties that increased tool life (Uhlmann and Klein, 2000). However, previous studies are mainly focused on optimizing residual stress for a certain coating or process. For instance, a recent study found that a compressive residual stress of 2-3 GPa is optimal for TiAlN coatings used in turning (G Skordaris *et al.*, 2017). However, in the current study, the authors presented that a wear mechanism-based approach would be more beneficial for studying the effects of residual stress.

Previously, the authors attempted to address the problems associated with dry machining of CGI by increasing the thickness of multilayer TiAlN coatings up to 17µm (Abdoos *et al.*, 2019). This was done by carefully adjusting the substrate bias voltage during deposition using a technology called super fine cathode (SFC) and resulted in the deposition of TiAlN coatings under compressive residual stresses as low as 500 MPa. These coatings outperformed commercial coatings because they delayed substrate exposure and reduced sticking and built-up edge formation. Next, the effect of deposition parameters on properties, especially on residual stress and the tool life of monolayer TiAlN coatings, was extensively studied (Abdoos, Rawal, *et al.*, 2020b). Contrary to the previous literature, a coating deposited with low compressive residual stress outperformed high compressive residual stress coatings that were subject to adhesion wear, despite its weaker mechanical properties. Upon further investigation, it was found that coatings with low compressive residual stress reduced the accumulation of sticking material on the cutting edge, delayed the formation of built-up edge, and improved tool life as well as product quality. It was concluded that this phenomenon is a result of residual stress and its effect on coating adhesion/cohesion behaviour. Although several studies discuss the effects of residual stress on coating performance, there is no information on the wear pattern, or the mechanisms affected by it. Moreover, high compressive residual stress might not always be beneficial. As the authors previously stated (Abdoos *et al.*, 2019), coatings that have low compressive residual stress might trigger a beneficial wear pattern under certain conditions.

The aim of this research work is to optimize and develop thick PVD TiAlN coatings that resolves the challenges and issues encountered while machining CGI that limits it

application for CGI in the automotive industry. This research work is developed in four stages as mentioned below:

In the first stage, it was demonstrated that thick (around 11µm) multilayer PVD TiAlN coating had longer tool life and excellent machining performance for CGI as compared to commercial TiAlN coatings, 5µm and 17µm thick TiAlN coatings (Abdoos *et al.*, 2019).

In the second stage, thick (11µm) monolayer TiAlN coating was optimized and the effect of the bias voltage and deposition pressure on various properties, residual stress and machining performance of CGI was reported (Abdoos, Rawal, *et al.*, 2020a).

In this third stage, the objective of the current research work is to investigate further the effects of residual stress on the properties, cutting edge quality, tool performance, and wear pattern of thick multilayer TiAlN coatings, focusing on adhesion wear during the machining of CGI. For this purpose, three thick, multilayer TiAlN coatings (around 11µm) with different target residual stress values were designed and deposited using the SFC technique at different combinations of substrate bias voltages, which were determined based on the findings reported in the stage two of these studies as mentioned above (Abdoos, Rawal, *et al.*, 2020a).

The fourth stage planned as a future work will focus on pre- and post- deposition treatment for the optimized thick multilayer TiAlN coatings as a method to increase coating coverage on the edge and solve the problem with geometrical stresses and the resulting coating breakage while machining CGI.

4.2. Experimental Detail

4.2.1. Sample Preparation

For this study, three different multilayer $Ti_{40}Al_{60}N$ coatings were deposited using a Kobelco AIP-S20 arc ion plating deposition system. This system uses a technology called super fine cathode (SFC) which enables better control for adjusting residual stress and can achieve high coating thicknesses up to 20 µm (Yamamoto *et al.*, 2018). The deposition process was carried out using two targets with a composition of 40 at.% Ti and 60 at.% Al, which were made by powder metallurgy. The multilayer structure was achieved by interrupting the growth process by slightly varying the substrate bias voltages between each layer. Each multilayer coating consisted of repeated bilayers in the range of nanometers (~200 nm), with minor differences in composition or properties caused by alternating the bias voltages. As presented in Table 4.1, the combinations of substrate bias voltages for each coating design were carefully selected based on a previous in-depth study on deposition parameters (Abdoos, Rawal, *et al.*, 2020b). The values were selected to vary the average compressive residual stress within a range of 1-5GPa. In all cases the deposition process started with the lower bias voltage layer to minimize stress at the coating/substrate interface. During the deposition process, only the combination of bias voltage and deposition time were varied, and all other deposition parameters were kept constant. Since bias voltage affects deposition rate and coating thickness (Devia *et al.*, 2011b), the deposition time for each coating was adjusted to get a thickness of around 11 µm. Kennametal CNGG432FS K313 and Sandvik Coromant SPGN120308 inserts were used for machining and characterization studies, respectively. Prior to deposition, the substrates

were all cleaned in acetone using an ultrasonic cleaner. The substrates were then mounted in the chamber, heated up to 550° C, and argon etched under a pressure of 1.3 Pa for 7.5 minutes.

4.2.2. Coating Characterization

To ensure that coating thickness was consistent in all the samples, thickness was measured using a BC-2 Miba Coating Group ball crater system and a steel ball with a diameter of 25mm. The residual stress of the coatings was determined on the (200) crystallographic plane using a Bruker D8 Discover 2-dimentional X-Ray diffraction system. This instrument was equipped with a cobalt target with an X-Ray wavelength of 1.79Å. Samples were scanned at six φ and seven ψ positions in the range of 0-257º and 10-50º respectively and the beam was collimated to 0.5 mm. To determine residual stress LEPTOS software was used. It should be also mentioned that as peaks from the WC-Co substrate were observed in the scans, determined residual stress refers to the average residual stress of the entire coating. The surface characteristics of the coatings were studied with an Anton Paar TOSCA 400 atomic force microscope (AFM). Moreover, the mechanical properties of the coatings were characterized using an Anton Parr RST^3 and a NHT^3 nanoindentation tester. Nanoindentation was done with a standard Berkovich tip under the load control mode with a maximum load of 100 mN. The indentation load was selected to limit the indentation penetration depth within 10% of the coating thickness in all the samples. Moreover, the same instrument was used to estimate yield strength using a spheroconical indenter with a tip radius of 20µm. To test the adhesion of the coating, scratch tests were performed using a Rockwell C indenter with a tip radius of 100µm under

a progressive load ranging from 0.5 N to 100 N, a scratch velocity of 7.5 mm/min, and a scratch length of 3mm. After the scratch test, critical failure loads (Lc_1 and Lc_2) were determined with an optical microscope following the ASTM C1624-05 standard.

Table 4.1. *Deposition parameters*

Coating	Bias voltage combination	Nitrogen pressure	Number of bilayers	Table rotation speed	Temperature	Arc source current
C1	-30V/-70V					
C2	-70V/-110V	4 Pa	28	5 rpm	550° C	150 A
C3	-110V/-150V					

4.2.3. Performance Evaluation

To evaluate the performance of the deposited coatings, finish turning was done on compacted graphite iron (CGI) workpiece material under dry cutting conditions. The CGI workpiece used was in the shape of a hollow cylinder with inner and outer diameters of 80 and 120 mm, and a length of 200 mm. The workpiece microstructure, as shown in fig. 4.1, consisted of 70% pearlite and 10% ferrite with a nodularity of 20%. Machining tests were done using a Boehringer VDF-180 lathe under dry cutting conditions with a cutting speed of 300 m/min, depth of cut of 0.25 mm, and feed rate of 0.2 mm/rev. During the machining process, cutting forces were collected with a Kistler dynamometer type 9121, and after each machining pass, flank wear was measured using a Keyence VHX-5000 optical microscope. Moreover, the tools were scanned and analysed at different cutting lengths with a Bruker Alicona InfiniteFocus microscope and a Vega II LSU scanning electron microscope equipped with an Oxford X-Max 80 energy dispersive spectroscopy (EDS). Tool life was considered up to a flank wear of 300µm, following the ISO 3685 standard. To better

understand the wear pattern, the built-up edge on the tool was then etched away with a mixture of nitric and hydrochloric acid.

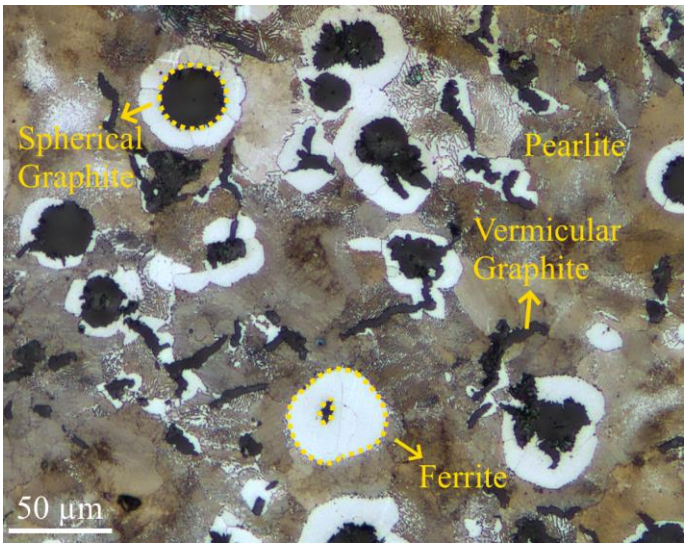

Figure 4.1. *Microstructure of compacted graphite iron.*

4.3. Result and Discussion

4.3.1. Residual Stress and Mechanical Properties of the Coatings

Table 4.2 shows the properties of the deposited multilayer TiAlN coatings. As can be seen in the table, when using a higher negative substrate bias voltage combination, a higher compressive residual stress was achieved. The major contributing factor to higher residual stress is increased ion bombardment energy and higher peening of already deposited atoms at a higher negative substrate bias voltage (Abdoos, Rawal, *et al.*, 2020b). Consequently, slightly higher hardness values were obtained when using a higher negative substrate bias voltage combination. In this case, the compressive residual stress in the coating opposed the stress generated by indentation, which caused the coating to resist indenter penetration (Chen, Yan and Karlsson, 2006). A similar phenomenon was observed by measuring the

yield strength with a spheroconical diamond indenter. Here, a maximum oscillating load of 400 mN with a frequency of 5 Hz and an amplitude of 30mN was applied to collect the required information from each coating. Stress and strain were then calculated from the following equations (Martínez *et al.*, 2003):

$$\varepsilon = 0.2\frac{a}{R} \quad (1)$$

$$\sigma = \frac{P}{K\pi a^2} \quad (2)$$

In these equations, a and R are the contact and indenter radius, respectively, P is the indentation load, and K, or constrain factor, is a constant determined by the deformation behaviour of the tested material. In this case, a constrain factor (K) of 1.5 was used, as suggested by the literature (Clausner and Richter, 2015). The resulting stress-strain curve is presented in fig. 4.2. Yield strength was then determined by recording the transition of the curve from the elastic region to plastic. Average yield strengths of 8.03 GPa, 8.95 GPa, and 10.13 GPa were calculated from fifteen indents for coatings C1, C2, and C3, respectively. The higher yield strength observed is due to compressive residual stress resisting indentation penetration, which is well reported by other researchers (G Skordaris *et al.*, 2017).

Table 4.2. *Properties of the deposited TiAlN coatings*

Coating	Thickness (μm)	Residual Stress (MPa)	Hardness (GPa)	Elastic Modulus (GPa)	Y.S (GPa)
C1	11.6 ± 0.2	-1277 ± 348	31.3 ± 2.4	407.8 ± 38.3	8.0 ± 0.6
C2	10.9 ± 0.2	-2110 ± 412	33.6 ± 3.2	400.9 ± 37.1	8.9 ± 0.6
C3	10.9 ± 0.1	-4483 ± 662	34.4 ± 2.7	417.5 ± 44.9	10.1 ± 0.8

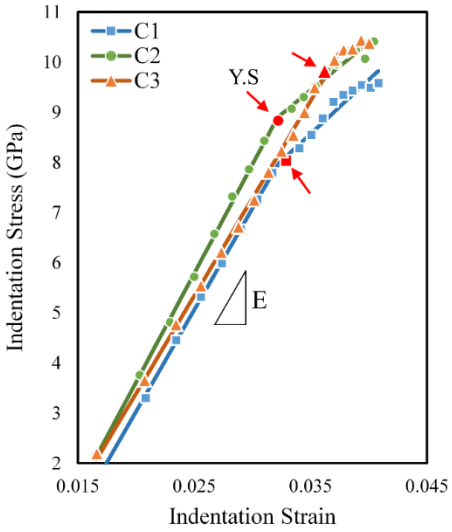

Figure 4.2. *Indentation stress-strain curves of coatings C1 to C3.*

4.3.2. Coating Adhesion

The most significant effect of residual stress was on coating adhesion as lower failure loads were observed when using higher negative bias voltage combinations. Fig. 4.3 shows the depth profile of the scratch tracks, SEM micrographs of the typical adhesive and cohesive failures, and the average critical failure loads. Brittle tensile cracks (A in fig. 4.3) and wedging spallation (B in fig. 4.3) were observed as the first (cohesive) and second (adhesive) modes of failure in all the coatings. The designations Lc_1 and Lc_2 were assigned to the critical loads causing each failure, respectively. Here, arc tensile crack is created by the tensile stress that the indenter generates behind itself, and wedging spallation is created by the compressive stress that the indenter applies in front of itself (Bull and G.-Berasetegui, 2006). In the case of wedging spallation, a crack forms ahead of the scratch path and then propagates in a wedge-shaped form, detaching the coating from the substrate (C in fig. 4.3). The lower Lc_2 values that were observed with higher substrate bias voltage

combination show how residual stress can expedite adhesive failure. Residual stress, in fact, adds to the stress generated in front of the indenter lowering the load necessary for the formation of a crack in the coating/substrate interface that leads to spallation. On the other hand, compressive residual stress also resists crack propagation and as a result, with higher compressive residual stress (for instance, in coating C3), a higher stress is needed for crack propagation. Therefore, the spallation from the test was contained in a smaller area near the scratch track where higher stress concentration was present during the test.

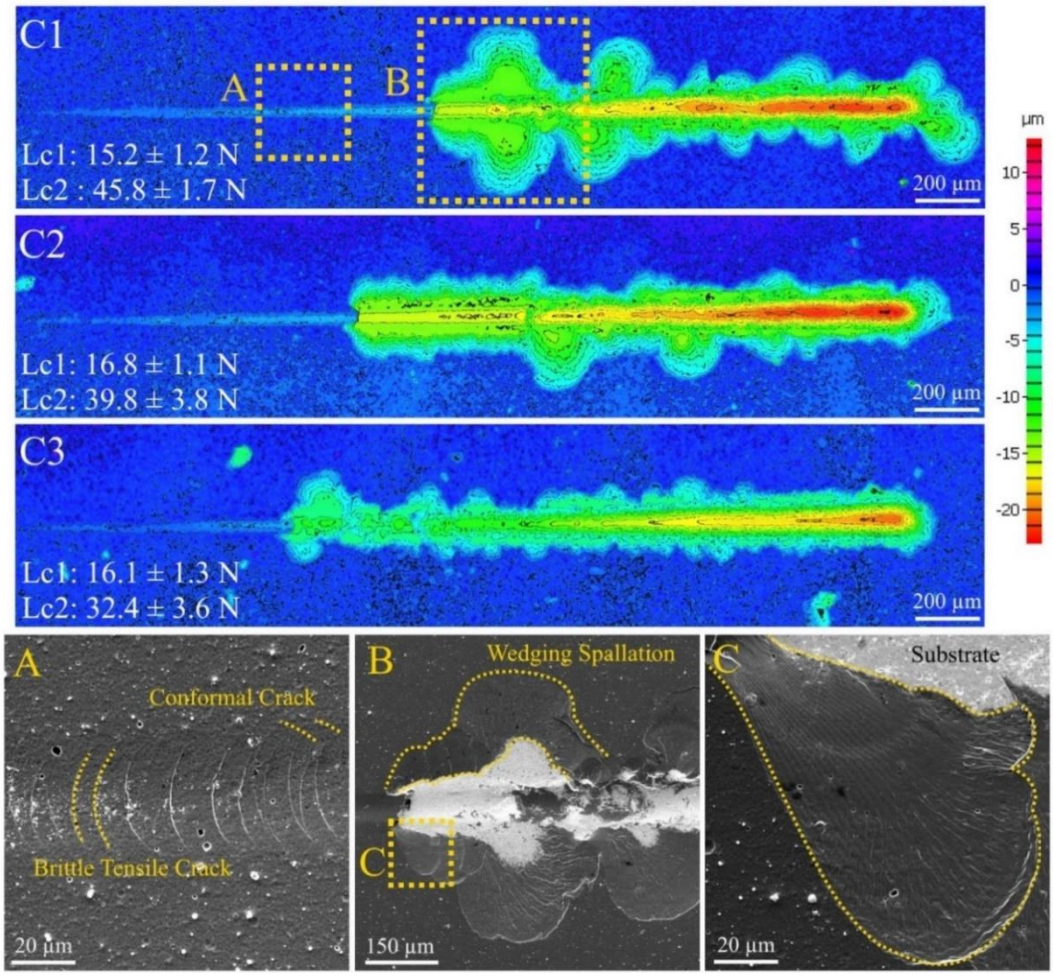

Figure 4.3. *Comparison of the scratch track and SEM micrographs of typical adhesion and cohesion failures in coatings C1 to C3.*

4.3.3. Surface roughness and defects

The surface characteristics of the coatings were studied with an atomic force microscope and a scanning electron microscope. Furthermore, a Bruker Alicona InfiniteFocus microscope was used to measure surface roughness, the results of which are presented in fig. 4.4. According to 3D images from the AFM in fig. 4.4 (a), the topography of the coatings was composed of peaks and valleys randomly distributed on the surface. The lowest surface roughness was observed in coating C1, while in coatings C2 and C3, the density of peaks was more concentrated, resulting in a slightly rougher surface. However, from the SEM micrographs in fig. 4.4 (b) the number of macroparticles appears to decrease with a higher negative substrate bias voltage from C1 to C2 and C3. Macroparticles are droplets of molten material that are separated from the target during the deposition process. These particles are one of main disadvantages of arc deposition systems as they are expected to weaken the mechanical properties and performance of a coating (Cai *et al.*, 2011). The presence of decreasing number of macroparticles under high substrate bias voltage is well reported in the literature and happens because of an increase in bombardment energy (Cai *et al.*, 2017; Abdoos, Rawal, *et al.*, 2020b).

4.3.4. Cutting Edge Condition

Both the geometry and quality of the cutting edges were inspected prior to the machining test to ensure consistency and to eliminate any possible effect of the edge radius on the machining experiment. All the coatings were used in the state in which they were deposited without any post-deposition treatments, which are commercially applied to improve the quality of the cutting edge. Moreover, the deposited TiAlN coatings were

thicker than commercial coatings, and therefore, the microgeometry of the tools was expected to be affected drastically. In this regard, SEM micrographs of typical, as-deposited defects along the cutting edges are presented in fig. 4.5.

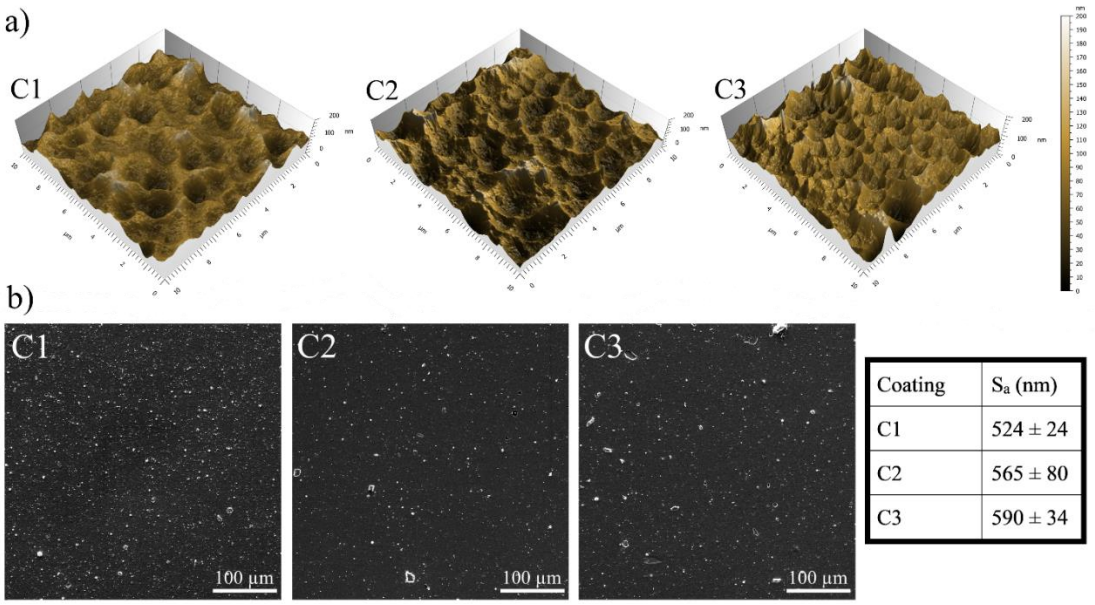

Coating	S_a (nm)
C1	524 ± 24
C2	565 ± 80
C3	590 ± 34

Figure 4.4. *AFM 3D images (a) and SEM micrographs (b) of the surface showing characteristics of the deposited coatings.*

Cohesive failure and microchipping were observed on all the coatings, the extent of which appeared to increase from coating C1 to C3. In extreme cases (coating C3), a high degree of chipping and tool substrate exposure was observed. In this situation, the edge was discarded for the machining test. Here, formation of these defects can be linked to both the complex geometry and residual stress of the coatings. Wiklund et al. (Wiklund, Gunnars and Hogmark, 1999) mentioned that compressive residual stress in a PVD coating can generate normal or shear stresses at the interface if the substrate is not perfectly flat. In the case of a cutting tool, compressive residual stress in the coating generates normal tensile stress at the interface, causing chipping along the cutting edge. Therefore, when high levels

of compressive residual stress are present, increased tensile stress at the interface and additional defects are expected, as observed in coatings C1 to C3. Consequently, when chipping occurs, controlling the edge radius becomes challenging, and decreased coating coverage is expected on the cutting edge, as shown in fig. 4.6. Chipping and coating delamination prior to machining are among the common problems that occur with thick coatings that have high compressive residual stresses (Tuffy, Byrne and Dowling, 2004; M Ahlgren and Blomqvist, 2005; Sargade *et al.*, 2011).

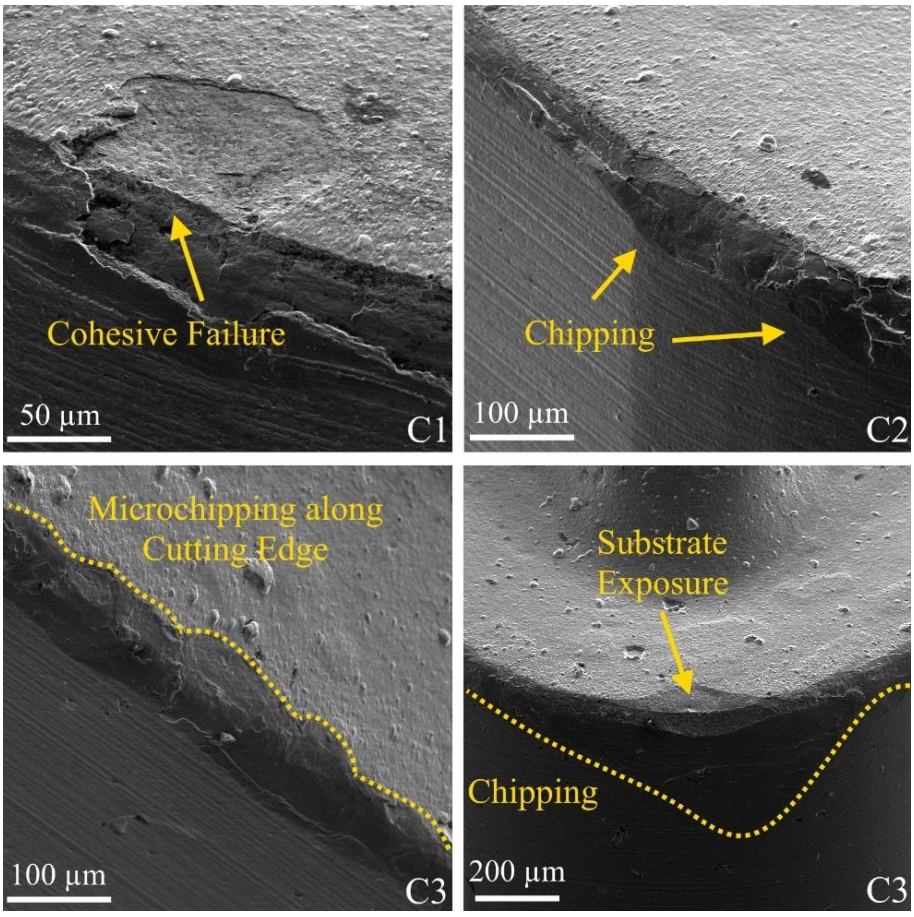

Figure 4.5. *SEM micrographs of post-deposition defects observed on coatings C1 to C3 showing substrate exposure and chipping along the cutting edge.*

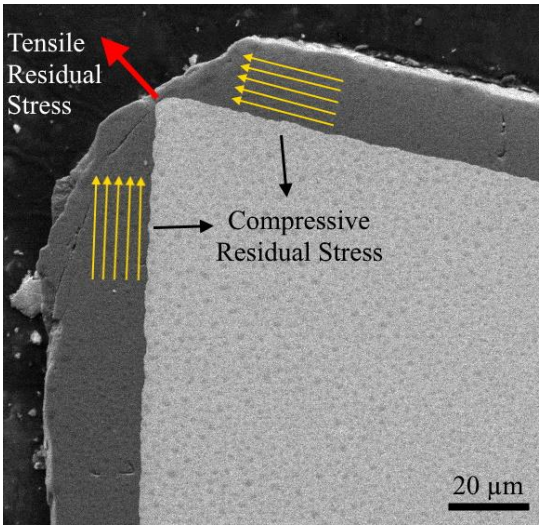

Figure 4.6. *Cross section of a thick TiAlN coating showing the effect of geometrical stresses on coating coverage along the cutting edge.*

4.3.5. Machining Test

As indicated in sections 4.3.1 to 4.3.3 with high negative bias voltage combination in coating C3, increased hardness and yield strength were observed. Coatings C2 and C3 also showed a lower density of macroparticles than coating C1; however, the difference in surface roughness between the coatings was insignificant. Coating C1 which showed the lowest compressive residual stress among the deposited coatings, resulted in better adhesion to the substrate as well as fewer post deposition defects along the cutting edge. These opposing factors are expected to affect coating performance, tool life, and wear behaviour. Therefore, to assess tool performance, machining tests were done on compacted graphite iron under a dry machining condition. During the machining test, to eliminate any effects of edge radius variation caused by microchipping along the cutting edge, only edges with a radius range of 40-44 µm were considered. Fig. 4.7 and fig. 4.8 show the results of the machining test pertaining to flank wear, cutting force (tangential force), and wear

volume in relation to cutting length. Coating C1, with the lowest substrate bias voltage combination, displayed the best tool life performance despite its slightly lower hardness and yield strength, followed by coatings C2 and C3. Scans from the worn tools, images A, B and C in fig. 4.7 (a), show that damages from the cutting process were mainly focused on the cutting edge, which indicates dominant adhesion wear. Moreover, the fluctuation of the cutting force in fig. 4.7 (b) can be attributed to the formation of BUE and the process of workpiece material sticking on and then removing from the tool. This affected the cutting force by changing the effective micro geometry of the tool during the machining test (Ahmed *et al.*, 2019). From the flank wear and wear volume data, it can be concluded that the tool life of a coated tool is significantly affected by the coating's bias voltage combination and the resulting compressive residual stress and adhesion. In this case, the lower compressive residual stress and higher adhesion in coating C1 resulted in a tool life around 30% longer than coating C2 and 75% longer than coating C3. Additionally, as shown in fig. 4.9, higher flank wear and cutting forces were observed in C2 and C3 coatings in the initial stage of wear. This can be attributed to pre-existing microchipping on the cutting edge, lower adhesion, and earlier substrate exposure caused by a higher negative bias voltage combination, which will be explained later in more detail.

To better understand the wear mechanism, fig. 4.10 shows SEM micrographs and EDS maps of Fe present on the cutting edge at various cutting lengths. Typical abrasive marks on the flank, and adhesion of the workpiece to both the flank and rake face can be seen in all coatings. According to previous studies, adhesion wear is the dominant wear mode in dry machining of CGI, and the sticking material is mainly ferrite as it has a high tendency

to stick to the tool (Rosa *et al.*, 2010; Nayyar *et al.*, 2013). Consequently, adhesion of the workpiece material to the rake face results in the formation of built-up edge.

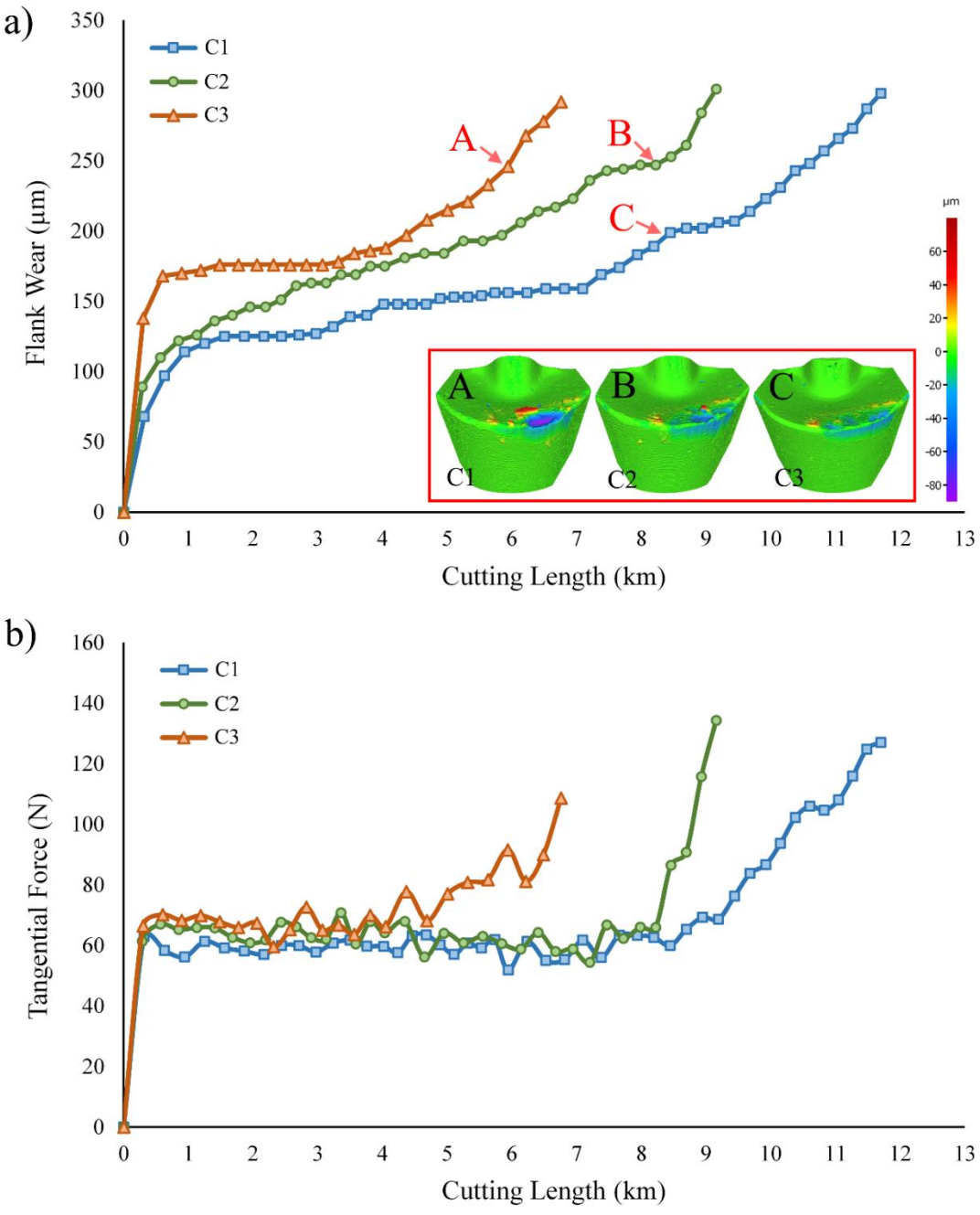

Figure 4.7. *Flank wear (a) and tangential cutting force (b) vs. cutting length for C1, C2 and C3 coatings.*

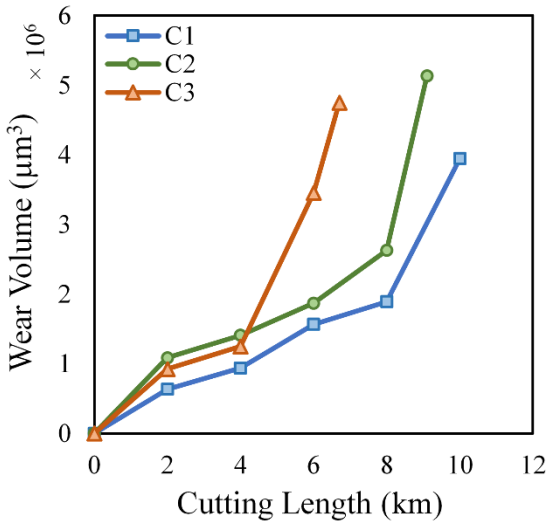

Figure 4.8. *Wear volume vs. cutting length for the deposited coatings.*

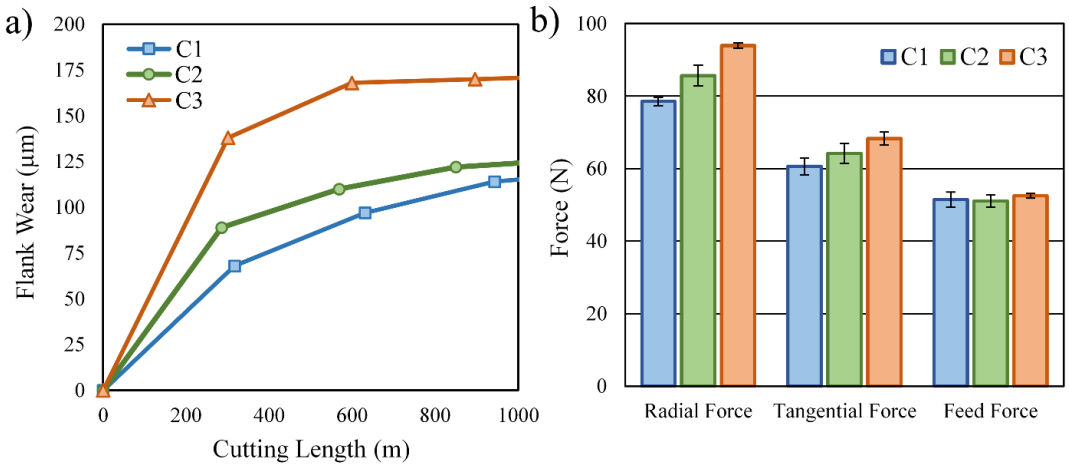

Figure 4.9. *Flank wear vs. cutting length at the running in stage (a) and initial cutting forces (b).*

Built-up edge is an unstable phenomenon that can decrease or increase in volume, as seen in coating C1 at 2 and 6 km. This repeated process of depositing and removing built-up edge on the cutting tool results in the sticking material gradually removing the coating/substrate, which ultimately destroys the cutting edge, as seen in coating C3 at 6 km. The degree of damage varies from a slight removal of the coating, as seen in coating

C1 at 6 km, to a complete removal of the coating and exposure of the substrate. From the SEM images, flank wear, and wear volume, it can be concluded that the coating C1 that was deposited with a low bias voltage combination protected the tool for a longer time against adhesion wear than the other coatings.

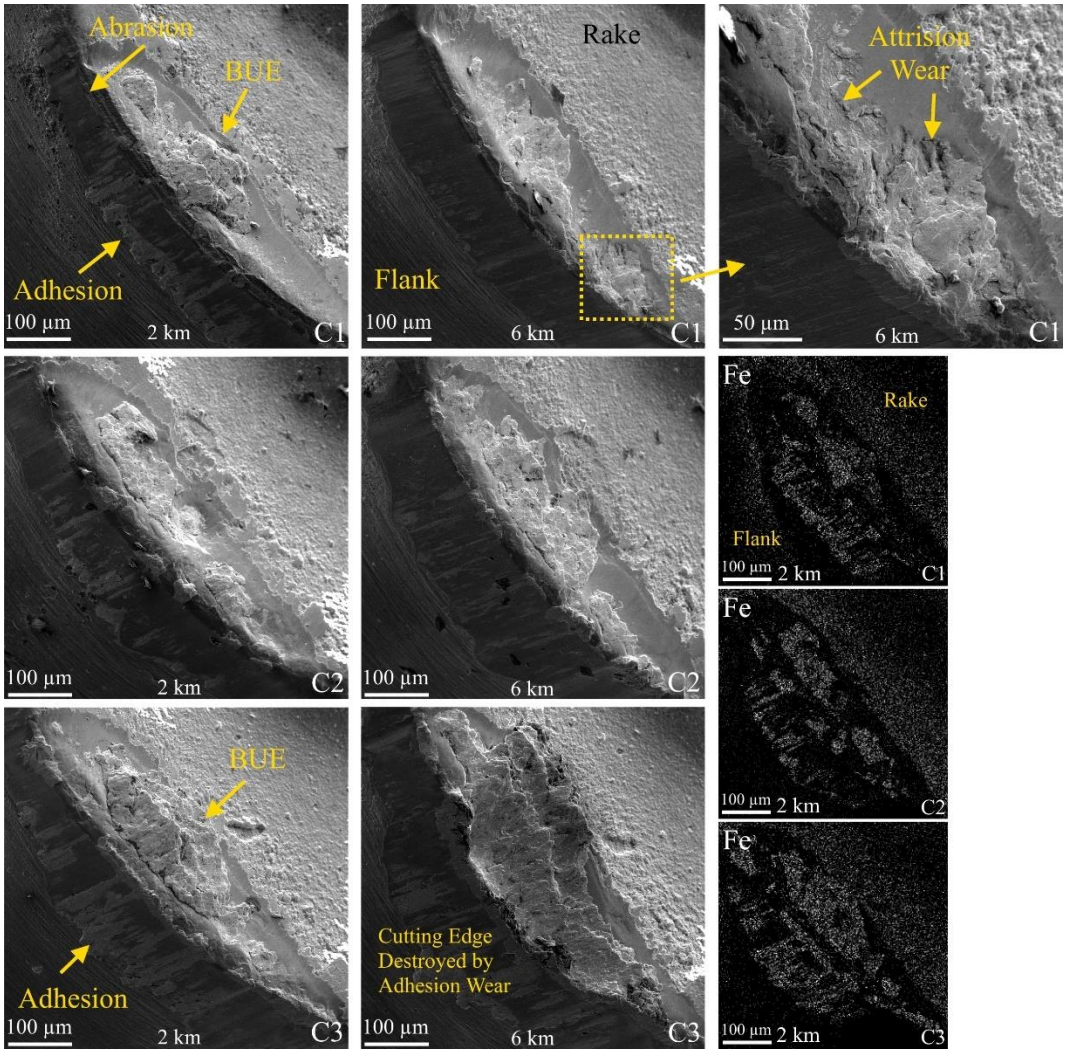

Figure 4.10. *SEM images and Fe EDS maps of coatings C1 to C3 at 2 and 6 km cutting lengths.*

In order to better investigate the wear process on the rake face and observe the coating/substrate removal pattern during adhesion wear, the built-up edge was etched away

from coatings C1 and C3 during a separate set of experiments at specific cutting lengths. SEM micrographs of the mentioned tools are shown in fig. 4.11 and fig. 4.12. Crack formation and coating delamination causing both adhesive failure (separation of coating from interface) and cohesive failure (separation of coating from itself) can be observed in both coatings, the degree of which appears to be higher in coating C3. Two different types of cracks are believed to form during machining: transverse cracks, which are detectable on the surface of the coating, and longitudinal cracks, which are hidden and cause coating delamination. The formation of these cracks is associated with microdeformation of the substrate and the tearing force caused by adhesion interaction between the coating and workpiece. However, defects such as pores or macro particles drastically affect crack formation (Vereschaka and Grigoriev, 2017; Vereschaka *et al.*, 2017). By comparing the micrographs of the two coatings, a drastic difference is observed in wear pattern. In coating C1, which was under approximately 1.3 GPa of compressive residual stress, transverse cracks and cohesion damage were observed at very early stages of machining (1 km). As wear on the tool continued, cohesive failure gradually expanded until the substrate was exposed at 4 km of cutting length. From this point, the substrate exposure expanded until it reached the cutting edge at around 7 km length. In coating C3, which was under approximately 4.5 GPa of compressive residual stress, transverse cracks, cohesive failure in the coating, and adhesive failure on the cutting edge could be observed after only 1 km of the machining length. By increasing the cutting length, tool substrate exposure appeared at various locations on the rake face, and it further expanded away from the cutting edge. Here, early coating adhesion failure and the resulting cutting-edge exposure can be

attributed to poor adhesion of the coating to the substrate due to high compressive residual stress and geometrical stress causing chipping on the cutting edge. Naturally, with an exposed cutting edge, the tool was no longer protected by the coating, and the tool wear process was accelerated. Hence, a reduced tool life is observed in coatings with a higher negative bias voltage combination.

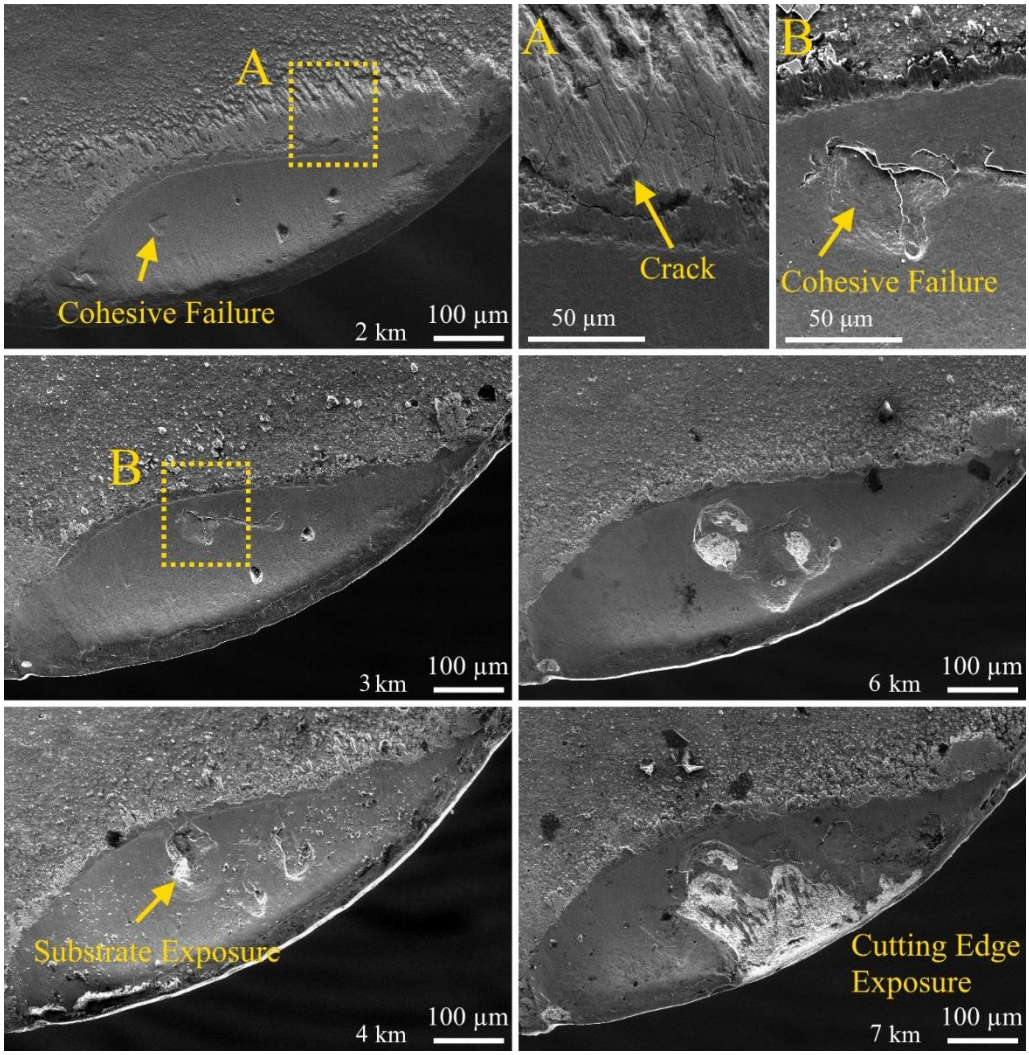

Figure 4.11. *SEM images from the rake face of coating C1 at different cutting lengths after removing the built-up edge.*

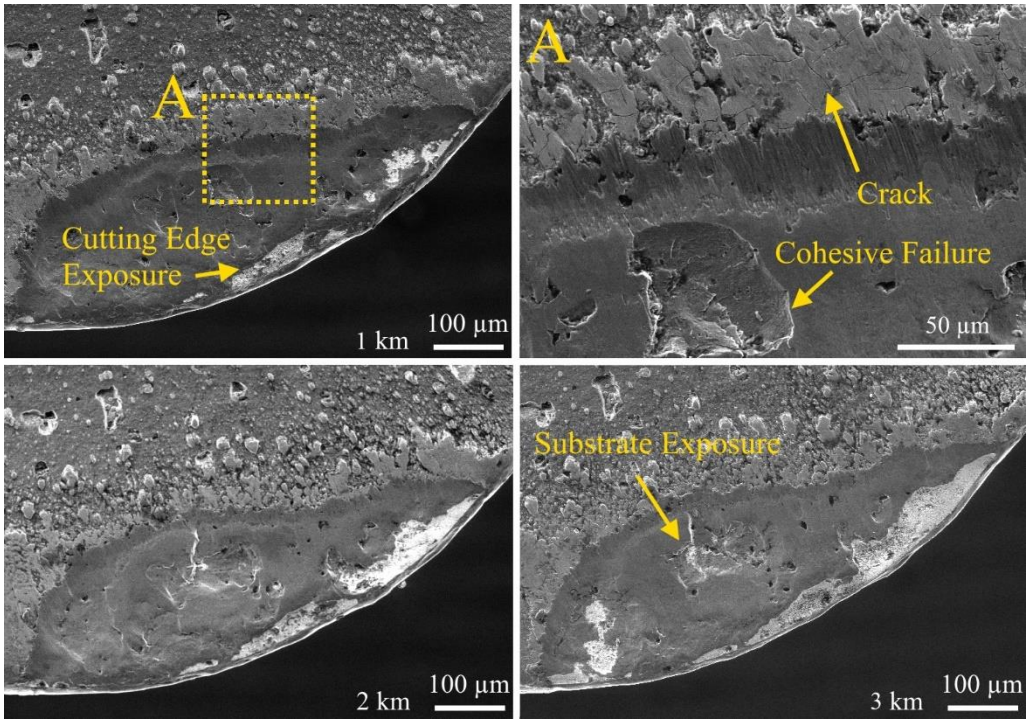

Figure 4.12. *SEM images from the rake face of coating C3 at different cutting lengths after removing the built-up edge.*

4.4. Conclusion

In this work, a technology called super fine cathode was used to deposit TiAlN multilayer coatings with a higher thickness range than commercial coatings (around 11 µm). Using this technology, three different multilayer TiAlN PVD coatings were designed and deposited with different substrate bias voltage combinations. The purpose of varying the substrate bias voltage was to achieve a range of 1-5 GPa of compressive residual stress in the coating. Next, the effect of residual stress on coating properties and wear behaviour/patterns was studied, the results of which are summarized below:

- By increasing the negative substrate bias voltage from -30/-70 (C1) to -70/-110 (C2) and -110/-150 (C3), the average compressive residual stress was increased from 1.3

GPa to 2.1 GPa and 4.5 GPa, respectively. Therefore, the SFC technology showed excellent capabilities for adjusting compressive residual stress by changing the substrate bias voltage.

- A high substrate bias voltage combination produced higher coating hardness and yield stress than other combinations. This increase is due to compressive residual stress resisting indenter penetration.
- The adhesion of the coating to the substrate weakened at higher negative substrate bias voltage combinations due to increased stress at the coating/substrate interface. However, spallation damage was contained in a smaller area due to the high compressive residual stress of the coating.
- All the coatings deposited for this investigation showed an insignificant difference in surface roughness. However, higher macroparticle density was observed in the coating with the lowest substrate bias voltage combination.
- As-deposited defects, such as microchipping, were observed in the coatings, the number of which increased with higher negative substrate bias voltage combination. Here, chipping was mainly observed along the cutting edge, and it was caused by the complex geometry of the tool and the resulting geometrically induced stresses. In extreme cases, the substrate was exposed due to a high degree of chipping and coating delamination.
- Adhesion and built-up edge formation were the major wear mechanisms leading to tool failure. Coating C1, which was under low compressive residual stress, showed

an improved tool life of 30% compared to coating C2 and 75% compared to coating C3. This coating was able to delay substrate exposure because of a combination of gradual cohesive failure and good adhesion to the substrate.

- After removing built-up edge formed on the rake face, significant differences were observed in the wear patterns of coatings C1 and C3. In coating C3, the first substrate exposure occurred at the cutting edge during an early stage of machining, whereas, in coating C1, the substrate was first exposed at later stages away from the cutting edge. This is due to the lower compressive residual stress of coating C1 and the resulting improved adhesion and lower geometrical stress on the cutting edge.

The developed thick coating showed promising results in machining CGI and can potentially increase tool life in machining similar hard to machine material. However, there was no pre- or post- deposition treatment done on the coating in this study and these methods can be implemented in the next step to improve tool life further.

4.5. References

Abdoos, M. et al. (2019) 'Effect of coating thickness on the tool wear performance of low stress TiAlN PVD coating during turning of compacted graphite iron (CGI)', Wear. Elsevier B.V., 422–423(January), pp. 128–136. doi: 10.1016/j.wear.2019.01.062.

Abdoos, M. et al. (2020a) 'A strategy to improve tool life by controlling cohesive failure in thick TiAlN coating during turning of CGI', The International Journal of Advanced Manufacturing Technology, 106(7), pp. 2793–2803. doi: 10.1007/s00170-019-04854-0.

Abdoos, M. et al. (2020b) ‘A strategy to improve tool life by controlling cohesive failure in thick TiAlN coating during turning of CGI’. The International Journal of Advanced Manufacturing Technology.

Ahlgren, M. and Blomqvist, H. (2005) ‘Influence of bias variation on residual stress and texture in TiAlN PVD coatings’, Surface and Coatings Technology, 200(1-4 SPEC. ISS.), pp. 157–160. doi: 10.1016/j.surfcoat.2005.02.078.

Ahmed, Y. S. et al. (2019) ‘Use of acoustic emission and cutting force signals to monitor built-up edge formation in stainless steel turning’, International Journal of Advanced Manufacturing Technology. doi: 10.1007/s00170-019-03607-3.

Ali, R., Sebastiani, M. and Bemporad, E. (2015) ‘Influence of Ti-TiN multilayer PVD-coatings design on residual stresses and adhesion’, Materials and Design, 75, pp. 47–56. doi: 10.1016/j.matdes.2015.03.007.

Bemporad, E. et al. (2006) ‘High thickness Ti/TiN multilayer thin coatings for wear resistant applications’, Surface and Coatings Technology, 201(6), pp. 2155–2165. doi: 10.1016/j.surfcoat.2006.03.042.

Bobzin, K. (2016) ‘High-performance coatings for cutting tools’, CIRP Journal of Manufacturing Science and Technology. doi: 10.1016/j.cirpj.2016.11.004.

Bouzakis, K. D. et al. (2011) ‘Optimization of wet micro-blasting on PVD films with various grain materials for improving the coated tools’ cutting performance’, CIRP Annals - Manufacturing Technology, 60(1), pp. 587–590. doi: 10.1016/j.cirp.2011.03.012.

Breidenstein, B. et al. (2016) ‘Influence of the residual stress state of coatings on the wear behavior in external turning of AISI 4140 and Ti–6Al–4V’, Production Engineering, 10(2), pp. 147–155. doi: 10.1007/s11740-015-0650-7.

Bull, S. J. and G.-Berasetegui, E. (2006) ‘An overview of the potential of quantitative coating adhesion measurement by scratch testing’, Tribology and Interface Engineering Series, 51, pp. 136–165. doi: 10.1016/S0167-8922(06)80043-X.

Cai, F. et al. (2011) ‘Effect of nitrogen partial pressure on Al-Ti-N films deposited by arc ion plating’, Applied Surface Science, 258(5), pp. 1819–1825. doi: 10.1016/j.apsusc.2011.10.053.

Cai, F. et al. (2017) ‘Influence of negative bias voltage on microstructure and property of Al-Ti-N films deposited by multi-arc ion plating’, Ceramics International, 43(4), pp. 3774–3783. doi: 10.1016/j.ceramint.2016.12.019.

Chen, X., Yan, J. and Karlsson, A. M. (2006) ‘On the determination of residual stress and mechanical properties by indentation’, Materials Science and Engineering A, 416(1–2), pp. 139–149. doi: 10.1016/j.msea.2005.10.034.

Clausner, A. and Richter, F. (2015) ‘Determination of yield stress from nano-indentation experiments’, European Journal of Mechanics, A/Solids, 51, pp. 11–20. doi: 10.1016/j.euromechsol.2014.11.008.

Dawson, S. and Schroeder, T. (2004) ‘Practical applications for compacted graphite iron’, AFS Transactions, 47(05), pp. 1–9.

Denkena, B. and Breidenstein, B. (2008) ‘Influence of the residual stress state on cohesive damage of PVD-coated carbide cutting tools’, Advanced Engineering Materials, 10(7), pp. 613–616. doi: 10.1002/adem.200800063.

Devia, D. M. et al. (2011) ‘TiAlN coatings deposited by triode magnetron sputtering varying the bias voltage’, Applied Surface Science, 257(14), pp. 6181–6185. doi: 10.1016/j.apsusc.2011.02.027.

Fox-Rabinovich, G. S. et al. (2008) ‘Effect of temperature of annealing below 900 °C on structure, properties and tool life of an AlTiN coating under various cutting conditions’, Surface and Coatings Technology, 202(13), pp. 2985–2992. doi: 10.1016/j.surfcoat.2007.10.034.

Heck, M. et al. (2008) ‘Analytical investigations concerning the wear behaviour of cutting tools used for the machining of compacted graphite iron and grey cast iron’, International Journal of Refractory Metals and Hard Materials, 26(3), pp. 197–206. doi: 10.1016/j.ijrmhm.2007.05.003.

Martínez, E. et al. (2003) ‘Nanoindentation stress-strain curves as a method for thin-film complete mechanical characterization: Application to nanometric CrN/Cr multilayer coatings’, Applied Physics A: Materials Science and Processing, 77(3–4), pp. 419–426. doi: 10.1007/s00339-002-1669-0.

Nayyar, V. et al. (2012) ‘An experimental investigation of machinability of graphitic cast iron grades; Flake, compacted and spheroidal graphite iron in continuous machining operations’, in Procedia CIRP, pp. 488–493. doi: 10.1016/j.procir.2012.04.087.

Nayyar, V. et al. (2013) ‘Machinability of compacted graphite iron (CGI) and flake graphite iron (FGI) with coated carbide’, International Journal of Machining and Machinability of Materials, 13(1), p. 67. doi: 10.1504/IJMMM.2013.051909.

Rosa, S. do N. et al. (2010) ‘Analysis of Tool Wear , Surface Roughness and Cutting Power in the Turning Process of Compact Graphite Irons with Different Titanium Content’, Journal of the Brazilian Society of Mechanical Sciences and Engineering, 32(3), pp. 234–240. doi: 10.1590/S1678-58782010000300006.

Sargade, V. G. et al. (2011) ‘Effect of coating thickness on the characteristics and dry machining performance of Tin film deposited on cemented carbide inserts using cfubms’, Materials and Manufacturing Processes, 26(8), pp. 1028–1033. doi: 10.1080/10426914.2010.526978.

Skordaris, G. et al. (2017) ‘Effect of PVD film’s residual stresses on their mechanical properties, brittleness, adhesion and cutting performance of coated tools’, CIRP Journal of Manufacturing Science and Technology, 18, pp. 145–151. doi: 10.1016/j.cirpj.2016.11.003.

Skordaris, G. et al. (2018) ‘Bias voltage effect on the mechanical properties, adhesion and milling performance of PVD films on cemented carbide inserts’, Wear, 404–405, pp. 50–61. doi: 10.1016/j.wear.2018.03.001.

Su, G. S. et al. (2016) ‘Effects of high-pressure cutting fluid with different jetting paths on tool wear in cutting compacted graphite iron’, Tribology International, 103, pp. 289–297. doi: 10.1016/j.triboint.2016.06.029.

Tanaka, S. et al. (2016) ‘Micro-blasting effect on fracture resistance of PVD-AlTiN coated cemented carbide cutting tools’, Surface and Coatings Technology. Elsevier B.V., 308, pp. 337–340. doi: 10.1016/j.surfcoat.2016.07.094.

Teixeira, V. (2001) ‘Mechanical integrity in PVD coatings due to the presence of residual stresses’, in Thin Solid Films, pp. 276–281. doi: 10.1016/S0040-6090(01)01043-4.

Teixeira, V. (2002) ‘Residual stress and cracking in thin PVD coatings’, Vacuum, 64(3–4), pp. 393–399. doi: 10.1016/S0042-207X(01)00327-X.

Tooptong, S., Park, K. H. and Kwon, P. (2018) ‘A comparative investigation on flank wear when turning three cast irons’, Tribology International. Elsevier Ltd, 120(December 2017), pp. 127–139. doi: 10.1016/j.triboint.2017.12.025.

Tuffy, K., Byrne, G. and Dowling, D. (2004) ‘Determination of the optimum TiN coating thickness on WC inserts for machining carbon steels’, Journal of Materials Processing Technology, 155–156(1–3), pp. 1861–1866. doi: 10.1016/j.jmatprotec.2004.04.277.

Uhlmann, E. and Klein, K. (2000) ‘Stress design in hard coatings’, Surface and Coatings Technology, 131(1–3), pp. 448–451. doi: 10.1016/S0257-8972(00)00837-9.

Vereschaka, A. A. et al. (2017) ‘Delamination and longitudinal cracking in multi-layered composite nano-structured coatings and their influence on cutting tool life’, Wear. Elsevier B.V., 390–391(August), pp. 209–219. doi: 10.1016/j.wear.2017.07.021.

Vereschaka, A. A. and Grigoriev, S. N. (2017) ‘Study of cracking mechanisms in multi-layered composite nano-structured coatings’, Wear. Elsevier, 378–379, pp. 43–57. doi: 10.1016/j.wear.2017.01.101.

Wang, C. et al. (2017) ‘Effect of different oil-on-water cooling conditions on tool wear in turning of compacted graphite cast iron’, Journal of Cleaner Production, 148, pp. 477–489. doi: 10.1016/j.jclepro.2017.02.014.

Wiklund, U., Gunnars, J. and Hogmark, S. (1999) ‘Influence of residual stresses on fracture and delamination of thin hard coatings’, Wear. Elsevier Sequoia SA, 232(2), pp. 262–269. doi: 10.1016/S0043-1648(99)00155-6.

Yamamoto, K. et al. (2018) ‘Cutting Performance of Low Stress Thick TiAlN PVD Coatings during Machining of Compacted Graphite Cast Iron (CGI)’, Coatings, 8(2), p. 38. doi: 10.3390/coatings8010038.

Chapter 5. Effect of Edge Preparation

Abdoos, M., Graf, H., Rawal, S., Arif, A. F. M., & Veldhuis, S. C. The effect of wet blasting as a pre-deposition treatment for thick TiAlN PVD coating. Submitted to The International Journal of Advanced Manufacturing Technology. November 2020.

Author's Contribution

Majid Abdoos	Designed and conducted the experiments Analyzed the results Wrote the manuscript
Heiko Graf	Prepared samples - wet blasting
Sushant Rawal	Assisted with experiment design Assisted with coating deposition
Abul Fazel Arif	Assisted with experimental design Assisted writing and editing the manuscript
Stephen Veldhuis	Supervised the project Edited the manuscript

Abstract

Edge preparation techniques are known to be an effective method to adjust the microgeometry and improve the mechanical properties of cutting tools. These techniques can also be used on tools prior to coating deposition to further improve the coating quality on the cutting edge and, consequently, tool life. In this research, wet blasting was used on indexable turning inserts to adjust the cutting-edge radius in order to address quality issues associated with thick PVD coatings while studying changes in the substrate properties. For this purpose, a multilayer TiAlN coating with an approximate thickness of 10 µm was deposited on prepared and unprepared inserts. Moreover, machining tests were conducted on compacted graphite iron (CGI) to understand the effect of pre-deposition edge preparation on cutting performance. The results show that wet blasting has minimal effects on substrate properties, such as hardness. However, it is an effective method to eliminate micro breakage along the cutting edge by reducing geometrically induced stresses. Wet blasting as a pre-deposition treatment provided a better coating quality, lower cutting forces, slightly longer tool life, and greater consistency in coated tool microgeometry.

Keywords: PVD coatings; Edge preparation; Wet blasting; Compacted graphite iron; Dry turning

5.1. Introduction

Edge preparation techniques are commonly used on indexable and solid tools to reduce production defects (such as burrs) and improve cutting edge stability (Fu *et al.*, 2019). These techniques can be utilized to adjust the microgeometry, surface roughness, and mechanical properties of the cutting edge to suit the application. Wet and dry abrasive blasting, brushing, drag finishing, grinding, laser, and electrical discharge machining are common edge preparation methods currently used (Bouzakis *et al.*, 2014; Denkena and Biermann, 2014). Although each method has its own limitations and advantages, prolonged tool life and better workpiece surface quality are generally observed with a prepared edge.

Edge preparation effects can be classified into three categories: microgeometry, properties, and topography. Many researchers have extensively reviewed the significance of tool geometry. Through their investigations, the radius and symmetry of the cutting edge has been shown to affect cutting forces, heat generation, chip formation, and, ultimately, wear mechanisms and tool life (Yen, Jain and Altan, 2004; M and N, 2020; Wang, Biermann, *et al.*, 2020). It has been mentioned that with a higher edge radius, the cutting forces and heat generated during the machining process increase; despite this, the cutting edge is more stable and is able to better dissipate heat due to higher area of contact with the workpiece. Therefore, there exists an optimal edge roundness which results in minimal thermal-mechanical load and, thus, the longest tool life possible (Denkena, Lucas and Bassett, 2011). Edge preparation can also alter the properties of the substrate or coating, depending on the stage it is applied at. Generally, with prepared edges, higher compressive residual stress, and therefore higher hardness, is achieved as the cutting edge is plastically

deformed during the material removal process (Zhong *et al.*, 2018). However, if excessive heat is generated during the preparation process, tensile residual stress can be observed as well (Tönshoff and Seegers, 2001). It is also worth mentioning that the effect of residual stress diminishes if a coating is deposited on the prepared edge due to annealing at high temperature during the deposition process (Bouzakis *et al.*, 2014). Naturally, edge preparation also affects the topography of the tool. It has been shown that depending on the preparation process, lower surface roughness can be achieved, which improves the mechanical bonding between the coating and substrate and, therefore, increase coating adhesion (Denkena *et al.*, 2014). However, Bouzakis et al. (Bouzakis *et al.*, 2005) observed that to improve adhesion on carbide tools, the surface roughness should be less than the WC particle radius to ensure the carbide is sufficiently embedded in the binder.

In wet/dry blasting or abrasive machining, an abrasive medium carried by pressurized air (dry blasting) or water (wet blasting) is accelerated through a jet nozzle which is then applied on the cutting edge. In general, the benefits of applying wet blasting include lower thermal effects (compared to dry blasting) on the substrate, inducing compressive residual stress on the blasted area, and the ability to prepare tools with complex shapes and geometry (Biermann *et al.*, 2016). Using water as the carrier medium results in a better surface finish due to the damping effect of water and prevents dust formation during the process (Bouzakis *et al.*, 2001). Wet blasting can also be implemented as an effective and inexpensive post-treatment to remove post-deposition defects present on a coating (Puneet, Valleti and Venu Gopal, 2017; Krebs *et al.*, 2018). This proved to be especially beneficial for CVD coatings since it increases hardness and reduces fracture formation by inducing

compressive residual stress in the coating (Zhong *et al.*, 2018). However, wet blasting is a very complex method of edge preparation with many process parameters affecting its reproducibility (Bouzakis, Bouzakis, *et al.*, 2011; Bouzakis, G Skordaris, *et al.*, 2011).

High thickness in PVD coatings can improve tool life significantly by providing more material to wear through, thus delaying substrate exposure, lowering stress concentration on the tool, and better protecting the tool against thermal and mechanical stresses (Bouzakis *et al.*, 2004; Bemporad *et al.*, 2006; Skordaris *et al.*, 2016; Vereschaka *et al.*, 2018). However, preliminary results showed a significant effect of coating thickness on the microgeometry, especially edge roundness. Moreover, due to the complexity of the cutting tool and geometrically induced stresses, as-deposited defects were observed along the cutting edge. Therefore, to improve cutting edge quality and tool performance and reduce unnecessary ploughing, pre-deposition edge treatments are necessary. Although prior literature showed the benefits of wet blasting for improving tool life, no research has been done on edge preparation for thick coatings since the coating itself is a new product under development. Therefore, the current work explores wet blasting as a means of adjusting the edge radius before deposition to reduce defects in order to improve overall tool quality and performance.

5.2. Experimental detail

To prepare the samples, wet blasting was done on Kennametal CNGG432FS K313 finishing inserts using a standard automatic wet blasting system (Graf-Technik GmbH, Germany), as illustrated in fig. 5.1. In order to adjust microgeometry, the blasting pressure

and size of the blasting media were adjusted according to the target values, and all other process parameters were kept constant, as shown in table 5.1. The microgeometry and surface roughness of the prepared edges were then measured using an Alicona InfiniteFocus microscope. The surface roughness was measured according to ISO standard 25178 on both the flank and rake face of the inserts near the cutting edge. Moreover, to study the effect of wet blasting on mechanical properties, an Anton Paar NH^3 nanoindentation tester was used to measure the hardness and elastic modulus of the cutting insert on the flank face near the cutting edge. Indentation was performed with a standard Berkovich indenter using the load control mode and applying a maximum load of 50 mN.

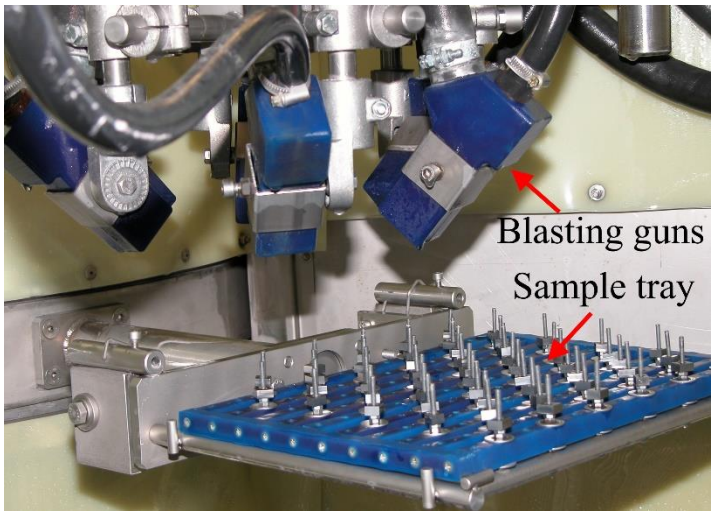

Figure 5.1. *Standard automatic wet blasting system.*

After the edge preparation, a thick, multilayer $Ti_{40}Al_{60}N$ PVD coating was deposited on the samples using a Kobelco AIP-S20 arc ion plating deposition system. The instrument uses a technology called superfine cathode (SFC) which enables the deposition of low residual stress PVD coatings up to 20 µm thick, details of which can be found elsewhere (Yamamoto *et al.*, 2018; Abdoos *et al.*, 2019; Abdoos, Bose, *et al.*, 2020; Abdoos, Rawal,

et al., 2020b). Prior to the deposition, samples were cleaned in acetone using an ultrasonic cleaner, then mounted in the chamber, preheated to 550º C, and etched by Ar for 7.5 min to increase adhesion and reduce any potential contamination. The properties of the deposited coating and the deposition parameters can be found in table 5.2. In order to keep track of any changes in coating adhesion caused by wet blasting, scratch tests were done on the coated samples with a maximum load of 100N, scratch velocity of 7.5 mm/min, and scratch length of 3mm. Lc_2, the critical load to initiate adhesive failure, was recorded in accordance with the ASTM C1624-05 standard.

Table 5.1. *Wet blasting process parameters.*

Sample name	E1	E2	E3	E4
Blasting media size (aluminum oxide)	180/220 mesh		220/240 mesh	
Concentration of blast media	19-21%			
Angle of blast guns/ Vert. axis	35º			
Blasting time (s)	10			
Air pressure (bar)	3.1	4.5	4.5	5.7

After the edge preparation was performed, a thick, multilayer $Ti_{40}Al_{60}N$ PVD coating was deposited on the samples using a Kobelco AIP-S20 arc ion plating deposition system. The instrument uses a technology called superfine cathode (SFC) which enables the deposition of low residual stress PVD coatings up to 20 µm thick, details of which can be found elsewhere (Yamamoto *et al.*, 2018; Abdoos *et al.*, 2019; Abdoos, Bose, *et al.*, 2020; Abdoos, Rawal, *et al.*, 2020b). Prior to the deposition, samples were cleaned in acetone using an ultrasonic cleaner, then mounted in the chamber, preheated to 550ºC, and etched by Ar for 7.5 min to increase adhesion and reduce any potential contamination. The properties of the deposited coating and the deposition parameters can be found in table 5.2. In order to keep track of any changes in coating adhesion caused by wet blasting, scratch

tests were done on the coated samples with a maximum load of 100 N, scratch velocity of 7.5 mm/min, and scratch length of 3mm. L_{C2}, the critical load needed to initiate adhesive failure, was recorded in accordance with the ASTM C1624-05 standard.

To evaluate the performance of the prepared samples, finish turning of compacted graphite iron was conducted on a Boehringer VDF-180 lathe under dry cutting conditions. A cutting speed of 300 m/min, depth of cut of 0.25 mm, and feed rate of 0.2 mm/rev were used. During the machining process, cutting forces were measured using a Kistler dynamometer type 9121. After a predefined cutting length, flank wear was measured using a Keyence VHX 5000 optical microscope, and the wear pattern was studied using a Vega II LSU scanning electron microscope. Tool life was considered up to a flank wear of 300 µm in accordance with ISO standard 3685.

Table 5.2. *Coating properties and deposition parameters.*

Coating	Bias voltage	Deposition time	Arc current	Rotation speed	Thickness	Hardness	Elastic modulus
$Ti_{40}Al_{60}N$	30/70 V	78 min	150 A	5 RPM	~10 µm	31.7 ± 2.8 GPa	446 ± 34 GPa

5.3. Results and discussion

5.3.1. Edge geometry

In order to characterize the cutting-edge, the form factor method was adopted for a more precise and specific measurement. In this method, rather than solely focusing on edge radius, a more complex measurement strategy was undertaken since the cutting edge was not well rounded (Denkena and Biermann, 2014). Here, the cutting edge was characterized by form factor K and average edge rounding $\bar{S}$, was found as follows:

$$K = \frac{S_\gamma}{S_\alpha} \qquad\qquad \bar{S} = \frac{S_\gamma + S_\alpha}{2}$$

Where S_γ is the cutting-edge segment on rake face and S_α is the cutting-edge segment on the flank face as shown in fig. 5.2.

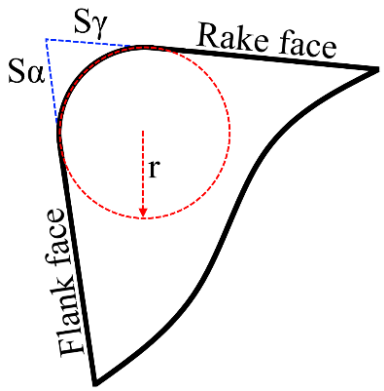

Figure 5.2. *Schematic of the form factor method.*

Table 5.3 shows the measured values of prepared and uncoated cutting edges; for comparison purposes, the measurements of unprepared cutting edges are represented by the label E0 for the reference. Each cutting edge was measured by an Alicona InfiniteFocus microscope using the built-in Edge Master module. The reported value for each sample was the average of 40 individual measurements covering a length defined by the angle spanning 80º around the cutting nose. As the values show, the edge roundness of the cutting edge can be effectively adjusted by wet blasting, with good repeatability. However, as the maximum standard deviation of 7.6% in average edge rounding shows, achieving a consistent value for higher edge radiuses is quite challenging. Moreover, there was a significant deviation in the microgeometry of the coated E0, E1 and E2 as shown in table 5.4. This could be due to post deposition defects such as micro breakage of the coating

along the cutting edge which caused some variation in the microgeometry, as discussed more thoroughly in another article by the author (Abdoos, Bose, *et al.*, 2020). Lower deviation in the coated E3 and E4 cutting edges' measured values tends to indicate less coating micro breakage. This will be discussed in more detail in the next section.

Table 5.3. *Edge characteristics of prepared and unprepared cutting edges.*

Cutting edge	r (µm)	S_α (µm)	S_γ (µm)	$\bar{S}$ (µm)	K
E0	6.08 ± 0.51	7.71 ± 0.79	7.62 ± 0.71	7.62 ± 0.71	0.98 ± 0.08
E1	16.80 ± 1.14	20.93 ± 1.60	21.34 ± 1.54	21.14 ± 1.51	1.02 ± 0.04
E2	25.66 ± 1.79	31.16 ± 2.26	34.07 ± 2.49	32.62 ± 2.32	1.09 ± 0.03
E3	32.53 ± 2.27	38.91 ± 3.05	45.05 ± 2.43	41.98 ± 2.65	1.16 ± 0.04
E4	42.45 ± 3.43	50.30 ± 4.20	61.78 ± 4.47	56.04 ± 4.27	1.22 ± 0.03

Table 5.4. *Edge characteristics of the coated inserts.*

Cutting edge	r (µm)	S_α (µm)	S_γ (µm)	$\bar{S}$ (µm)	K
E0	43.26 ± 8.69	63.78 ± 6.34	53.28 ± 11.27	58.53 ± 7.51	0.83 ± 0.15
E1	52.01 ± 6.33	68.25 ± 8.80	62.02 ± 7.15	65.13 ± 7.90	0.91 ± 0.03
E2	64.51 ± 7.94	83.34 ± 9.10	78.42 ± 8.67	80.88 ± 8.59	0.94 ± 0.05
E3	36.36 ± 1.18	44.70 ± 1.22	58.81 ± 1.04	51.76 ± 1.13	1.31 ± 0.01
E4	46.09 ± 1.84	56.98 ± 2.34	76.33 ± 1.13	66.65 ± 0.60	1.34 ± 0.07

5.3.2. Edge Quality and Surface Roughness

The effect of edge preparation is not only limited to edge geometry. It has been established that edge preparation also alters superficial mechanical properties and surface roughness and reduces manufacturing defects, such as burrs or grinding marks, and, overall, contributes to the quality of the cutting edge (Wang, Saifullah, *et al.*, 2020). The SEM micrographs of the prepared and unprepared cutting edges in fig. 5.3 are evidence of this effect. In E0, the unprepared edge, grinding marks can be seen on the flank face. After wet blasting the cutting edge in E1, grinding marks can still be observed; however, a smooth edge was achieved. Finally, neither grinding marks nor any other manufacturing defects can be observed on the E2, E3, and E4 cutting edges. The effect of edge blasting was also

evident from the surface roughness measurement on the flank and rake face of the cutting edge, reported in fig. 5.4. Moreover, fig. 5.4 shows the 3D scans of the flank and rake side obtained using an Alicona InfiniteFocus microscope. Similarly, the SEM micrographs revealed lower level surface features on the prepared inserts than on the unprepared cutting edge. Due to wet blasting a smoother surface, with lower surface roughness was also observed on the rake face. Despite eliminating grinding marks, surface roughness was slightly increased on the flank face of the prepared inserts; however, the differences between samples in both flank and rake face were quite insignificant.

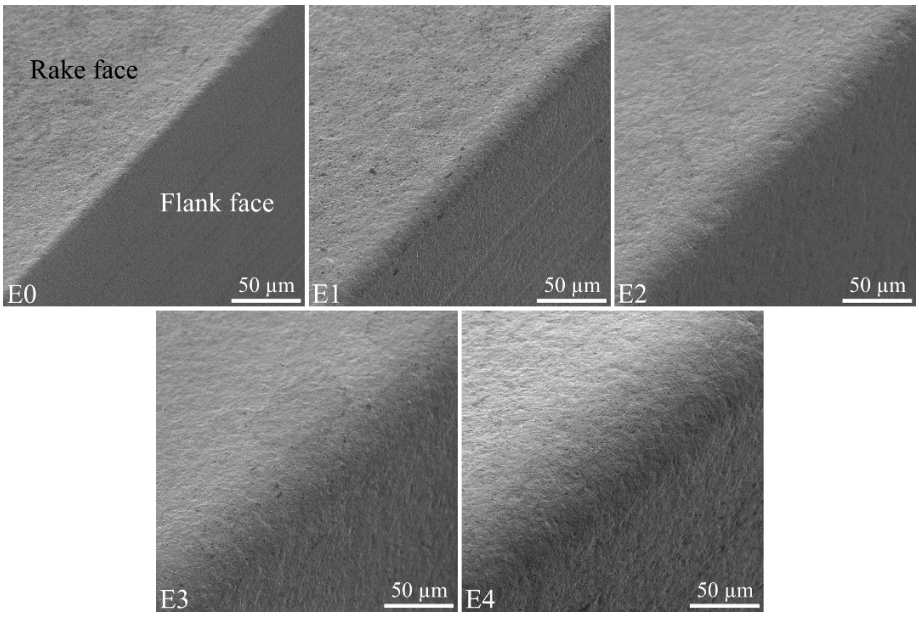

Figure 5.3. *SEM micrograph of the uncoated prepared and unprepared edges.*

Despite improving the cutting-edge quality, the most significant effect of wet blasting was observed after coating deposition. As fig. 5.5 shows, after adjusting the microgeometry of the cutting edge to a desired edge rounding, coating micro breakage can no longer be observed in E3 and E4. It is worth mentioning that coating micro breakage is caused by

compressive residual stress in the deposited coating and geometrically induced stress due to the complex geometry of the cutting tool. In this regard Wiklund et al. (Wiklund, Gunnars and Hogmark, 1999) mentioned that compressive residual stress in the coating causes tensile stress at the coating-substrate interface along a sharp edge, which can result in coating breakage or spallation. Micro breakage can be clearly observed on the cutting edge of E0, E1, and E2. Naturally, tensile stress at the interface can be lowered by making the transition from rake face to flank face more gradual, or, in other words, by increasing edge rounding. Coating micro breakage has been shown to be more severe in the case of thick PVD coatings and was observed to drastically change with residual stress (Abdoos, Bose, *et al.*, 2020). However, as seen in fig. 5.5, increasing edge rounding was an effective method for lowering the geometrically induced stress and, thus, eliminating micro breakage completely. By eliminating micro breakage, a consistent edge microgeometry can be expected, as seen in table 5.4.

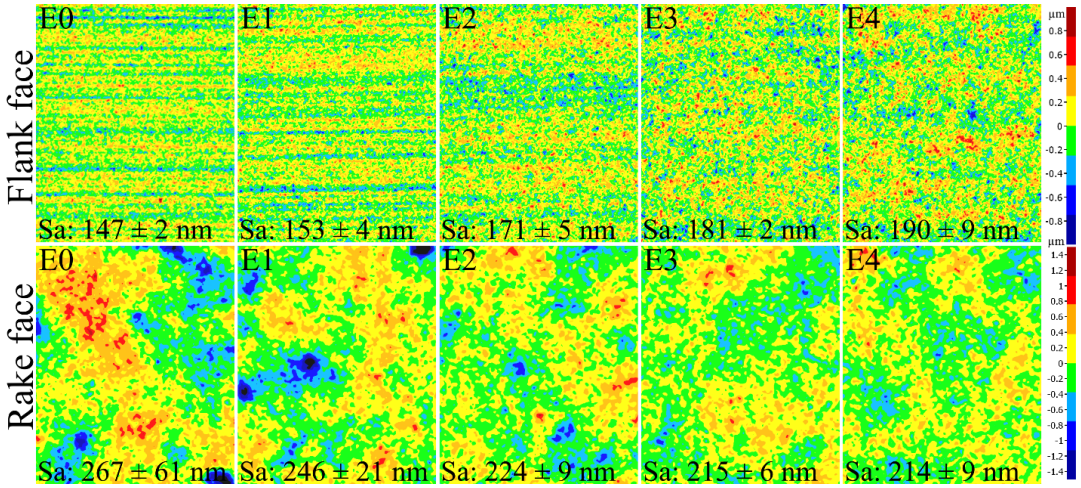

Figure 5.4. *3D scan of the rake and flank face of uncoated prepared and unprepared inserts.*

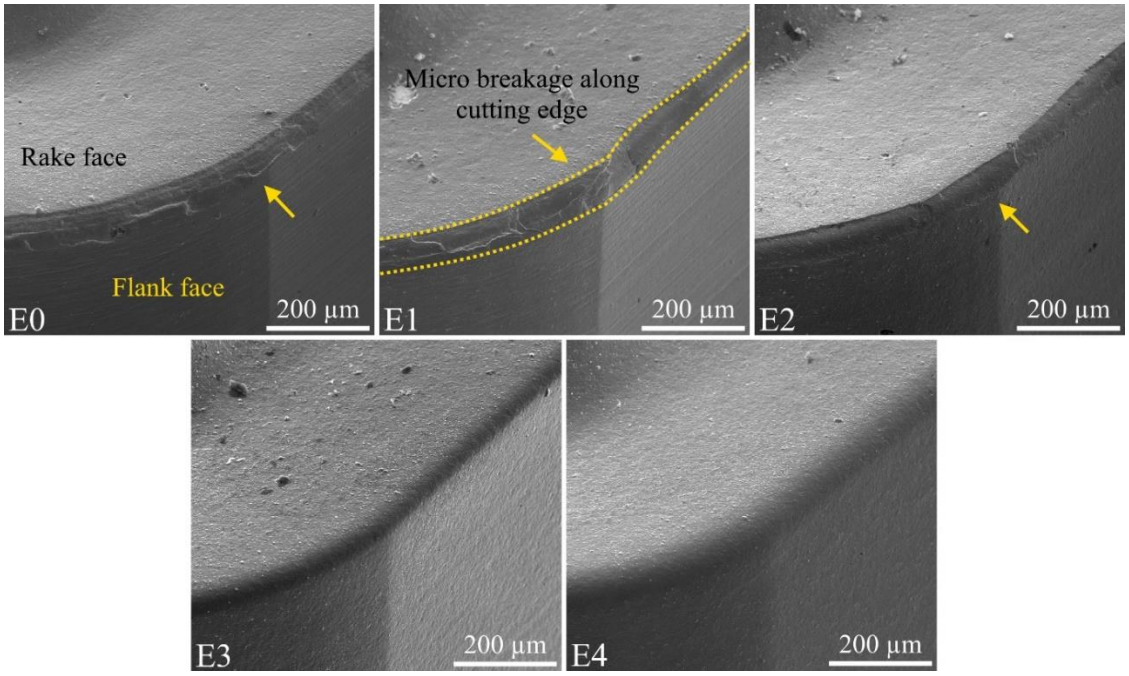

Figure 5.5. *SEM micrograph of the coated unprepared and prepared edges.*

5.3.3. Hardness and Adhesion

To understand the effect of wet blasting on the mechanical properties of the substrate, nanoindentation was done on uncoated inserts near the cutting edge. In order to measure only the superficial hardness, a maximum load of 50 mN was used which resulted in an approximate maximum penetration depth of 350 nm. Moreover, to measure adhesion, scratch testing was carried out on the flank face after coating deposition and Lc_2 was recorded as the critical load to initiate adhesive failure. The average hardness, elastic modulus, and critical load to initiate adhesive failure are presented in fig. 5.6. It is worth mentioning that the data was obtained from a minimum of 30 indents and 3 scratch tests. Despite affecting microgeometry, the results clearly show that the effect of wet blasting on the hardness of the substrate was measured to be insignificant. This can be linked with the benefits of using water as the medium in blasting and its damping effect during the particle

impact. However, there is a slight increase in adhesion which can be attributed to higher surface roughness and better mechanical interlocking of the coating and substrate, as Jacob et al. mentioned (Jacob *et al.*, 2017).

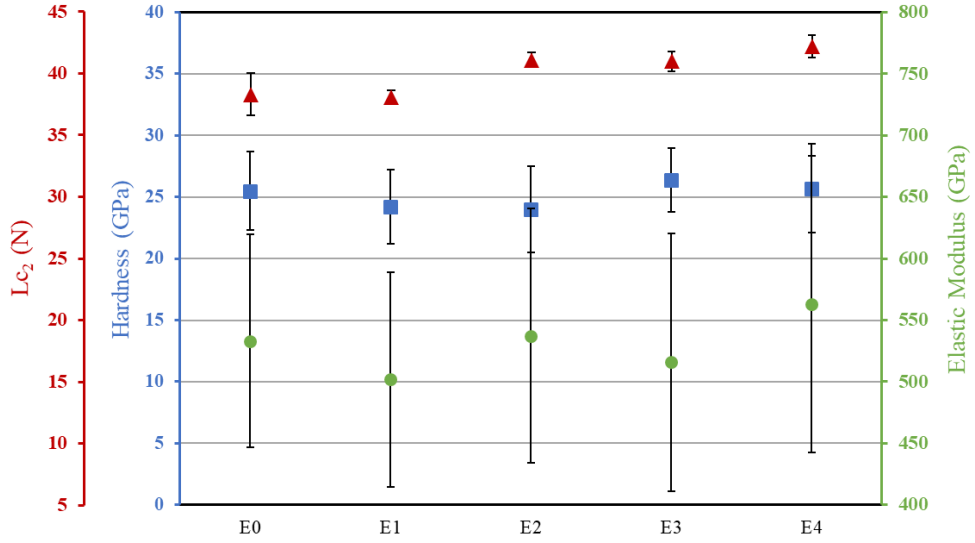

Figure 5.6. *Hardness and elastic modulus of different substrates and adhesion of the coating measured on the flank face.*

5.3.4. Machining results

As observed in the previous sections, despite minimizing manufacturing defects such as grinding marks, wet blasting has an insignificant effect on substrate properties. Thus, the main effects of this process are improving the microgeometry of coated and uncoated inserts as well as slightly increasing coating adhesion. It was shown that increasing the average edge rounding to around 42 µm can completely eliminate coating micro breakage and significantly improve coating quality along the cutting edge. This is expected to affect cutting forces and tool life during the machining process. Therefore, to study tool performance, machining tests were done on compacted graphite iron (CGI) with the

prepared and unprepared coated inserts. The cutting edges used for the machining experiment were mainly ones with a radius close to average to better understand the effect of preparation. Fig. 5.7 and fig. 5.8 present tool life data and the initial cutting forces obtained from the machining experiments performed. E1 and E2 showed the shortest tool life which was expected due to its significantly higher edge rounding and high degree of micro breakage along the cutting edge. The longest tool life was achieved by sample E3 followed by E0 and E4; however, the difference in tool life between the mentioned samples was less than 20%. Moreover, the lowest machining forces was achieved with sample E3 with the lowest edge rounding. Lower machining forces with a lower edge rounding are well reported in the literature as a sharper tool causes less ploughing and a lower degree of plastic deformation (Ventura *et al.*, 2017). This can be clearly observed in fig. 5.8, where cutting forces followed the same trend as the edge rounding mentioned in table 5.4.

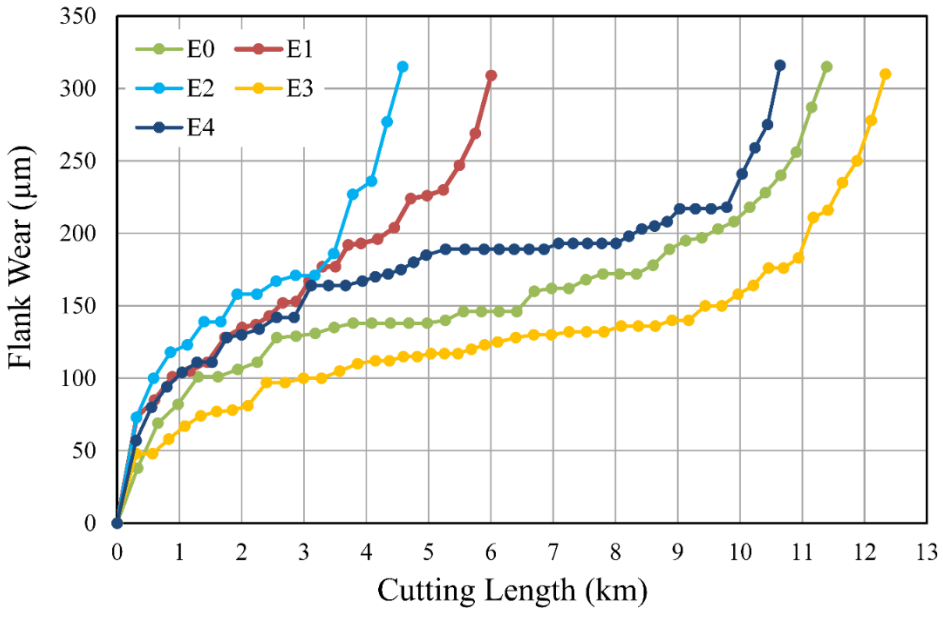

Figure 5.7. *Flank wear vs. cutting length for different coated tools.*

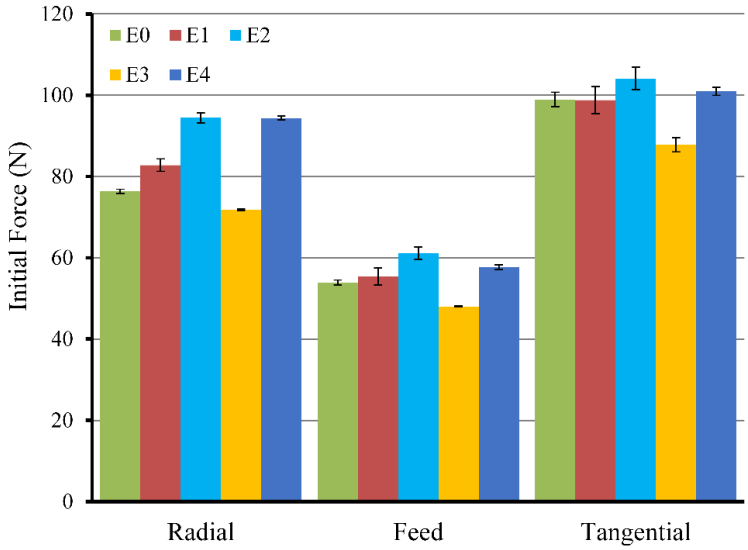

Figure 5.8. *Initial cutting forces.*

In order to better understand the wear process, SEM micrographs of the cutting edges prior to tool failure are shown in fig. 5.9. It can be observed that the dominant wear mode was adhesion wear as the cutting edge was destroyed during the cutting process. Sticking of the workpiece material and formation of BUE can be also be observed on all tools. The wear mechanism can be summarized in this way: during the cutting process, the workpiece material sticks to the cutting edge, forming built-up edge. Built-up edge is extremely unstable as it gets removed and redeposited during the cutting process. During the removal of the material forming the built-up edge, part of the coating can also be removed. This process continued until the substrate was exposed, which leads to the destruction of the cutting edge. Naturally, if the coating is able to withstand the adhesion wear for a longer time, tool life can be prolonged. Therefore, the short tool life of samples E1 and E2 can be linked with high levels of micro breakage due to built-up edge removal and subsequent reduced coating coverage as well as high edge rounding and the resulting high cutting

forces associated with the larger edge radius. Similarly, tool life for E0, E3, and E4, seems to correlate mainly with the cutting forces, however there was a slight difference in wear behaviour. As can be seen from table 5.4, K, or the form factor, increased from 0.83 in E0 to 1.34 in E4. According to Denkena and Biermann (Denkena and Biermann, 2014), form factor greatly influences the ploughing force vector and, therefore, stress on the cutting edge. When K values were low, ploughing forces were focused toward the rake face, and when the form factor increased to values higher than 1, it shifted toward the flank face. Here, as the SEM micrographs show, substrate exposure shifts from being focused on the rake face in E0 to the flank face in E3 and E4. Moreover, it can be seen that part of the cutting edge was destroyed in E0 at 10 km of cutting length; however, the cutting edge still mostly retains its shape in E3 and E4 at the same cutting length.

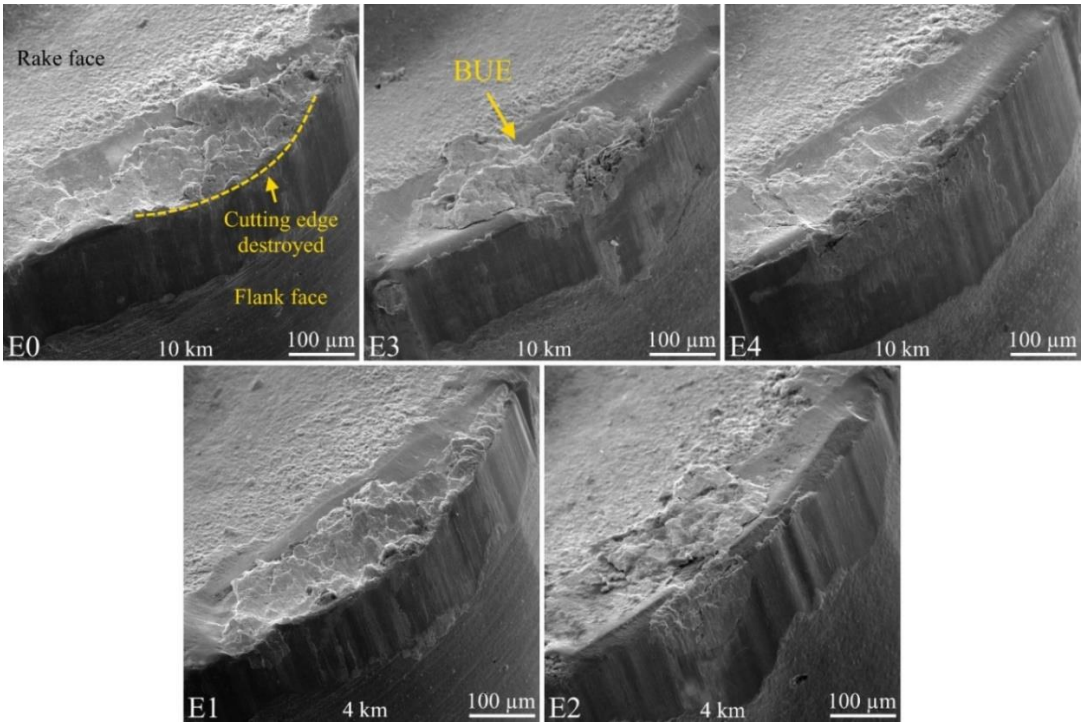

Figure 5.9. *SEM micrograph of the cutting edge close to the end of tool life.*

5.4. Conclusion

In this work, wet blasting was used to prepare turning tools before coating deposition. The edge radii of the cutting tools were adjusted to a range of 15-45 µm by changing the size of the blasting media and the air pressure. After preparation, a low residual stress TiAlN coating was deposited on the inserts with an approximate thickness of 10 µm. The properties and cutting performance of the prepared inserts were then studied to understand the effect of wet blasting. The results of this study are summarized as follows (it should be noted that these results are specific to the coating, edge preparation, and workpiece material):

- By increasing the size of the blasting media or air pressure, greater edge rounding was achieved on the prepared inserts.
- Wet blasting was able to reduce manufacturing defects such as grinding marks on inserts. Moreover, surface roughness was slightly affected by the process. In this case, by increasing the air pressure or blasting media size, surface roughness was increased on the flank face and reduced on the rake face.
- Edge rounding after deposition followed the same trend as observed for the uncoated inserts. However, at an uncoated edge rounding of 42 µm (E3), the edge roundness of the coated insert was significantly reduced due to the elimination of geometrically induced stresses. At this point, a higher consistency in coating microgeometry was achieved.
- Wet blasting did not show any significant effect on substrate properties such as hardness and elastic modulus. Furthermore, scratch testing on the coated inserts

showed a slight increase in coating adhesion which can be linked with better mechanical interlocking of the coating/substrate system.

- By adjusting the uncoated edge rounding to 42 µm (E3), cutting forces were reduced and tool life was slightly lengthened when machining with the coated insert.
- Tool life was mainly affected by the degree of micro breakage and changes in cutting forces due to differences in edge rounding. Moreover, the wear pattern was slightly changed due to different form factors for the cutting edge.
- Overall, wet blasting greatly improved coating quality along the cutting edge. However, its impact on tool life is dependent on the cutting parameters as well as coating and workpiece material. Variation in tool life improvement should be expected under different cutting conditions.

5.5. References

Abdoos, M. et al. (2019) ‘Effect of coating thickness on the tool wear performance of low stress TiAlN PVD coating during turning of compacted graphite iron (CGI)’, Wear. Elsevier B.V., 422–423(January), pp. 128–136. doi: 10.1016/j.wear.2019.01.062.

Abdoos, M., Rawal, S., et al. (2020) ‘A strategy to improve tool life by controlling cohesive failure in thick TiAlN coating during turning of CGI’. The International Journal of Advanced Manufacturing Technology.

Abdoos, M., Bose, B., et al. (2020) ‘The influence of residual stress on the properties and performance of thick TiAlN multilayer coating during dry turning of compacted graphite iron’, Wear. Elsevier Ltd, 454–455, p. 203342. doi: 10.1016/j.wear.2020.203342.

Bemporad, E. et al. (2006) ‘High thickness Ti/TiN multilayer thin coatings for wear resistant applications’, Surface and Coatings Technology, 201(6), pp. 2155–2165. doi: 10.1016/j.surfcoat.2006.03.042.

Biermann, D. et al. (2016) ‘Wet Abrasive Jet Machining to Prepare and Design the Cutting Edge Micro Shape’, Procedia CIRP. Elsevier B.V., 45, pp. 195–198. doi: 10.1016/j.procir.2016.02.071.

Bouzakis, K. D. et al. (2001) ‘Improvement of PVD coated inserts cutting performance, through appropriate mechanical treatments of substrate and coating surface’, Surface and Coatings Technology, 146–147, pp. 443–450. doi: 10.1016/S0257-8972(01)01485-2.

Bouzakis, K. D. et al. (2004) ‘The effect of coating thickness, mechanical strength and hardness properties on the milling performance of PVD coated cemented carbides inserts’, Surface and Coatings Technology, 177–178(178), pp. 657–664. doi: 10.1016/j.surfcoat.2003.08.003.

Bouzakis, K. D. et al. (2005) ‘Effect on PVD coated cemented carbide inserts cutting performance of micro-blasting and lapping of their substrates’, Surface and Coatings Technology, 200(1-4 SPEC. ISS.), pp. 128–132. doi: 10.1016/j.surfcoat.2005.02.119.

Bouzakis, K. D., Bouzakis, E., et al. (2011) ‘Effect of PVD films wet micro-blasting by various Al2O3 grain sizes on the wear behaviour of coated tools’, Surface and Coatings Technology, 205(SUPPL. 2). doi: 10.1016/j.surfcoat.2011.03.046.

Bouzakis, K. D., Skordaris, G., et al. (2011) ‘Optimization of wet micro-blasting on PVD films with various grain materials for improving the coated tools’ cutting

performance', CIRP Annals - Manufacturing Technology, 60(1), pp. 587–590. doi: 10.1016/j.cirp.2011.03.012.

Bouzakis, K. D. et al. (2014) 'Effect of cutting edge preparation of coated tools on their performance in milling various materials', CIRP Journal of Manufacturing Science and Technology, 7(3), pp. 264–273. doi: 10.1016/j.cirpj.2014.05.003.

Denkena, B. et al. (2014) 'Influence of the cutting edge preparation method on characteristics and performance of PVD coated carbide inserts in hard turning', Surface and Coatings Technology. Elsevier, 254, pp. 447–454. doi: 10.1016/j.surfcoat.2014.07.003.

Denkena, B. and Biermann, D. (2014) 'Cutting edge geometries', CIRP Annals - Manufacturing Technology, 63(2), pp. 631–653. doi: 10.1016/j.cirp.2014.05.009.

Denkena, B., Lucas, A. and Bassett, E. (2011) 'Effects of the cutting edge microgeometry on tool wear and its thermo-mechanical load', CIRP Annals - Manufacturing Technology, 60(1), pp. 73–76. doi: 10.1016/j.cirp.2011.03.098.

Fu, X. et al. (2019) 'Edge micro-creation of Ti(C, N) cermet inserts by micro-abrasive blasting process and its tool performance', Machining Science and Technology, 23(6), pp. 951–970. doi: 10.1080/10910344.2019.1636275.

Jacob, A. et al. (2017) 'Influences of micro-blasting as surface treatment technique on properties and performance of AlTiN coated tools', Journal of Manufacturing Processes. The Society of Manufacturing Engineers, 29, pp. 407–418. doi: 10.1016/j.jmapro.2017.08.013.

Krebs, E. et al. (2018) ‘High-quality cutting edge preparation of micromilling tools using wet abrasive jet machining process’, Production Engineering, 12(1), pp. 45–51. doi: 10.1007/s11740-017-0787-7.

M, P. and N, S. P. (2020) ‘Effect of cutting edge form factor (K-factor) on the performance of a face milling tool’, CIRP Journal of Manufacturing Science and Technology. doi: 10.1016/j.cirpj.2020.06.004.

Puneet, P. C., Valleti, K. and Venu Gopal, A. (2017) ‘Influence of surface preparation on the tool life of cathodic arc PVD coated twist drills’, Journal of Manufacturing Processes, 27, pp. 233–240. doi: 10.1016/j.jmapro.2017.05.011.

Skordaris, G. et al. (2016) ‘Film thickness effect on mechanical properties and milling performance of nano-structured multilayer PVD coated tools’, Surface and Coatings Technology, 307, pp. 452–460. doi: 10.1016/j.surfcoat.2016.09.026.

Tönshoff, H. K. and Seegers, H. (2001) ‘X-Ray diffraction characterization of pre-treated cemented carbides for optimizing adhesion strength of sputtered hard coatings’, Surface and Coatings Technology, 142–144, pp. 1100–1104. doi: 10.1016/S0257-8972(01)01282-8.

Ventura, C. E. H. et al. (2017) ‘The influence of the cutting tool microgeometry on the machinability of hardened AISI 4140 steel’, International Journal of Advanced Manufacturing Technology. The International Journal of Advanced Manufacturing Technology, 90(9–12), pp. 2557–2565. doi: 10.1007/s00170-016-9582-4.

Vereschaka, A. et al. (2018) ‘Influence of Thickness of Multilayered Nano-Structured Coatings Ti-TiN-(TiCrAl)N and Zr-ZrN-(ZrCrNbAl)N on Tool Life of Metal Cutting Tools at Various Cutting Speeds’, Coatings, 8(2), p. 44. doi: 10.3390/coatings8010044.

Wang, W., Saifullah, M. K., et al. (2020) ‘Effect of edge preparation technologies on cutting edge properties and tool performance’, International Journal of Advanced Manufacturing Technology. The International Journal of Advanced Manufacturing Technology, 106(5–6), pp. 1823–1838. doi: 10.1007/s00170-019-04702-1.

Wang, W., Biermann, D., et al. (2020) ‘Effects on tool performance of cutting edge prepared by pressurized air wet abrasive jet machining (PAWAJM)’, Journal of Materials Processing Technology. Elsevier Ltd, 277. doi: 10.1016/j.jmatprotec.2019.116456.

Wiklund, U., Gunnars, J. and Hogmark, S. (1999) ‘Influence of residual stresses on fracture and delamination of thin hard coatings’, Wear. Elsevier Sequoia SA, 232(2), pp. 262–269. doi: 10.1016/S0043-1648(99)00155-6.

Yamamoto, K. et al. (2018) ‘Cutting Performance of Low Stress Thick TiAlN PVD Coatings during Machining of Compacted Graphite Cast Iron (CGI)’, Coatings, 8(2), p. 38. doi: 10.3390/coatings8010038.

Yen, Y. C., Jain, A. and Altan, T. (2004) ‘A finite element analysis of orthogonal machining using different tool edge geometries’, Journal of Materials Processing Technology, 146(1), pp. 72–81. doi: 10.1016/S0924-0136(03)00846-X.

Zhong, Z. Q. et al. (2018) ‘Cutting performances and the related characteristics of CVD coated hardmetal inserts changed by post-treatments’, International Journal of Refractory

Metals and Hard Materials. Elsevier Ltd, 70, pp. 162–168. doi: 10.1016/j.ijrmhm.2017.10.003.

Chapter 6. Conclusions and Future Work

6.1. General Conclusion

Despite its high hardness and tensile strength, compacted graphite iron has limited applications in the manufacturing industry due to its low machinability. During continuous cutting of CGI, the cutting tool shows tool life as low as 10% compared to grey cast iron which is commonly used in different industrial components such as engine blocks. Challenges associated with the machining of CGI are mainly high abrasive wear with the presence of lubricants, and high adhesive wear and formation of built-up edge in dry machining. To solve the aforementioned challenges, the development of a thick TiAlN PVD coating under low compressive residual stress was attempted in this research. A greater thickness of coating can lower the mechanical and thermal load on the substrate and, therefore, protect it for a longer period of time. The coating was developed using a new technology called super fine cathode (SFC) which enabled the deposition of PVD coatings under low compressive residual stress.

To develop a thick TiAlN PVD coating, this research was divided into four different studies, each trying to understand an important aspect of coating/substrate design such as thickness, the parameters affecting coating properties, the effect of coating properties on wear pattern, and the effect of tool geometry. In each study, various in-depth characterisation studies and machining experiments were conducted including XRD, SEM/EDS, FIB/TEM, nano and micro indentation, scratch test, AFM, optical 3D

microscope, wear measurement, and cutting force collection. The major findings of this research can be summarized as follows:

1. By using the SFC technology and controlling residual stress generation during the deposition process, coating thickness was successfully increased up to 17μm. It was observed that thickness greatly affects tool microgeometry, cutting forces as well as tool life.
2. Residual stress significantly affected wear pattern and coating performance. It was observed that with a high compressive residual stress coating, the substrate was exposed at a very early stage of the machining process due to reduced adhesion and coating coverage along the cutting edge. Here, the coating was shown to fail adhesively, and the failure started from the cutting edge. In contrast, in the coating with low compressive residual stress, the coating started to fail cohesively, and the substrate was first exposed away from the cutting edge. It was determined that this mechanism (gradual cohesive failure) was the main reason for the better tool performance of the tools with a low residual stress coating when machining CGI.
3. The properties of the coating can be adjusted mainly using nitrogen pressure and substrate bias voltage. These parameters affected properties such as deposition rate, density of defects, residual stress, and hardness as well as cutting performance and tool life under the influence of bombardment energy, the re-sputtering effect, and target poisoning. By increasing nitrogen pressure during the deposition process in a range of 1 to 5.5 Pa, residual stress was reduced as a

result of lower bombardment energy. Moreover, target poisoning took place at a nitrogen pressure of 5.5 Pa, which reduced the deposition rate as well as the density of defects. Increasing the substrate bias voltage in a range of -30 V to -150 V had an opposite effect on coating properties as higher compressive residual stress, lower deposition rate, and a lower microparticle density was achieved.

4. Coating micro breakage along the cutting edge was observed commonly after the deposition of thick coatings. With higher compressive residual stress, the degree of micro breakage was higher. In extreme cases, this led to chipping and substrate exposure. This was found to be due to geometrically induced residual stresses and the resulting tensile stress generated on the cutting edge.
5. Wet blasting was an effective method to adjust the microgeometry of the cutting edge. The edge radius of the uncoated tool was successfully increased from 6 µm to 15-45 µm by increasing the air pressure and size of the blasting media during wet blasting. The process had an insignificant effect on the hardness of the substrate; however, it reduced manufacturing defects, such as grinding marks, and improved the coating quality.

In summary, the developed coating under low compressive residual stress significantly outperformed the commercially available coatings, provided lower machining forces as well as better surface quality of the finished product. Moreover, quality issues with thick coating can be solved with wet blasting, and the edge radius can be adjusted for the specific application by using this method.

In this work, the coating was designed in a step by step manner. The emphasis was on tuning the properties in order to inhibit the dominant wear mechanism rather than focusing on different compositions, an approach which is not commonly used in the literature. This systematic coating design approach was done in the following steps:

- The feature which greatly affected coating performance and tool life subjected to the dominant wear mechanism was identified as thickness and residual stress.
- The limiting factors for each feature was comprehensively studied such as the effect of thickness on microgeometry and the effect of residual stress on coating quality.
- Each feature was then tuned in the direction of improving tool life while considering the limiting factors associated with the machining process.
- Substrate microgeometry was adjusted to accommodate challenges associated with the designed coating and further increasing tool life.

Using a similar approach is highly suggested for designing a coating as the same concept can be utilized for different applications, workpiece materials and coating systems. It should be also noted that although the resulted features are dependent on the instruments used, they follow the same trend. In this regard, a high edge radius in accordance to the depth of cut should be avoided to reduce ploughing. Moreover, geometrically induced stresses should be considered when selecting a proper substrate for thick coatings to avoid microbreakage along the cutting edge.

6.2. Research Contributions

The main contributions of this research can be summarized as follows:

1. SFC technology was identified as an effective method to generate higher coating thicknesses while keeping residual stress at lower levels typical of commonly used coatings for this application. The added thickness, possible with SFC, provided for more coating material which increased the time to substrate exposure under abrasive and adhesive wear conditions. This research also demonstrated the effect of coating thickness on tool microgeometry where thicker coatings rounded the cutting edge resulting in an increase in machining forces due to the larger cutting-edge radius. An overall 35% improvement in performance in terms of tool life over commercially available tool was measured for machining.
2. A strategy to control residual stress was identified by varying the deposition process parameters. The substrate bias voltage of -30 to -150 V and nitrogen pressure of 1 to 4 Pa were the most effective range to adjust residual stress. The correlation between deposition parameters and other coating properties such as hardness, yield strength, adhesion, microparticle density, and deposition rate was established.
3. Gradual cohesive failure was identified as the dominant failure mechanism for thick coatings with low compressive residual stress. Based on this mechanism, a tool life enhancing strategy was formulated and verified. This strategy resulted

in 70% higher tool life compared to coating with high residual stress due to delayed substrate exposure.

4. Wet blasting before coating deposition was demonstrated to be an effective method to adjust the tool microgeometry and reduce substrate tool surface defects. Furthermore, wet blasting improved the quality of the deposited coatings by reducing coating defects which resulted in enhanced tool performance.

In this research, a thick multilayer TiAlN PVD coating was designed along with a favourable compressive residual stress and tool microgeometry which increased tool life, reduced cutting forces, and improved the machined part quality in finish turning of CGI. The knowledge gained and the approach used in this research can be implemented for various workpiece materials to tailor the coating according to the need and achieve similar results.

6.3. Recommendations for Future Research

This study showed that by adjusting residual stress and thickness tool life can be improved when machining CGI. However, the same concept can be implemented for other applications and workpiece materials. According to the findings of this research, the developed coating should provide higher performance if the main wear mechanism is adhesion wear. Therefore, other workpiece materials and other applications, such as drilling or tapping, need to be tested to understand the full potential of this coating. Furthermore, as this research was focused on coating development, the effect of residual stress on the

properties of the machined workpiece was not fully studied. A more in-depth characterization study on the workpiece material is required to understand the impact of the developed coating on the workpiece.

Coating micro breakage along the cutting edge was studied. It was shown that increasing the edge radius reduces the geometrically induced stresses and, therefore, eliminates micro breakage. However, it is not possible to measure such stresses without modeling. Therefore, to better understand the phenomena, a comprehensive finite element model is needed to calculate the stresses applied on the interface. Once developed this FE model could be applied to help improve the design of the cutting edge.

Wet blasting was explored as a method to adjust tool microgeometry without significantly affecting tool properties. However, implementing another edge preparation method might improve substrate properties and, therefore, further prolong tool life. An in-depth study on different edge preparation techniques is needed to fully understand the preparation process. Furthermore, edge preparation can be done after deposition which can further improve the coating quality and performance.